

No. WREM I / 2 89

FTE/1657  
30/01/2021

Roll No. FOTE/950

From:

Vikas Kumar Rana  
K/2, Old Vikram Baug,  
Vadodara-390002  
Mob No: 9033908837

Date: 30-01-2021

To,  
The Registrar (Academic)  
The Maharaja Sayajirao University of Baroda  
Vadodara -390002

Sub.: To submit Synopsis of the Thesis "Remote Sensing and Geographic Information System Approach for Hydrological, Morphometrical and Spatial Analysis of Vishwamitri Watershed"

Through: The Guide, WREMI  
The Director, WREMI  
The Dean, Faculty of Technology and Engineering

Sir,

I have registered for Ph.D. in Civil Engineering, my Registration Number is FOTE/950 dated 09-02-2018.

I am submitting herewith Synopsis of my Thesis in PDF format. The final Thesis will be submitted as per the University Rules (Within One Year)

Thanking you,

Yours sincerely,

  
(Vikas Kumar Rana)

Encl: Synopsis

  
(Dr. T. M. V. Suryanarayana)  
Guide

  
Director  
WREMI  
DIRECTOR  
WATER RESOURCES ENGINEERING  
AND MANAGEMENT INSTITUTE  
FACULTY OF TECHNOLOGY AND ENGINEERING  
THE M. S. UNIVERSITY OF BARODA  
SAMIALA - 391 410.

  
Dean  
Faculty of Tech. & Engg.  
Dean  
Faculty of Tech. & Engg.  
M. S. University of Baroda,  
Baroda.

Remote Sensing and Geographic Information System  
Approach for Hydrological, Morphometrical and Spatial  
Analysis of Vishwamitri Watershed

A Synopsis Submitted to  
The Maharaja Sayajirao University of Baroda  
in Fulfilment of the Requirements for the Award of Degree of

DOCTOR OF PHILOSOPHY

In

CIVIL ENGINEERING

**GUIDE**

**Dr. T.M.V SURYANARAYANA**

**Director, WREMI  
PH.D. IN CIVIL ENGINEERING  
M.I.A.H.S., M.I.W.R.S., M.A.H.I.,  
M.I.S.G., M.I.S.H., M.A.A.M., M.I.A.E.M.E**

**SUBMITTED BY**

**VIKAS KUMAR RANA  
M.E (CIVIL)**

WATER RESOURCES ENGINEERING AND MANAGEMENT INSTITUTE  
FACULTY OF TECHNOLOGY & ENGINEERING  
THE MAHARAJA SAYAJIRAO UNIVERSITY OF BARODA  
SAMIALA-391410 DIST: VADODARA

**January 2021**

## CERTIFICATE

This is to certify that the synopsis entitled "Remote Sensing and Geographic Information System Approach for Hydrological, Morphometrical and Spatial Analysis of Vishwamitri Watershed" which is being submitted to The Maharaja Sayajirao University of Baroda in fulfilment of the requirements for the award of degree of Doctor of Philosophy in Civil Engineering by Mr. Vikas Kumar Rana written by him under my supervision and guidance. This is an original work carried out by him independently. The matter presented in this synopsis has not been submitted for the award of any other degree.



Dr. T.M.V. Suryanarayana  
Supervisor  
W. R. E. M. I.



Director  
W. R. E. M. I.  
DIRECTOR

30/01  
2021

WATER RESOURCES ENGINEERING  
AND MANAGEMENT INSTITUTE  
FACULTY OF TECHNOLOGY AND ENGINEERING  
THE M. S. UNIVERSITY OF BARODA  
SAMIALA - 391 410.



Dean  
Faculty of Technology & Engineering  
The Maharaja Sayajirao University of Baroda

Dean  
Faculty of Tech. & Engg.  
M. S. University of Baroda,  
Baroda.

## ACKNOWLEDGEMENT

Firstly, I would like to express my sincere gratitude to my guide Dr.T.M.V. Suryanarayana, Director of WREMI, Faculty of Technology & Engineering, The Maharaja 'Sayajirao University of Baroda, for the continuous support of my Ph.D study, for his patience, motivation and immense knowledge. His guidance helped me in all the time of research and writing of this Synopsis. I could not have imagined having a better advisor and mentor for my Ph.D study.

Besides my advisor, I would like to thank the WREMI teaching staff, Dr. Falguni Parekh, Inayatoli Shah, Pranav Mistry, Sumitra Sonaliya and Mugdha Trivedi for their support and inspiration.

I would also like to thank the agencies, United States Geological Survey (USGS), European Space Agency (ESA), Indian Space Research Organisation (ISRO), State Emergency Operation Centre Gandhinagar, National Bureau of Soil Survey and Land Use Planning (NBSS&LUP) for providing data and platforms to carry out the research work.

Date: 30/01/2021

Place: Vadodara

  
Vikas Kumar Rana

LIST OF TABLES	i
LIST OF FIGURES	ii

Sr. No.	Title	Page No.
1	INTRODUCTION	1-3
2	LITERATURE REVIEW	4-7
3	STUDY AREA AND DATA COLLECTION	8-11
4	METHODOLOGY	12-20
5	RESULTS AND ANALYSIS	21-46
6	CONCLUSIONS AND RECOMMENDATIONS	47-47
7	REFERENCES	48-49

## LIST OF TABLES

<b>Table No.</b>	<b>Name of Tables</b>	<b>Page No.</b>
1	Data characteristics of Cartosat DEM and Sentinel-2 data used in the study	10
2	Specifications of Sentinel-1 and Sentinel-2 products	10
3	Specifications of Sentinel-1 and Sentinel-2 products	11
4	Linear, aerial, and relief morphometric parameters	14
5	Metadata of the satellite data	19
6	Correlation coefficients for ASTER, SRTM, and Cartosat derived elevation	23
7	Slope classes	23
8	Covariance (Correlation) matrix of sentinel-2 bands	28
9	Comparison of user's accuracy (UA), producer's accuracy (PA), overall accuracy (%), and kappa coefficient using random forest tree and support vector machine algorithms for VV and VH polarization over Kerala region	36
10	Inundated area statistics of RF and SVM over cloud-free optical data for Kerala region	37
11	Comparison of user's accuracy (UA), producer's accuracy (PA), overall accuracy (%), and kappa coefficient using random forest tree and support vector machine algorithms for VV and VH polarization over Assam region	37
12	Inundated area statistics of RF and SVM over cloud-free optical data for Assam region	37
13	Estimated Daily runoff for the period 30-07-2019 to 03-08-2019 using weighted CN	39
14	Calculated area and percentage of each temperature class for summer and winter.	44
15	Administrative wards with green spaces requirement	44
16	Calculated bias and RMSE of the predictive models.	45

## LIST OF FIGURES

Figure No.	Name of Figures	Page No.
1	Study area	8
2	Study area Kerala	11
3	Study area Asssam	11
4	Methodology adopted for watershed delineation	13
5	Multi criteria decision making (MCDM) technique workflow using AHP for identification of potential runoff storage zones for water storage	15
6	Methodology of SAR workflow	17
7	Flowchart of the methodology for LST	18
8	(a) Histogram of ASTER data (b) Histogram of SRTM data (c) histogram of Cartosat data (d) Quantile-Quantile Plot of ASTER data (e) Quantile-Quantile Plot of SRTM data (f) Quantile-Quantile Plot of Cartosat data (g) Detrended Normal Q-Q Plot of ASTER data (h) Detrended Normal Q-Q Plot of SRTM data (I) Detrended Normal Q-Q Plot of Cartosat data	23
9	(a) Scatterplot showing linear regression of ASTER derived elevation vs Cartosat derived elevation (b) Scatterplot showing linear regression of SRTM derived elevation vs Cartosat derived elevation	24
10	Map showing ASTER, SRTM, and Cartosat derived river deviation from the actual river	24
11	Delineated watershed boundaries from ASTER, SRTM and Cartosat data	25
12	Area and perimeter of delineated watersheds	25
13	Visual Inspection of Watersheds derived from ASTER, SRTM, and Cartosat over the Shaded Relief map and Satellite imagery	26
14	(a) Filled sinks in ASTER (b) Filled sinks in Cartosat (c) Filled sinks in SRTM	26
15	Loading plot of component 1, 2 and 3.	29
16	Visual comparison of the principal component bands derived from the Sentinel-2 data (a) PCA band 1 (b) PCA band 2 (c) PCA band 3 and (d) Frequency distribution of principal component band 1 (e) Frequency distribution of principal component band 2 (f) Frequency distribution of principal component band 3	29
17	Figure 17: Curve number for antecedent moisture condition II generated from traditional approach (a) MLE (b) RF (c) SVM classifiers and PCA based approach in (d) MLE (e) RF (f) SVM classifiers	29
18	Hypsometric curve of Vishwamitri watershed	33
19	Sub watersheds of Vishwamitri watershed	33
20	Potential runoff storage zones of the study area	34
21	Identified sites for water storage structures on potential runoff storage zones	35
22	Already built water storage structures on the derived potential runoff storage zones.	35
23	Kerala (a) Random forest tree classification on filtered VH; (b) Support vector machine classification on VH; (c) Random forest tree classification on filtered VV; (d) Support vector machine classification on VV	37
24	Assam (a) Random forest tree classification on filtered VH; (b) Support vector machine classification on VH; (c) Random forest tree classification on filtered VV; (d) Support vector machine classification on VV	37
25	(a) Natural colour composite R-B04 G-B03 B-B02, (b) Green band (c) Near-infrared (d) Calculated NDWI over cloud-free extent for Kerala region	38
26	(a) Natural colour composite R-B04 G-B03 B-B02, (b) Green band (c) Near-infrared (d) Calculated NDWI over cloud-free extent for Assam region	38
27	Inundation map of Vadodara city using 2D modelling	40

28	Map validation using sites visit	41
29	Estimated land surface temperatures for the summer and winter seasons using Landsat 8 data	45
30	Spatial distribution of (A) NDVI, (B) NDWI, (C) DBSI and (D) Land use/land cover over Vadodara city.	45
31	Classification of heat zones into UHI and non-UHI zones, and contribution index of land use/land cover classes in summer and winter seasons.	45
32	Maps A,B, C, D,E,F,G and H show the predicted LST using the K-NN (2×2), K-NN (5×5), NN (2×2), NN(5×5) ,RT (2×2), RT (5×5), SVM (2×2) and SVM (5×5) models, respectively. Map I shows the observed LST estimated using Landsat 8.	46
33	Absolute error maps A1-H1 and corresponding frequency histogram of error A2-H2 of predictive models	46

# 1. Introduction

## 1.1 General

This chapter describes the objectives of the present study and also give brief introduction of electromagnetic energy, remote sensing, geographic information system, digital elevation model, morphometric analysis and weighted overlay analysis.

## 1.2 Introduction

Remote sensing relies on the measurement of electromagnetic (EM) energy. EM energy can take several different forms. The most important source of EM energy at the Earth's surface is the Sun, which provides us, for example, with (visible) light, heat (that we can feel) and UV-light, which can be harmful to our skin. Many sensors used in remote sensing measure reflected sunlight. Some sensors, however, detect energy emitted by the Earth itself or provide their own energy. A basic understanding of EM energy, its characteristics and its interactions is required to understand the principle of the remote sensor. This knowledge is also needed in order to interpret remote sensing data correctly. The most important source of energy is the Sun. Before the Sun's energy reaches the Earth's surface, three fundamental interactions in the atmosphere are possible absorption, transmission and scattering. The energy transmitted is reflected or absorbed by the surface material. Electromagnetic energy travelling through the atmosphere is partly absorbed by various molecules. The most efficient absorbers of solar radiation in the atmosphere are ozone (O<sub>3</sub>), water vapour (H<sub>2</sub>O) and carbon dioxide (CO<sub>2</sub>).

Geographic Information System (GIS) is a computer based information system used to digitally represent and analyze the geographic features present on the Earth's surface and the events (non-spatial attributes linked to the geography under study) that are taking place on it. The meaning to represent digitally is to convert analog (smooth line) into a digital form. "Every object present on the Earth can be geo referenced", is the fundamental key of associating any database to GIS. Here, term 'database' is a collection of information about things and their relationship to each other and 'geo-referencing' refers to the location of a layer or coverage in space defined by the co-ordinate referencing system.

Land surfaces of the earth are continuous phenomena rather than discrete objects. To fully model the surface, it would need an infinite amount of points. Digital Elevation Model (DEM) or Digital Terrain Model (DTM) is one of the methodologies to represent the surface. The term Digital Elevation Model (DEM) is frequently used to refer to any digital representation of ground surface topography or terrain; however, most often it is used to refer specifically to a raster or regular grid of spot heights. In a DEM, each cell has a value corresponding to its elevation.

Hydrologists and geomorphologists have recognized that certain relations are most important between runoff characteristics and geographic characteristics of drainage basin system. Various important hydrologic phenomena can be correlated with the physiographic characteristics of drainage basins such as size, shape, slope of drainage area, size and length of the tributories. Morphometry is the measurement and mathematical analysis of the configuration of the earth's surface, shape and dimension of its landforms. The morphometric analysis of the drainage basin and channel network play an important role in understanding the geo-hydrological behaviour of drainage basin and expresses the prevailing climate, geology, geomorphology, structural antecedents of the catchment.

Weighted Overlay is a technique for applying a common measurement scale of values to diverse and dissimilar inputs to create an integrated analysis. Geographic problems often require the analysis of many different factors. Weighted Overlay only accepts integer rasters as input, such as a raster of land use or soil types.

## Objectives of the Present Study

1. To demonstrate a comparative assessment of discrepancy in the hydrological behaviour of the DEMs in terms of terrain representation at the catchment scale.
  - I. To compare Digital Elevation Models of satellites ASTER, SRTM and Cartosat of 30 meter resolution for the selection of most appropriate DEM for Vishwamitri watershed.
  - II. To delineate watershed and sub - watersheds of Vishwamitri river using remote sensing and GIS.

Hydrological research on watersheds in developing countries is considered a relatively new field. Therefore, for the development of mathematical watershed models that can simulate and evaluate the existing and proposed management scenarios, the application of hydrologic data is considered necessary. Thus, the evaluation of the accuracy of watershed boundaries derived from different sources of elevation data becomes necessary. To evaluate the sensitivity of data sources and their vertical accuracies, two hydrologic applications, watershed boundary and river network extraction, were used along with various statistical measures. Hydrologic applications are selected because they heavily rely on DEM data.

2. To develop an approach to analyze Sentinel–2 satellite images using traditional and principal component analysis based approaches to create land use and land cover map, which is a prerequisite for developing the curve number.
  - I. To prepare Landuse map of entire watershed using spectral separability method from Landsat data.

*Instead of Landsat data, more recent and better resolution Sentinel-2 data has been used. Supported sources: [USGS](#) , [Astola et al. \(2019\)](#).*

In this study, PCA is used to condense the information of high dimensional Sentinel–2 multispectral satellite data into fewer channels (represented by the higher-order components) and use the principal components as inputs to the classifiers, thus reducing the computational demands and possibly improving performance. The study will also show the performances of state-of-the-art classification methods, the Maximum Likelihood Estimation, Random Forest Tree, and Support Vector Machine tested on Sentinel–2 multispectral satellite data in order to observe if principal component analysis improves land use and land cover classification.

3. To perform Morphometrical analysis of Vishwamitri watershed and prioritization of sub-watersheds for assessing the flood influencing characteristics of the five sub-watersheds of the Vishwamitri watershed.
4. To identify potential runoff storage zones based on the various physical characteristics of the Vishwamitri watershed using a GIS-based conceptual framework that combines through analytic hierarchy process using multi criteria decision-making method.

The conceptual framework will help to identify potential runoff storage zones for water storage sites based on the various physical characteristics (rainfall, slope, land use/land cover, height above the nearest drainage, stream order, curve number, topographic wetness index) of the watershed.

5. To develop an approach for operational flood extent mapping using Synthetic Aperture Radar (SAR) and preparation of flood inundation map for data scarce region using 2D flow modelling using rain on grid model.

Some most preferred speckle filters are assessed for the data from Sentinel-1 to map flood extent. The Sentinel-1 (VV-vertical transmit, vertical receive and VH- vertical transmit, horizontal receive) polarizing filter data were used. Moreover, flood inundation map for Vishwamitri River was prepared using 2D flow modelling using rain on grid model.

6. To quantify the effects of urban land forms on land surface temperature and modeling the spatial variation using machine learning. The models can help to predict land surface temperature under temporary cloud cover spots, which are present in the data at the time of the acquisition, using neighboring biophysical (cloud-free) independent variables relationship with land surface temperature.

The specific objectives of this study are:

- (1) To derive land surface temperature from the Landsat 8 thermal band
- (2) To examine the distributions of land surface temperature and land use/land cover types in the study area and also, to understand the overall relationship between the land surface temperature and urban landforms in summer and winter seasons in Vadodara city, India
- (3) To determine contribution indexes of land use/land cover classes to land surface temperature under different temperature conditions;
- (4) To examine the relationship between LST with Normalized Difference Vegetation Index (NDVI), Normalized Difference Water Index (NDWI) and Dry Bare-Soil Index (DBSI);
- (5) To evaluate the machine learning models' performances for K-Nearest Neighbor (K-NN) regression, Neural Networks (NN), Random Trees (RT) regression and Support Vector Machine (SVM) regression with the mean moving kernel (observation grid) of 2×2 and 5×5 for each explanatory variable (NDVI, NDWI and DBSI).

## 2. Literature Review

### 2.1 General

This chapter briefly shows the research papers studied for the individual objective. The chapter is divided into six sections, each section contains the literature reviewed for the specific objective.

1. **Objective:** Comparative assessment of discrepancy in the hydrological behaviour of the DEMs in terms of terrain representation at the catchment scale.

Hydrological research on watersheds in developing countries is considered a relatively new field. Therefore, for the development of mathematical watershed models that can simulate and evaluate the existing and proposed management scenarios, the application of hydrologic data is considered necessary. Thus, the evaluation of the accuracy of watershed boundaries derived from different sources of elevation data becomes necessary. To evaluate the sensitivity of data sources and their vertical accuracies, two hydrologic applications, watershed boundary and river network extraction, were used along with various statistical measures. Hydrologic applications are selected because they heavily rely on DEM data. For various hydrological and geomorphological models, the digital elevation model is applied as inputs. A set of morphometric parameters, which are used to construct relationships between hydrological features and morphometric properties, can be used to deterministically identify terrain features. The study of [Sharma & Tiwari, \(2014\)](#) shows noteworthy contrasts in hydrological properties of the two contemplated DEMs considering vertical accuracy assessment, hydrological simulation, empirical USLE model, and physical SWAT model. ArcSWAT simulation results uncover runoff predictions that are less sensitive to the selection of the DEMs. To delineate the drainage network that causes a significant effect on hydrological or hydraulic modeling and the comprehension of fluvial processes, [Persendt & Gomez, \(2016\)](#) selected different progressive flow accumulation threshold values. [Ficklin et al., \(2015\)](#) concluded that the DEM source and DEM resampling techniques (nearest neighbor, bilinear interpolation, cubic convolution, and majority) are less sensitive parameters as compared to DEM resolution in the SWAT model. [Guth, \(2010\)](#) compared the GDEM with SRTM 3 arcsecond data and computed the elevation, slope distributions, and geomorphometric parameters. Furthermore, they determined that the ASTER GDEM is essentially equivalent to SRTM 3 arcsecond data. In addition, they also reported that GDEM contains data anomalies or inconsistencies that corrupt its utilization for most applications. However, many studies have demonstrated that the outputs of hydrological models are influenced by DEM resolution [Chaplot, \(2014\)](#); [Wolock & Price, \(1994\)](#), DEM source [Wang, Yang, & Yao, \(2012\)](#) and DEM resampling .

The evaluation of lower resolution data such as the Shuttle Radar Topography Mission (SRTM) and Advanced Thermal Emission and Reflection Radiometer (ASTER) was carried out by [Jarhani, Callow, Mcvigar, Niel, & Larsen, \(2015\)](#)- using the hydrodynamic models by (i) assessing the point accuracy and geometric co-registration error of the original DEMs; (ii) quantifying the effects of DEM preparation methods (vegetation smoothed and hydrologically corrected) on hydrodynamic modeling relative accuracy; and (iii) quantifying the effect of the grid size (30–2000 m) of the digital elevation hydrodynamic model and the associated relative computational costs (run time) on relative accuracy in model outputs. The study highlights the important impact of the quality of the underlying DEM and, in particular, how sensitive hydrodynamic models are to preparation methods and how important vegetation smoothing and hydrological correction of the base topographic data are for modeling floods in low gradient and multichannel environments.

- Objective:** To develop an approach to analyze Sentinel-2 satellite images using traditional and principal component analysis based approaches to create land use and land cover map, which is a prerequisite for developing the curve number.

Numerous effective methods and advanced classifiers have been applied to improve the performance of land use and land cover classification that is based on moderate resolution data. Researchers have used various methods to incorporate Landsat data into land-use change analyses [Ozesmi & Bauer, \(2002\)](#). The complexity of the landscape, the selected remote sensing data, image processing, and classification methods, make it difficult to obtain reliable and accurate land use and land cover information [Manandhar, Odehi, & Ancevt, \(2009\)](#). Researchers have tried to overcome this problem from many different perspectives, with the purpose of seeking an efficient method for mapping LULC patterns. These studies range from conventional statistical approaches to more powerful machine learning algorithms that have enhanced the quality of the solutions for this problem. Traditional remote sensing data classification methods include maximum-likelihood classifier, distance measure, clustering, or logistic regression. Over the last decade, more advanced methods such as decision trees, k-nearest-neighbors, random forest, neural networks and support vector machines have been used for LULC mapping [Cheng et al., \(2015\)](#); [Han, Zhang, Cheng, Guo, & Ren, \(2015\)](#). Recently, a study on the state of the art of supervised methods for land use and land cover classification was performed by [Khatami et al., 2016](#). It was reported that Support Vector Machine, k-nearest-neighbors, and Random Forest Tree generally provide better performance than other traditional classifiers, SVM being the most efficient method.

PCA is a statistical procedure that transforms the input bands (with correlated variables) orthogonally from an input multivariate attribute space to a new multivariate attribute space (having linearly uncorrelated variables) whose axes are rotated with respect to each other. Transformation or dimensionality reduction of the data in the analysis compresses data by eliminating noise, redundancy, and irrelevant information. The linearly uncorrelated variables in new multivariate attribute space are called principal components. The first principal component (PC1 derived from the first eigenvector) is the direction in space along which projections have the largest variance. The subsequent principal component (PC2) is the direction that maximizes variance among all directions orthogonal to the previous principal component. The variances of the remaining principal component images decrease in order, as denoted by the magnitudes of the corresponding eigenvalues.

- Objective:** To perform Morphometrical analysis of Vishwamitri watershed and prioritization of sub-watersheds for assessing the flood influencing characteristics of the five sub-watersheds of the Vishwamitri watershed

Measurement and statistical study of the shape of the earth's surface, form and scale is called morphometry. Morphometric study of the watershed provides a detailed overview of the drainage system, which is an important part of the characterisation of the watershed. It's an indicator of evolutionary phase that the basin landform is currently undergoing, as illustrated in different morphometric studies. Morphometric parameters such as stream order, basin area and perimeter, stream length, basin length, drainage density, stream frequency, bifurcation ratio, drainage texture, relief ratio, ruggedness number, form factor, circulatory ratio, compactness index, and lemniscate ratio have been used to establish a primary hydrological diagnosis and to prioritize sub-watersheds according to their flood potential ([Masoud,\(2016\)](#) and [Bhat et al., \(2019\)](#) . Ungauged watersheds with scarce information on soil, geology, geomorphology and hydrology, morphometric analyses are an excellent alternative to understanding the underlying factors that

regulate the hydrological behaviour (Altaf et al., (2013) and Romshoo et al., (2013)). Traditional methods have generally been used for the morphometric characterization of basins in the past (Magesh and Chandrasekar, (2014) and Ozdemir and Bird, (2009)). However, the assessment of basin morphometry has become more reliable, speedy and economically productive with the advancement of the geographic information system, high resolution digital elevation models (DEMs) and remote sensing techniques Ahmed et al., (2010). Bhat et al., (2019) evaluated the flood influencing factors in the upper Jhelum basin, they delineated the upper Jhelum basin into ten sub-basins, followed by extraction of drainage network and morphometric parameters using ASTER DEM and topographic maps in Geographic Information System. The overall flood potential was determined on the basis of compound value obtained for all morphometric parameters of each sub-basin.

4. **Objective:** To identify potential runoff storage zones based on the various physical characteristics of the Vishwamitri watershed using a GIS-based conceptual framework that combines through analytic hierarchy process using multi criteria decision-making method.

In this study, a GIS-based conceptual framework is applied with multi criteria decision making (MCDM) technique using analytic hierarchy process (AHP) to produce suitability map of potential runoff storage zones within the watershed. The conceptual framework will help to identify potential runoff storage zones for water storage sites based on the various physical characteristics (Rainfall, Slope, Land use/land cover, Height above the nearest drainage, Stream order, Curve number, Topographic wetness index) of the Vishwamitri watershed. This will help concerned authorities in the proficient arranging and execution of water-related plans and schemes, improve water shortage, reduce dependability on ground water and

A number of studies have been reported for site suitability using Multi Criteria Decision Making (MCDM) and Analytic Hierarchy Process (AHP) in GIS environment (Al-Adamat, (2008); Pauw, Oweis and Youssef, (2008); Kahinda et al., (2008); Mahmoud and Alazba, (2014)). AHP is a popular weighting method in the field of MCDM (Saaty, (1977); Rozos et al. 2011; Karimi and Zeinivand, (2019)). The AHP is a theory of measurement through a pairwise comparison matrix and relies on the judgments of experts to derive priority scales. It is used as higher cognitive process tool to determine the percentage importance of various criteria used in the determination of suitable sites. The AHP method consists of three main phases: construction of hierarchy, priority analysis of data and confirmation of consistency.

5. **Objective:** To develop an approach for operational flood extent mapping using Synthetic Aperture Radar (SAR) and preparation of flood inundation map for data scarce region using 2D flow modelling using rain on grid model.

In recent years, severe rainfall events have afflicted the state of Kerala in southern India causing damage to houses and infrastructures. Remotely sensed data can provide significant mapping capabilities during such severe rainfall events. However, obtaining remotely sensed data with an ideal combination of fine spatial and temporal resolution with the ability to see through clouds and discriminate flooding under forest cover is a difficult task. The extent of inundation, caused by river flooding and/or coastal storm surges, is required quickly to expedite relief and repair services. The precipitation over Kerala amid June, July and August (1–19 August 2018) were 15%, 18% and 164% above normal, respectively. Due to intense rainfall, all the major reservoirs were full by the end of July 2018 and had no buffer storage to accommodate the inflows from 10th of August 2018 (Central Water Commission, 2018). Serious spell of precipitation from the 14 August 2018 to 19 August 2018

brought appalling flood in 13 out of 14 districts. The perpetuated exceptional rainfall in August (170% above normal) in the catchment areas compelled the authorities to resort to hefty

Synthetic Aperture Radar (SAR) imaging is an efficient remote sensing technique offering well-developed, consistent, efficient, and reliable means of collecting information to extract earth's surface dielectric properties (Lee and Pottier 2009). The ability of SAR to penetrate clouds is extremely useful in flood-related studies. Synthetic aperture radar uses microwave radiation to illuminate the earth's surface for recording the amplitude and phase of the back-scattered radiation, which makes the imaging process coherent. The active sensor of Sentinel-1 forms a SAR image by coherently processing the returning signals from successive radar pulses. Stronger or weaker final signals (output) are generated by the out-of-the-phase waves by constructively or destructively interfering with each other. These interferences produce a seemingly random pattern of brighter and darker pixels giving the radar images a distinctly grainy appearance known as 'Speckle' (Goodman, 1976). Speckle noise changes the spatial statistics of the underlying scene backscatter making the classification of imageries a difficult task (Durand et al.,1987). A brief introduction of some well-known despeckling methods is presented below.

6. **Objective:** To quantify the effects of urban land forms on land surface temperature and modeling the spatial variation using machine learning. The models can help to predict land surface temperature under temporary cloud cover spots, which are present in the data at the time of the acquisition, using neighboring biophysical (cloud-free) independent variables relationship with land surface temperature.

The land surface temperature is defined as the temperature felt when long-wave radiation and turbulent heat fluxes are exchanged within the surface-atmosphere interface Tomlinson, (2011); Avdan and Jovanovska, (2016). It has been used in several fields, including hydrological cycles, urban climate, climate change and evapotranspiration. Studies show that urban growth is increasing with associated vegetation loss, leading to urban microclimate alterations. In Baltimore City, USA, Zhao et al., (2016) were keen to build correlations between the land surface temperature and land use/land cover indices. In the study carried out in Tehran City of Iran, Haashemi et al., (2016) noted a seasonal variation in the land surface temperature and land use/land cover relationship. Different simulation techniques are available to model future land cover changes in an area, as a result, future land surface temperature modeling of that area is equally possible. However, there is relatively limited work on the simulation of land surface temperature. Mallick et al., (2008) used linear regression for predicting surface temperature over land use/land cover classes using normalized difference vegetation index and fractional vegetation cover.

Two or more satellite images from different timescales were used to analyze land surface temperature patterns because cloud-free images were not available for a large number of studies. However, any resulting land surface temperature configuration can be affected by different environmental factors (wind speed, Sun's radiation, surface moisture, and humidity) by differing acquisition time conditions. Zeng et al., (2014) tried to reconstruct MODIS land surface temperature based on multitemporal classification and robust regression. In a recent study, Shafizadeh-Moghadam et al, (2020) used machine learning models to simulate urban land surface temperature based on independent factors such as land use/land cover, solar radiation, altitude, appearance, distance to major roads, and Normalised Difference Vegetation Index (NDVI) models. Performance evaluation of the four models revealed a close performance in which their  $R^2$  and Root Mean Square Error (RMSE) were between 60.6–62.1% and 2.56–2.60 °C, respectively.

### 3. Study Area and Data Collection

#### 3.1 General

In the present work, Vishwamitri watershed is selected as a site of the study. Due to the unavailability of SAR data for the Vadodara region, the applicability of the SAR for inundation mapping is shown over Kerala and Assam region.

#### 3.2 Study areas and data collection

The study area is located in the Vadodara district of Gujarat State of India. In this work, the Vishwamitri Watershed has been selected as the study area. The Vadodara district area, which is located south of the Tropic of Cancer and in the transition zone of heavy rainfall areas of South Gujarat and arid areas of North Gujarat plains, has a subtropical climate with moderate humidity. The Vadodara district forms a part of the great Gujarat plain. The eastern portion of the district is hilly terrain with several ridges, plateaus, and isolated relict hills that have an elevation in the range of 150–481 m above the mean sea level. The southeastern plateau has the highest peaks of the district—Amba Dungar and Mandai Dongar 637 m above the mean sea level. The Vishwamitri river, which falls in the Vadodara taluka, is considered as a major tributary of the Dhadhar river. The Vishwamitri river originates from the hills of Pavagadh, which is 43 km northeast of Vadodara. The Pavagadh hill is made of trappean rocks that emerge abruptly 830 m above the mean sea level. The Vishwamitri river has a channel length of around 70 km and 58 km of this channel length flows through the Vadodara District. It meets the Dhadhar river at Pingalwada in the Vadodara district.

Figure 1 shows the geographical location of the study area.

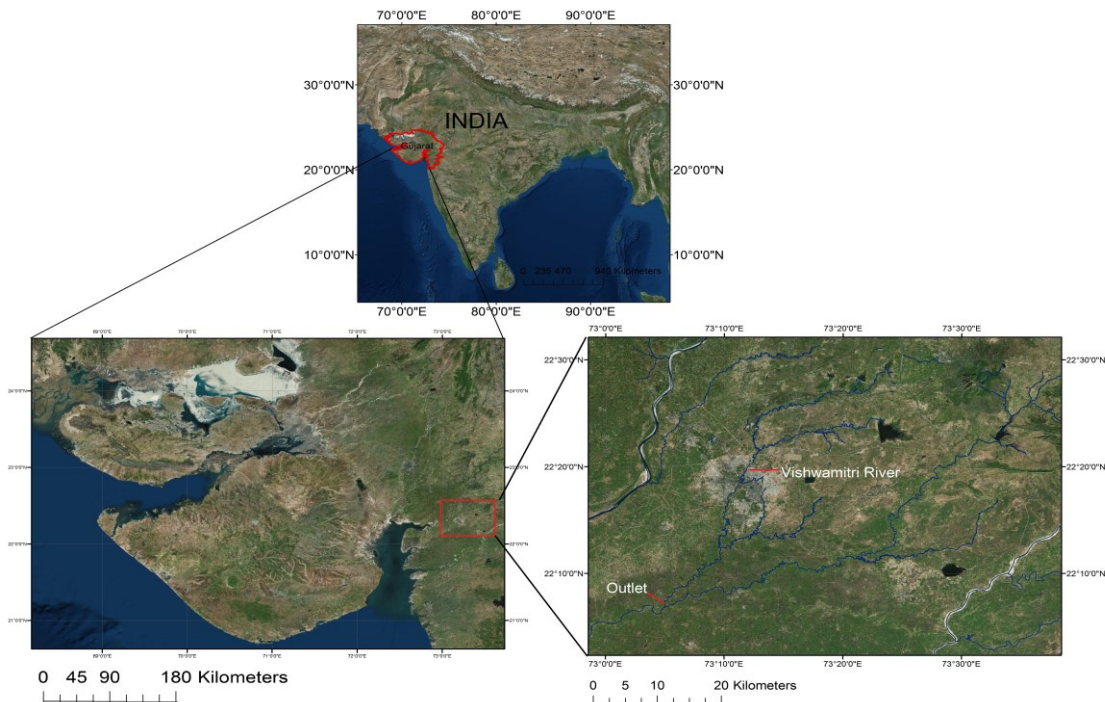


Figure 2: Study area

#### Cartosat-DEM:

With the prime objective of delivering high-resolution satellite data of 2.5 m in-track stereo, Indian Space Research Organization (ISRO) launched Cartosat –1 on May 5, 2005. The quality verification process is performed by panning and draped visualization in order to demarcate distortions. The DEM is referenced to WGS84.

**SRTM-DEM:**

The SRTM data are projected in a geographic (lat./long.) projection taking into consideration the WGS84 horizontal datum and the EGM96 vertical datum. It is considered global DEM with one-arcsecond resolution (approximately 30 m at the equator). Two different C-band and X-band interferometric radar images of the same area are captured by two antennas that are about 60 m apart. C-RADAR Vertical reference and Polarization are EGM96 geoid and HH VV, respectively, whereas X-RADAR Vertical reference and Polarization are WGS84 ellipsoid and VV, respectively. Elevation data are obtained after processing interferograms.

**ASTER-GDEM:**

ASTER GDEM was generated by using the stereo-correlation of more than 1.5 million along-track stereo images of 15 m horizontal resolution, which are obtained by the visible and near-infrared (VNIR) sensor covering land surfaces between 83°N and 83°S. Initially, ASTER (GDEM-V1) with 30 m horizontal resolution and absolute vertical accuracy of 20 m (95% confidence interval) were made open for public use. The data are referenced to WGS84 and EGM96 vertical datum.

**Sentinel-2:**

The European Space Agency's Sentinel-2 Multispectral Imager measures the reflected solar spectral radiances in 13 spectral bands ranging from the visible to the shortwave infrared bands. The primary purpose is to monitor vegetation, water bodies, cropland, urban areas, land use and land cover change at local, regional, national and global scales. Sentinel-2A and -2B can together revisit the same region every five days with data acquisitions available in Level 1C processing. The data characteristics of Cartosat DEM and Sentinel-2 data used in the study are given in [Table 1](#). Bands 1, 9 and 10 at 60 m resolution are dedicated mainly to atmospheric corrections and cirrus-cloud screening. As they do not contain surface information, those 3 bands were omitted after the pre-processing phase from the analysis.

**Kerala**

Kerala is a small, elongated coastal state in peninsular India's south-western tip. It is surrounded by the Western Ghats in the east and the Arabian Sea in the west. A part of the state of Kerala was considered in this study. The state faces severe and varied damages due to floods and heavy rainfall. Monsoon circulation dominates the climate of India and Kerala in particular. The wind blows from the oceans to the south of the Asian land masses during the half of the year, while a seasonal wind blows from the Asian land masses to the oceans in the south during the other half of the year causing a spectacular reversal of pressure and wind patterns between the two six-month periods. South-west monsoon (June-September) and post-monsoon (October-November) are the main rainy seasons in Kerala. The state witnessed heavy floods in the year 1924 and 1961. The IMD recorded rainfalls for 15 to 17 August 2018 were found to be comparable to the rigorous storm that occurred in 1924 ([Central Water Commission, 2018](#)). Heavy rainfall resulted in high surface runoff in Kerala's major river basins, filling all dams and subsequent opening of these dams, causing widespread flooding in downstream areas, low-lying coastal areas, and Kerala's backwaters. [Figure 2](#) shows the area covered under the study.

The National Aeronautics and Space Administration Alaska Satellite Facility (NASA/ASF) houses a complete archive of Sentinel-1 SAR data processed by the European Space Agency (ESA). The Sentinel-1 Level-1 ground range detected (GRD) data acquired in interferometric wide swath (IW) mode, which is the predefined mode over land with VV and VH polarizations, were downloaded via the ASF application programming interface (API). Sentinel-1 and Sentinel-2 data that are available closest to event date were acquired on 21 August 2018 at 00:40:44 and 22 August 2018 at 05:06:49,

respectively. The specific parameters of the Sentinel-1 and Sentinel-2 products are given in [Table 2](#).

### Assam

Assam is a state in northeast India, situated south of the eastern Himalayas along the Brahmaputra and Barak River valley. The state has recently witnessed heavy flood in July 2019. The Brahmaputra basin falls within the monsoon rainfall regime, getting an average rainfall of about 230 cm. The heavy floods in the Brahmaputra river in Assam owing to the increase in water concentrations of the Brahmaputra river and its related tributaries likely led from high continuous rainfall in the upper catchment regions of the Brahmaputra Basin. [Figure 3](#) shows the area covered under the study. Sentinel-1 and Sentinel-2 data that are available closest to event date were acquired on 14 July 2019 at 11:57:18 and 16 July 2019 at 04:27:09, respectively. The specific parameters of the Sentinel-1 and Sentinel-2 products are given in [Table 3](#).

Table 1: Data characteristics of Cartosat DEM and Sentinel-2 data used in the study

	Acquisition technique	Spatial resolution	Projection
<i>Cartosat DEM</i>	Satellite stereo images	1 arc-second or 30 meters	WGS84
<i>Sentinel-2</i>	Multispectral Imager (MSI)	Band 2-Blue	10 m
		Band3-Green	10 m
		Band4-Red	10 m
		Band5- Vegetation Red Edge	20 m
		Band6- Vegetation Red Edge	20 m
		Band7- Vegetation Red Edge	20 m
		Band8-NIR	10 m
		Band8A- Narrow NIR	20 m
		Band11-SWIR	20 m
Band12-SWIR	20 m		

Table 2: Specifications of Sentinel-1 and Sentinel-2 products

	PRODUCT NAME	REPEAT CYCLE	INSTRUMENT	PRODUCT TYPE	ACQUISITION MODE	SENSING DATE	PASS	TRACK	ORBIT	POLARIZATION
SENTINEL-1A	S1A_IW_GRDH_1SDV_20180821T004109_20180821T004134_023337_0289D5_B2B2	12 days	C-SAR	Ground Range Detected	Interferometric Wide swath (IW)	21-Aug-18	DESCENDING	165	23337	DV (dual VV+VH polarization)
SENTINEL-2B	S2B_MSIL1C_20180822T050649_N0206_R019_T43PFL_20180822T085140	10 days	Multi-Spectral Instrument	S2MSI1C	INS-NOBS	22-Aug-18	DESCENDING	-	7624	-

Table 3: Specifications of Sentinel-1 and Sentinel-2 products

	PRODUCT NAME	REPEAT CYCLE	INSTRUMENT	PRODUCT TYPE	ACQUISITION MODE	SENSING DATE	PASS	TRACK	ORBIT	POLARIZATION
SENTINEL-1A	S1A_IW_GRDH_1SDV_20190714T115653_20190714T115718_028113_032_CCD_F972	12 days	C-SAR	Ground Range Detected	Interferometric Wide swath (IW)	14-Jul-19	ASCENDING	41	28113	DV (dual VV+VH polarization)
SENTINEL-2B	S2B_MSIL2A_20190716T042709_N0213_R133_T46RDQ_20190716T083530	10 days	Multi-Spectral Instrument	S2MSI1C	INS-NOBS	16-Jul-19	DESCENDING	-	12314	-

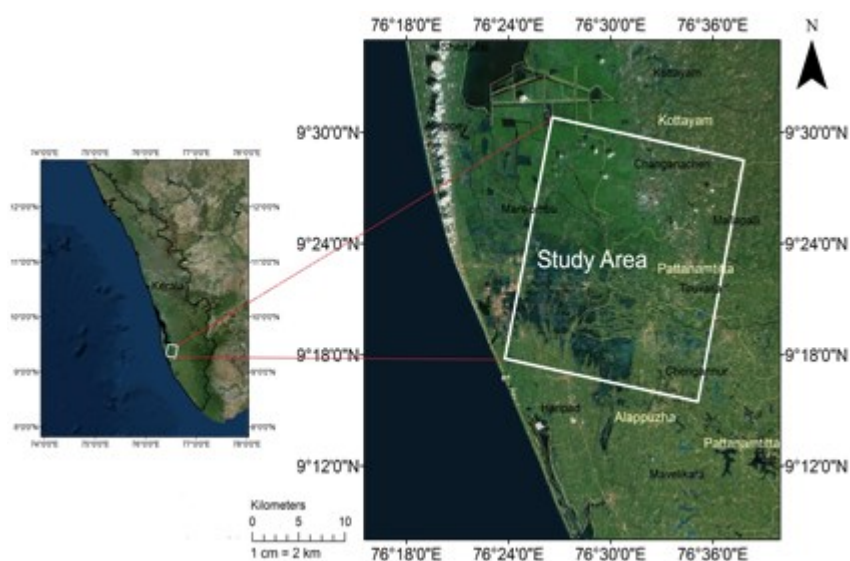


Figure 3: Study area Kerala

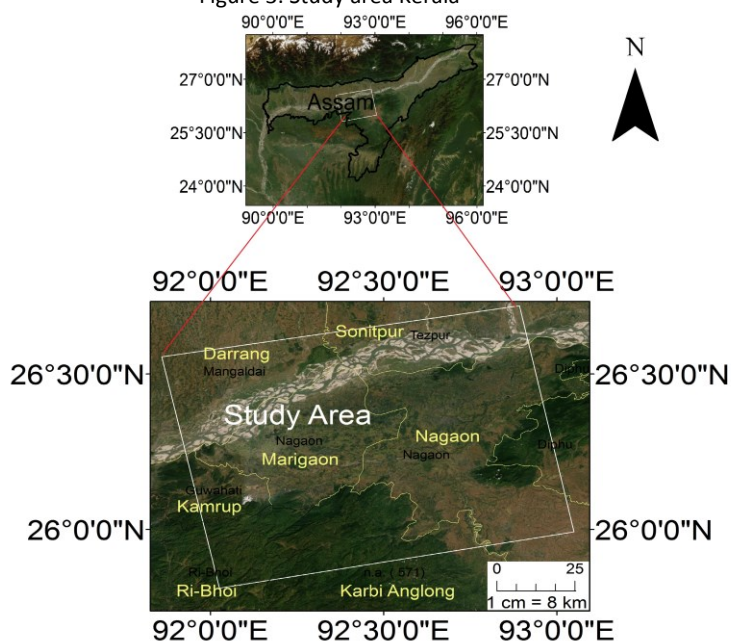


Figure 4: Study area Assam

## 4. Methodologies

### 4.1 General

This chapter briefly shows the methodology adopted for the individual objective. The chapter is divided into six sections, each section contains the specific methodology for the specific objective.

### 4.2 Methodology

1. **Objective:** To demonstrate a comparative assessment of discrepancy in the hydrological behaviour of the DEMs in terms of terrain representation at the catchment scale.

**Datum Transformation:** The ellipsoidal height of terrain (in meters), with WGS84 ellipsoid as a horizontal and a vertical datum, in Geographic Projection System (i.e., X and Y in terms of latitude and longitude) is provided by Cartosat DEM. The 27,4476 elevation values extracted from Cartosat DEM have been reprojected by using the Vdatum transformation tool provided by NOAA's National Ocean Service in a Geographic (lat./long.) projection, with WGS84 as a horizontal datum and EGM96 as a vertical datum. SRTM and ASTER data are referenced to WGS84 and EGM96 vertical datum.

**Statistical Comparison:** Several descriptive statistic measures were employed to describe and compare the elevation distributions in each DEM. The root-mean-square error (RMSE), a typical proportion of measuring vertical exactness in DEMs, was computed for DEMs. The elevation of each ASTER and SRTM DEM pixel was compared with that of the respective Cartosat DEM pixel. The RMSE was calculated directly from data. In addition, skewness and kurtosis were determined for DEMs. The degree of asymmetry of a distribution around its mean is measured by skewness. The range of skewness is considered to be from minus infinity ( $-\infty$ ) to positive infinity ( $+\infty$ ). A distribution with a tail extending out to the right is called positively skewed distribution, whereas a distribution with an asymmetric tail extending out to the left is called negatively skewed. The degree to which a distribution is more or less peaked than a normal distribution is measured by excess kurtosis. Kurtosis is a unitless measure that indicates how sharp the data peak is. A kurtosis value of  $>0$  indicates a peaked distribution, whereas a kurtosis value of  $<0$  indicates a flat distribution.

**Visual Comparison:** The aim of visual comparison was to detect changes between the results, such as streams and watershed derived from the different DEMs by using the shaded relief map and the high-resolution satellite imagery. The Cartosat watershed was selected for comparison between the slope map generated by ASTER, SRTM, and Cartosat DEMs taking into consideration heterologous comparisons of the ridge line and stream. The maximum rate of change of the elevation of the plane (the angle that the plane makes with a horizontal surface) is called the slope gradient. A declivity map with a pixel size of 30 m was created for analyzing the influence of the terrain slope on the models. Based on the Brazilian Agricultural Research Corporation standards, the slope values were classified. The Brazilian Agricultural Research Corporation (Embrapa), which is a state-owned research corporation, is affiliated with the Brazilian Ministry of Agriculture. Watershed delineation was performed by GIS software by importing DEMs. A pixel or a set of spatially connected pixels whose flow direction cannot be assigned to one of the eight valid values in a raster of the flow direction is called a sink. In order to remove small imperfections in the data, the Fill Sink tool was used. Sinks must be filled to ensure a proper delineation of basins and streams. A derived drainage network may be discontinuous if the sinks are not filled. A raster of the flow direction from each pixel to its downslope neighbors is created by the flow-direction tool. The accumulated flow as the accumulated weight of all pixels flowing into each downslope pixel in the

output raster is calculated by the flow accumulation tool. Pixels with a high flow accumulation are termed as areas of concentrated flow, which may be used for identifying stream channels. Similarly, pixels with a flow accumulation of 0 are termed as local topographic highs, which may be used for identifying ridges. A stream network can be delineated by applying a threshold value to the flow accumulation raster. A user-defined and important parameter, which is known as the stream threshold, directly affects the drainage network and basin boundaries that would be obtained by hydrological analysis. In this study, the stream threshold has been considered as 1% of the maximum flow accumulation value. The point on the surface at which water flows out of an area is called the outlet or the pour point. The outlet is the lowest point along the boundary of a watershed. Figure 4 shows the methodology adopted for watershed delineation. Map algebra that determines where the Fill tool had filled the sinks was used to investigate the cause of the errors in the streams network.

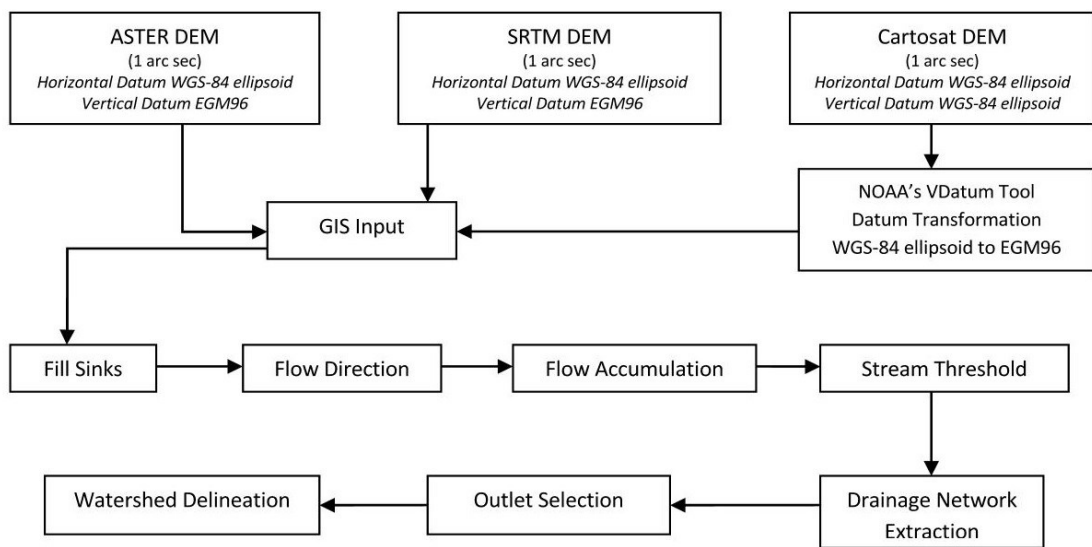


Figure 5: Methodology adopted for watershed delineation

2. **Objective:** To develop an approach to analyze Sentinel-2 satellite images using traditional and principal component analysis based approaches to create land use and land cover map, which is a prerequisite for developing the curve number.

The Sentinel-2 cloud-free Level 1C data product (L1C\_T43QCE\_A008039\_20180920T054434) acquired on 20 September 2018 was downloaded from the Sentinel Hub developed by European Space Agency. Sentinel-2 Level 1C data were processed from Top-Of-Atmosphere Level 1C to Bottom-Of-Atmosphere Level 2A. QGIS desktop 3.6.1 is a free and open-source cross-platform desktop geographic information system application that supports viewing, editing, and analysis of geospatial data. QGIS desktop 3.6.1 interface was used with Semi-Automatic Classification Plugin (SCP), to convert the Sentinel-2 MSI data to reflectance values and for dark object subtraction atmospheric correction (DOS1) of the data.

After atmospheric correction, ten bands (2–8, 8A, 11 and 12) were composited and clipped to the study area. The processed data were georeferenced to the WGS 84 UTM 43N projected coordinate system. In order to test the effectiveness of PCA, two stacks were created for the classification in ESRI's ArcGIS Desktop 10.5 software. Stack 1 contained atmospherically corrected bands (2–8, 8A, 11 and 12) and Stack 2 contained 3 major PCA bands accounting for the 97.96% of eigenvalues. The PCA technique was used to reduce the number of bands or dimensions necessary for classification.

Dimension reduction leads to a reduction in the computation costs without compromising the desired variability in the data. The process of PCA can be divided into three steps. The first step is to calculate the covariance or correlation matrix of multiband images.

The traditional approach and PCA based approach used Stack 1 and Stack 2, respectively, as inputs for land use and land cover classification. The training data were collected based on the manual interpretation of the original Sentinel–2 data and DigitalGlobe's WorldView-4 high-resolution imagery and was kept the same for all the three classifiers to avoid the optimistic bias in classification. The training sample size was kept below 1000 pixels per class to evaluate the influence of the training sample size, as well as the performance of classification algorithms. Training data for each land use and land cover class were collected as a group of pixels. The input data and corresponding ground truth data (training sample) were used to train the classifiers. The classifiers learn the complex relationships between the input and ground truth data (training sample). To determine the accuracy of each classification and class, thematic accuracy assessment was performed. For this purpose, firstly a reference data set including a total of 100 points was created. Stratified random sampling was used with 100 points to obtain the ground truth data from the manual interpretation of the original 10 m resolution Sentinel–2 data (Band 2, 3 and 4) and DigitalGlobe's WorldView-4 data (Product Id: 1ba34688-3ee0-41e4-9187-de68fdb075df-inv) acquired on 25-10-2018 at 5:30 am with 31 cm resolution. The results of the classifications were not post-processed (e.g., filtered). The classification maps were evaluated in terms of their overall accuracy (OA), producer's accuracy (PA), user's accuracy (UA) and the Kappa index of agreement (k) or Kappa coefficient and a Confusion matrix was created.

3. **Objective:** To perform Morphometrical analysis of Vishwamitri watershed and prioritization of sub-watersheds for assessing the flood influencing characteristics of the five sub-watersheds of the Vishwamitri watershed.

Five basic morphometric parameters such as: area, basin length, perimeter, stream order and stream length, were directly calculated from the Cartosat-1 30m DEM by using Arc-hydro tools. The derived parameters were calculated using formulas given in below table 4. The prioritization of the sub-watersheds was done assigning ranks to individual parameter based on their flood influencing characteristics.

Table 4: linear, aerial, and relief morphometric parameters

Morphometric parameters	Formulae	Units
Basin length ( $L_b$ )	Maximum length of the watershed measured parallel to the main drainage line	Km
Area (A)	Area of watershed	Km <sup>2</sup>
Perimeter (P)	Length of the watershed boundary	Km
Stream order ( $S_u$ )	Hierarchical rank (Strahler Scheme)	Dimensionless
Stream Length ( $L_u$ )	$L_u = L_1 + L_2 + \dots + L_n$ ; Length of the stream	Km
Stream number ( $N_u$ )	$N_u = N_1 + N_2 + \dots + N_n$	Dimensionless
Bifurcation Ratio ( $R_b$ )	$R_b = N_u / N_{u+1}$ ; $R_b$ was computed as the ratio between the number of streams of any given order to the number of streams in the next higher order	Dimensionless
Mean Bifurcation Ratio (Rbm)	$R_{bm}$ = Average of bifurcation ratios of all orders	Dimensionless
Drainage density ( $D_d$ ):	$D_d = \sum L_u / A$ ; The ratio between the total stream length of all orders to the area of the basin	(km/km <sup>2</sup> )

Drainage frequency ( $F_s$ ):	$F_s = \Sigma Nu/A$ ; The ratio between total number of streams and area of the basin	(no./km <sup>2</sup> )
Drainage Texture ( $R_t$ ):	$T = \Sigma Nu/P$ ; Where, $R_t$ = Drainage texture; $\Sigma Nu$ = Total no. of streams of all orders; $P$ = Perimeter (km)	(no./km)
Relief ratio ( $R_r$ ):	$R_r = H/L$ ; Where, $R_r$ = Relief ratio; $H$ = Total relief of the basin in Kilometre; $L_b$ = Basin length	Dimensionless
Ruggedness number ( $R_n$ ):	$R_n = B_h \times D_d$ ; Where, $B_h$ = Basin relief; $D_d$ = Drainage density	Dimensionless
Form factor ( $F_f$ ):	$F_f = A/L_b^2$ ; The ratio of the basin area to the square of the basin length	Dimensionless
Circularity ratio ( $R_c$ ):	$R_c = 4 * \pi * A/p^2$ ; Where, $R_c$ = Circularity ratio; $\pi$ = "Pi" value that is 3.14; $A$ = Area of the basin (km <sup>2</sup> ); $P$ = Perimeter (km)	Dimensionless
Elongation ratio ( $R_e$ ):	$R_e = (2/L_b) * \text{sqrt}(A/\pi)$ ; Where, $R_e$ = Elongation ratio $A$ = Area of the basin (km <sup>2</sup> ); $\pi$ = "Pi" value that is 3.14; $L_b$ = Basin length	Dimensionless
Length of Overland Flow ( $L_g$ ):	$L_g = 1/(D_d * 2)$ ; Where, $L_g$ = Length of overland flow; $D_d$ = Drainage density	Km

4. **Objective:** To identify potential runoff storage zones based on the various physical characteristics of the Vishwamitri watershed using a GIS-based conceptual framework that combines through analytic hierarchy process using multi criteria decision-making method. To find the potential runoff storage zones, workflow was divided into 4 steps (Figure 5). Firstly, the rainfall analysis was carried out using SPI and annual rainfall. Secondly, processing of spatial data and creation of spatial data layers. Thirdly, criteria weights were determined using AHP. Lastly, executing weighted overlay process (WOP) within GIS.

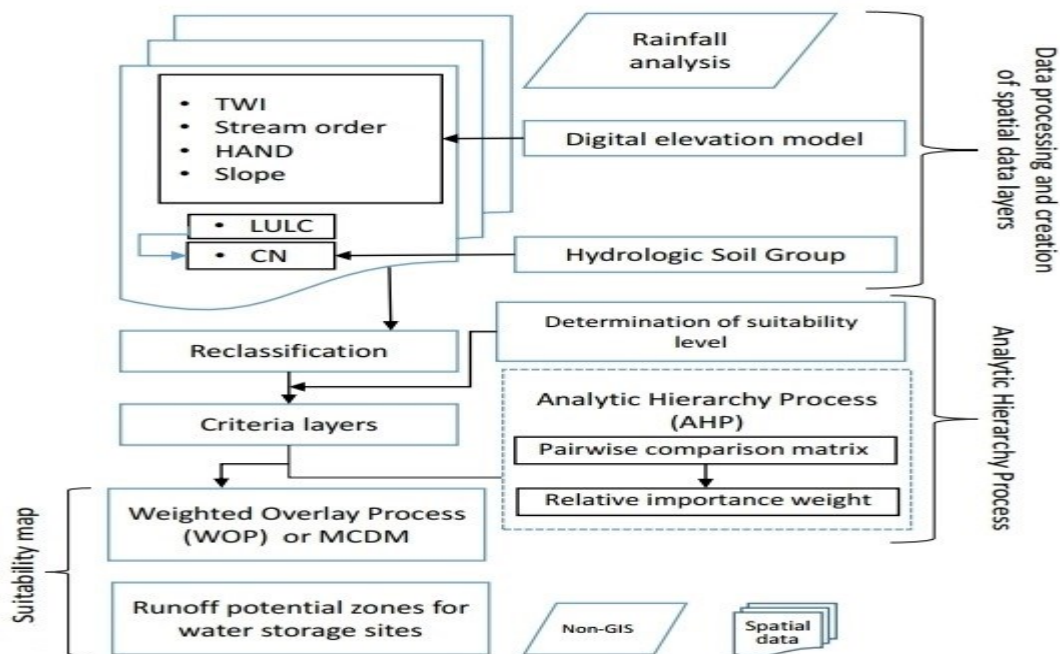


Figure 6: Multi criteria decision making (MCDM) technique workflow using AHP for identification of potential runoff storage zones for water storage.

Processing and creation of spatial data layers:

**Topographic Wetness Index (TWI):** TWI is widely used topographically based soil wetness model that identifies wet areas. It is based on the assumption that local topography controls the movement of water in sloped terrain which quantifies the effect of the local topography on runoff generation. The index is represented as the natural logarithm of the ratio of upslope flow accumulation area and slope at the cell.

$$TWI = \ln(\text{flow accumulation} + 1) / (\tan(((\text{slope in degrees})3.14)/180))$$

**Generation of slope map using Topography Position Index (TPI):** The TPI is the difference of a cell elevation in a digital elevation model from the mean elevation ( $\bar{X}$ ) of a user specified neighborhood surrounding. Local mean elevation is subtracted from the elevation value at centre of the local window. The range of TPI depends not only on elevation differences but also on the adopted local window. Large local window values mainly reveal major landscape units, while smaller values highlight smaller features, such as minor valleys and ridges.

$$TPI_i = X_0 - \bar{X}$$

$$\bar{X} = \frac{\sum_{i=1}^n X_i}{n}$$

Where,

$X_0$	=	elevation at the central point
$\bar{X}$	=	average elevation around the central point within the local window
$n$	=	total number of surrounding points employed in the evaluation

**Height above nearest drainage (HAND):** HAND allows for the calculation of the elevation of each point in the catchment above the nearest stream it drains to, following the flow direction. HAND raster was prepared for the 4<sup>th</sup> and 5<sup>th</sup> order streams of Vishwamitri watershed as they are highly susceptible to flooding.

**Determining criteria weights using AHP:** Analytic Hierarchy Process (AHP) is one of Multi Criteria Decision Making (MCDM) method, it has been widely applied to solve decision-making problems related to water resources. The approach combines mathematics and psychology in dealing with complex decision and in turn converts it into a simpler system of hierarchy. The determination of the relative importance weight of each criterion (Slope, TWI, LULC, Curve Number, Stream Order and HAND) for potential runoff storage zones is calculated by using the pair-wise comparison matrix method. The number of comparison can be determined using:

$$\text{Number of comparison} = \frac{n(n-1)}{2}$$

where, n = number of criterion

The resulting pair-wise comparison matrix is used to obtain the Eigen value of each criterion, which represents its relative importance weight.

- Objective:** To develop an approach for operational flood extent mapping using Synthetic Aperture Radar (SAR) and preparation of flood inundation map for data scarce region using 2D flow modelling using rain on grid model.

**Pre-processing:** A schematic of the Sentinel-1-based processing chain is outlined in [Figure 6](#). The downloaded Sentinel-1 Level-1 GRD data acquired in IW with VV and VH polarizations were loaded onto Sentinel Application Platform (SNAP). SNAP offers a wide range of tools and features for Sentinel-1 imagery processing and analysis. Due to the large swath width of the Sentinel-1 data, the image was first divided into a subset for the study sites to reduce the processing time. Multi-

looking was then performed to reduce the standard deviation of the noise. The number of Azimuth looks and the number range of looks (2×2) with mean GR mean pixel of 20 meters were applied to a 1 m × 5 m (single look). The multi-looked data were then calibrated to transform the pixel values from the digital values recorded by the sensor into backscatter coefficient values or Sigma<sub>0</sub> (σ<sub>0</sub>). This was achieved using the following equation:

$$\sigma_0 = \frac{|DN_i|^2}{A_i^2}$$

$DN_i$  = pixel's digital number

$A_i$  = absolute calibration constant

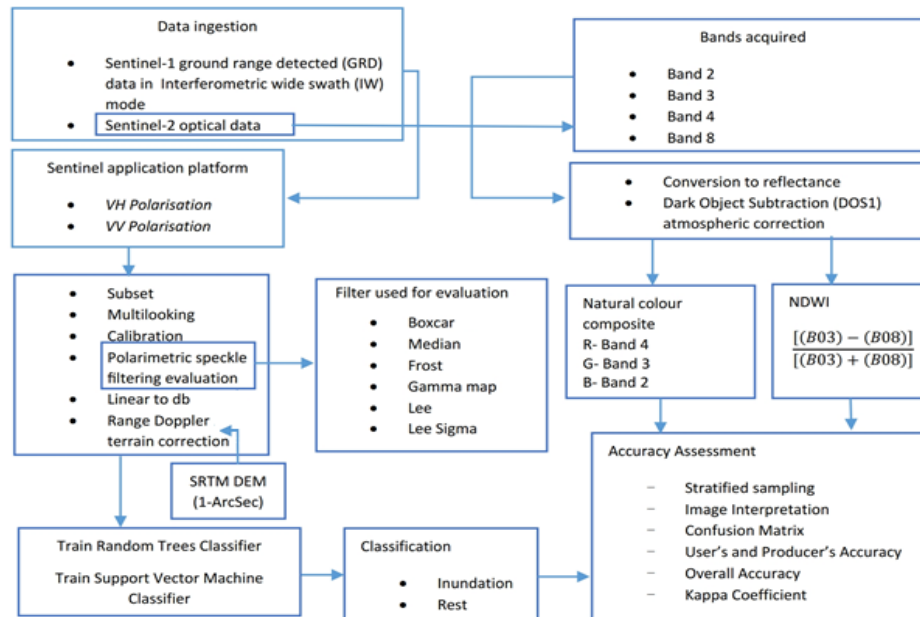


Figure 7: Methodology of SAR workflow

**Application of filters:** Speckles inherently corrupt all radar images, degrading the image quality, and making it more difficult to interpret features. Thus, it is often necessary to enhance the image by filtering speckles before data can be used in different applications. All of the filters, namely, Boxcar, Median, Frost, Gamma map, Lee and Lee sigma with 3×3 and 5×5 kernel size, used in the study were available in SNAP and applied using default system parameters.

#### Machine learning algorithms for classification

The terrain corrected images were classified using the random forest and support vector machine algorithms as a next step. For both the classifiers, the same number of training samples was used. The training inundated pixels covered 5.2 Km<sup>2</sup> and the rest of the training pixels covered 3.1 Km<sup>2</sup> of the study area Kerala. Similarly, for the study area Assam, the training inundated pixels covered 11 Km<sup>2</sup> and the rest of the training pixels covered 54 Km<sup>2</sup>.

During the southwest monsoon season, it is nearly impossible to obtain 100% cloud-free data, however, a small extent of the cloud-free data can be used for validation. The normalized difference water index (NDWI) is defined for Sentinel–2 data as ((B03) – (B08))/(B03) + (B08)), where B03 is a green band and B08 is the near-infrared band. When NDWI is applied over a multispectral image, the water feature has positive values, while soil and terrestrial vegetation features have zero or negative values. This is because NIR is absorbed strongly by water but reflected strongly by terrestrial vegetation and dry soil, while in a green light, water has high reflectance than terrestrial

vegetation and soil. Therefore, the NDWI was applied to extract water from the optical data. A cloud-free part of satellite optical image was collected by Sentinel-2 at 05:06:49 on 22 August 2018, 28 h after the Sentinel-1 pass over the study area Kerala. Similarly, a cloud-free part of satellite optical image was collected by Sentinel-2 at 04:27:09 on 15 July 2019, 40 h after the Sentinel-1 pass over the study area Assam. Sentinel-2 data were converted to reflectance and dark object subtraction atmospheric correction (DOS1) was applied. The corrected Sentinel-2 image was used to validate the extent of the flood. The normalized difference water index (NDWI), established earlier to extract the water from the optical data, was calculated as:

$$NDWI = \frac{\rho_{Green} - \rho_{NIR}}{\rho_{Green} + \rho_{NIR}}$$

6. **Objective:** To quantify the effects of urban land forms on land surface temperature and modeling the spatial variation using machine learning. The models can help to predict land surface temperature under temporary cloud cover spots, which are present in the data at the time of the acquisition, using neighboring biophysical (cloud-free) independent variables relationship with land surface temperature.

The methodology used in the study is presented in Figure 7. The workflow was divided into six steps. First, the satellite data were subjected to image pre-processing and atmospheric correction to remove the atmospheric effect and sensor defects for land surface temperature retrieval. Second, the classification of the heat zones. Third, derivation of land use/land cover and accuracy assessment. Fourth, derivation of NDVI, NDWI and DBSI. Fifth, calculate Land Contribution Index (LCI) and Landscape index (LI). Sixth, model fitting and evaluation. Each step has been discussed in detail in the following sections.

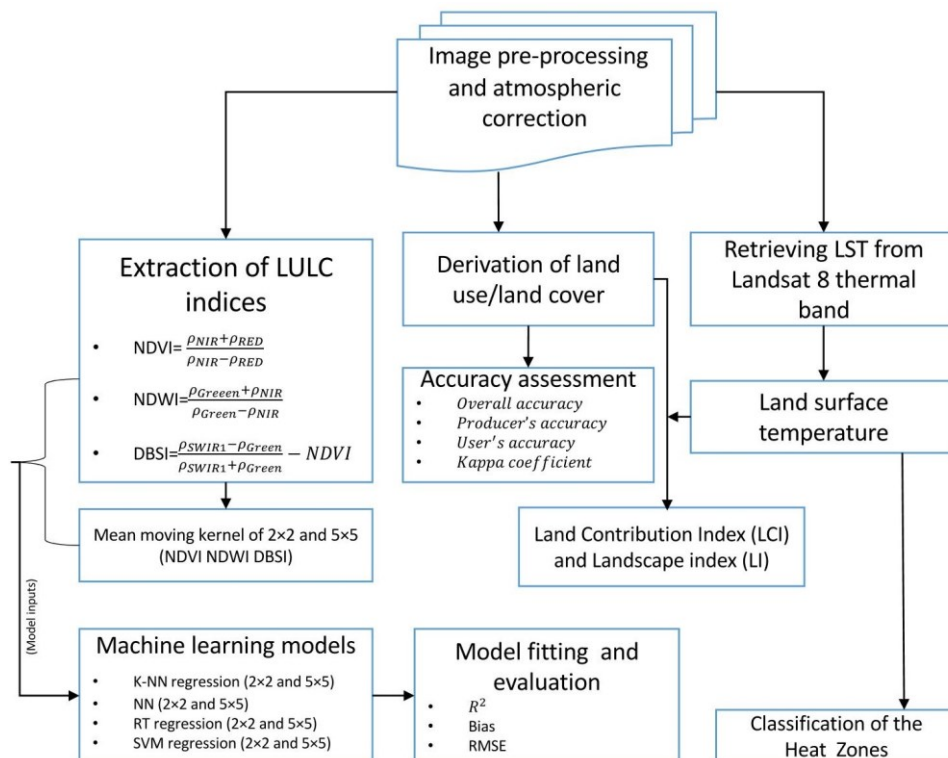


Figure 8: Flowchart of the methodology for LST.

**Retrieval of Land Surface Temperature:** The two cloud-free Landsat 8 level 1T data products (ID: LC08\_L1TP\_148045\_20180423\_20180502\_01 and LC08\_L1TP\_148045\_20181101\_20181115\_01) were acquired from the United States Geological Survey (USGS) Earth Resources Observation and Science (EROS) Center. Landsat 8 level 1T data products are orthorectified images of the thermal infrared radiance-at-the-sensor. The land surface temperature data in summer and winter were derived from the thermal infrared sensor (TIRS) Band 10 (10.30–11.30  $\mu\text{m}$ ) at a spatial resolution of 100 m, resampled to 30 m using a cubic convolution resampling method, which were respectively acquired at 11:02:51.19 AM local time for both summer (23 April) and winter (1 November) in 2018. TIRS data were converted to top of atmospheric spectral radiance using the radiance rescaling factors provided in the metadata file using Equation:

$$L_{\lambda} = M_L \times Q_{cal} + A_L - O_i$$

- $L_{\lambda}$  = at-sensor spectral radiance ( $\text{W}/(\text{m}^2 \cdot \text{sr} \cdot \mu\text{m})$ )
- $M_L$  = multiplicative rescaling factor
- $Q_{cal}$  = quantized and calibrated standard product Digital Numbers (DNs)
- $A_L$  = additive rescaling factor
- $O_i$  = correction for Band 10

At-sensor spectral radiance of Band 10 was converted into at-sensor brightness temperature ( $T_B$ ) using the thermal constants provided in the metadata file (Table 5). To obtain the results in Celsius from Kelvin, the radiant temperature is adjusted by adding the absolute zero ( $-273.15^{\circ}\text{C}$ ).

$$T_B = \frac{K_2}{\ln \left[ \left( \frac{K_1}{L_{\lambda}} \right) + 1 \right]} - 273.15$$

Table 5: Metadata of the satellite data

Thermal constant, Band 10	K1	774.8853
	K2	1321.0789
Rescaling factor, Band 10	$M_L$	3.3420E-04
	$A_L$	0.1
Correction, Band 10	$O_i$	0.29

Emissivity-corrected LST was based on Fractional Vegetation Cover ( $P_V$ ) and was calculated using Equation:

$$P_V = \left[ \frac{NDVI - NDVI_{min}}{NDVI_{max} - NDVI_{min}} \right]^2$$

$$LST(^{\circ}\text{C}) = \frac{T_B}{1 + \left( \lambda \times \frac{T_B}{\rho} \right) \ln \varepsilon}$$

Where  $T_B$  is the Landsat-8 Band 10 at-sensor brightness temperature;  $\lambda$  is the wavelength of emitted radiance;  $\rho = \left( \frac{hc}{\sigma} \right) = 1.438 \times 10^{-2} \text{ m K}$  (where,  $\sigma$  is the Boltzmann constant ( $1.38 \times 10^{-23} \text{ J/K}$ );  $h$  is Planck's constant ( $6.626 \times 10^{-34} \text{ Js}$ );  $c$  is the velocity of light ( $2.998 \times 10^8 \text{ m/s}$ ); Emissivity ( $\varepsilon$ ) is calculated using Equation (5) :

$$\varepsilon = m P_V + n$$

$$m = \varepsilon_v - \varepsilon_s - (1 - \varepsilon_s) F \varepsilon_v$$

$$n = \varepsilon_s + (1 - \varepsilon_s)F\varepsilon_v$$

$\varepsilon_s$  and  $\varepsilon_v$  are soil and vegetation emissivity, respectively. The  $\varepsilon_s$  and  $\varepsilon_v$  values obtained for band 10 from the ASTER spectral library are 0.97 and 0.99, respectively. The final expression for land surface emissivity is given by Equation

$$\varepsilon = 0.004 P_V + 0.986$$

**Model fitting and evaluation:** The land surface temperature is estimated and explored by four machine learning and statistical models, including K-NN regression, NN, RT regression and SVM regression. We hypothesized that the explanatory variables (NDVI, NDWI and DBSI) influence the spatial changes of land surface temperature significantly in the study area. Meanwhile, all these three explanatory variables were also calculated at the 2 levels of the observation grids unit. Since, apart from sunlight, the land surface temperature is also affected by the surrounding land cover. A mean moving kernel of 2×2 and 5×5 were used as the observation grids unit for each explanatory variable. A mean moving kernel calculates for each input pixel location a mean of the values within a specified neighborhood around it. To develop the models, the original dataset was divided into three parts, 70% of the whole dataset (124,578 pixels) were used as the training dataset, 20% (35,568 pixels) data were used as the testing dataset, and 10% (18,056 pixels) data were used as validation dataset. Three measures, namely, coefficient of determination (R<sup>2</sup>; Equation (24)), bias (Equation (25)), and root-mean-square error (RMSE; Equation (26)) were used to evaluate the performance of the models for training, testing and validation. In the equation below, R<sup>2</sup> is the coefficient of determination between the original and predicted land surface temperatures. A high R<sup>2</sup> indicates a satisfactory prediction.

$$R^2 = 1 - \frac{\sum(LST_p - LST_a)^2}{\sum(LST_p - \overline{LST}_a)^2}$$

Where  $LST_p$  is the predicted land surface temperature,  $LST_a$  is the actual land surface temperature and  $\overline{LST}_a$  is the average of actual land surface temperature.

Bias and RMSE were used to test the errors between the predicted land surface temperature and the actual land surface temperature. The calculation formulas for bias and RMSE are as follows:

$$\text{Bias} = \frac{\sum_{i=1}^n (LST_p - LST_a)}{n}$$

$$\text{RMSE} = \sqrt{\frac{1}{n} \sum_{i=1}^n (LST_p - LST_a)^2}$$

Where n represents the number of pixels of the data.

## 5. Results and analysis

### 5.1 General

This chapter briefly shows the results obtained for the individual objective. The chapter is divided into six sections, each section contains the obtained for the specific objective.

### 5.2 Results and analysis

1. **Objective:** To demonstrate a comparative assessment of discrepancy in the hydrological behaviour of the DEMs in terms of terrain representation at the catchment scale.

**Statistical Comparison:** In order to provide evidence of the statistical significance of the results, the amount of data (274476 pixels) from all three DEMs was used. The absolute difference between the mean value of SRTM and Cartosat is 1.55 m and between the mean value of ASTER and Cartosat was found to be 5.38 m. The standard deviation showed that the Cartosat dataset was less spread out as compared to the other two datasets, which was also confirmed by the difference between the upper and lower quartiles (interquartile range). For the samples, the positive value of skewness showed that the distributions of the data were positively skewed or skewed right, i.e., the right tail of the distribution was longer as compared to the left tail of the distribution. For ASTER, the value of kurtosis was 0.02, which showed that the distribution is leptokurtic, i.e., its tails are longer and fatter. For SRTM and Cartosat, the negative value of kurtosis showed that the distribution is platykurtic, i.e., its tails are shorter and thinner. The normal quantile-quantile (Q–Q) plot and the detrended normal Q–Q plot were also drawn to support or refute the claim of normality. The quantile-quantile plot is shown in [Figure 8 \(d\)–\(f\)](#), which compares the observed quantiles of the data with those of the normally distributed data. The observed quantiles of the data are depicted as circles, whereas the quantiles of data that we would expect to see if the data were normally distributed are depicted as a solid line. The data are approximately normally distributed, if the points are on or close to the line. Similarly, the sample data are not normally distributed if the points are not clustered on the 45° line or they, in fact, follow a curve. Moreover, the detrended normal Q–Q plot provides the same information as the normal Q–Q plot, but in a different way. In the detrended plot, the horizontal line at the origin represents the quantiles if the data were normally distributed, whereas the dots represent the magnitude and direction of deviation in the observed quantiles. Each dot is calculated by subtracting the expected quantile from the observed quantile. [Figure 8 \(g\)–\(i\)](#) also shows the detrended normal Q–Q plot. In order to assess the level of correlation between the DEMs, the correlation scatter-plots were drawn as shown in [Figure 9 \(a\)](#) and [\(b\)](#). It was difficult to create a scatter plot from each pixel in a DEM as each DEM contains over a million pixels. However, a total of 274,476 pixels were used for the analysis. As shown in [Table 6](#), the correlation coefficient of 0.83, 0.94, and 0.85 was obtained by Pearson's correlation analysis between the ASTER and Cartosat, SRTM and Cartosat, and ASTER and SRTM, respectively (correlation is found to be significant at the level of 0.01). For instance, the correlation value of 0.94 indicates a strong positive linear correlation between SRTM and Cartosat. Similarly, the simple linear regression analysis is demonstrated by means of scatter-plots. In this case, the analysis of the determination coefficients ( $R^2$ ) of the regression line shows that the Cartosat DEM is considered adequate for describing the ASTER DEM in 68.9% and the SRTM DEM in 87.9%. Considering Cartosat as the reference DEM, the RMSE calculated was used for evaluating the vertical accuracy of the ASTER DEM and the SRTM DEM. For ASTER the RMSE was calculated to be 7.21 m, whereas for SRTM, the RMSE was calculated to be 3.24 m.

**Slope Gradients Classes:** Moreover, six classes of slope were established for a better understanding of terrain. As shown in [Table 7](#), the slope values were classified according to the Brazilian Agricultural Research Corporation standards. According to the SRTM and Cartosat, the result showed that the maximum area in watershed belongs to flat relief with a declivity value (in %) between 0 and 2.99. According to the ASTER, however, the maximum area belongs to smooth relief with a declivity value (in %) between 3 and 7.99.

**Stream Comparison:** When the delineated streams are overlaid over high-resolution imagery, the Cartosat-generated network is much closer to the actual river network followed by the SRTM-derived drainage network as shown in [Figure 10](#). It has been observed that the drainage network delineated by ASTER is highly misleading. Moreover, sinks around the actual river have considerably contributed to the deviation of ASTER DEM- and SRTM DEM-derived streams.

**Watershed Comparison:** The area enclosed by the watershed generated by SRTM and ASTER is comparatively much larger than that generated by Cartosat as shown in [Figures 11](#) and [12](#). The area of the watershed delineated by Cartosat is 1285.4 km<sup>2</sup>, whereas the area of the watershed delineated by ASTER is 1624.8 km<sup>2</sup> (26.40% larger). Moreover, the SRTM-based watershed area is 2026.3 km<sup>2</sup>, which is 56.63% larger than the Cartosat boundary. The perimeter of the watershed delineated by Cartosat is 209.9 km, whereas the perimeter of the watershed delineated by ASTER is 315.4 km (50.26% larger). Moreover, the SRTM-based watershed perimeter is 294.9 km, which is 40.5% larger than the Cartosat watershed perimeter.

**Ridge Line Inspection:** The cartographic relief depiction shows the shape of the terrain in a realistic fashion and also demonstrates the three-dimensional surface that is illuminated from a point light source. Moreover, the watersheds overlaid over the relief map and satellite imagery show that the watersheds delineated by ASTER and SRTM could not follow the ridgeline and hence they have encompassed the Dhadhar river in them. As shown in [Figure 13](#), the highlighted yellow circles show the locations where the ASTER watershed and the SRTM watershed encompass the Dhadhar river. Clearly, it can also be observed that the Cartosat-derived boundary follows the actual ridgeline. In the flow-direction process, a depressionless DEM is considered to be the desired input. An erroneous flow-direction raster may be resulted in the presence of sinks. Moreover, there may be legitimate sinks in the data in some of the cases. By taking into consideration the flow networks associated with each type of elevation data, the cause of the difference in the watershed boundaries can be found. It has been observed that the flow networks generated from the ASTER- and SRTM-based DEM had several errors. Map algebra was used to find where the Fill tool had filled the sinks in order to determine the cause of the errors in the streams network. As shown in [Figure 14](#), it was found that the errors in the stream network occurred where filling greater than 3 m in ASTER and 5 m in SRTM along the actual river had occurred. Moreover, in the deviation of ASTER DEM- and SRTM DEM-derived streams from the actual stream, a large number of sinks around the actual river have considerably contributed. Such error indicates that there were probably residual and artifactual anomalies that most certainly degraded the overall accuracy of ASTER and SRTM DEMs. As a result of underestimating the elevation at certain points, pit, and depressions are considered false in the Fill method as mentioned above. Therefore, the depressions are filled, and thus raising the elevation until it reaches the lower neighbor. As a result, the larger the number of continuously affected pixels, the more the result of the flow-direction assignment is affected. [Figure 14 \(a\)–\(c\)](#) shows that ASTER data contain a large number of depressions or pits followed by the SRTM data, whereas the Cartosat data contain the least amount of depressions or pits.

Table 6: Correlation coefficients for ASTER, SRTM, and Cartosat derived elevation

	ASTER	SRTM	Cartosat
ASTER	1.00		
SRTM	0.85	1.00	
Cartosat	0.83	0.94	1.00

Table 7: Slope classes

Declivity (%)	Relief classes	ASTER AREA(Km2)	Cartosat AREA(Km2)	SRTM AREA(Km2)
0 – 2.99	Flat	252.58	687.16	638.32
3 – 7.99	Smooth	677.55	481.20	600.01
8 – 19.99	Corrugated	335.48	89.73	38.94
20 – 44.99	Heavily Corrugated	16.07	20.05	5.15
45 – 74.99	Mountainous	2.18	4.78	1.56
< 75	Steepest	1.39	2.34	1.26

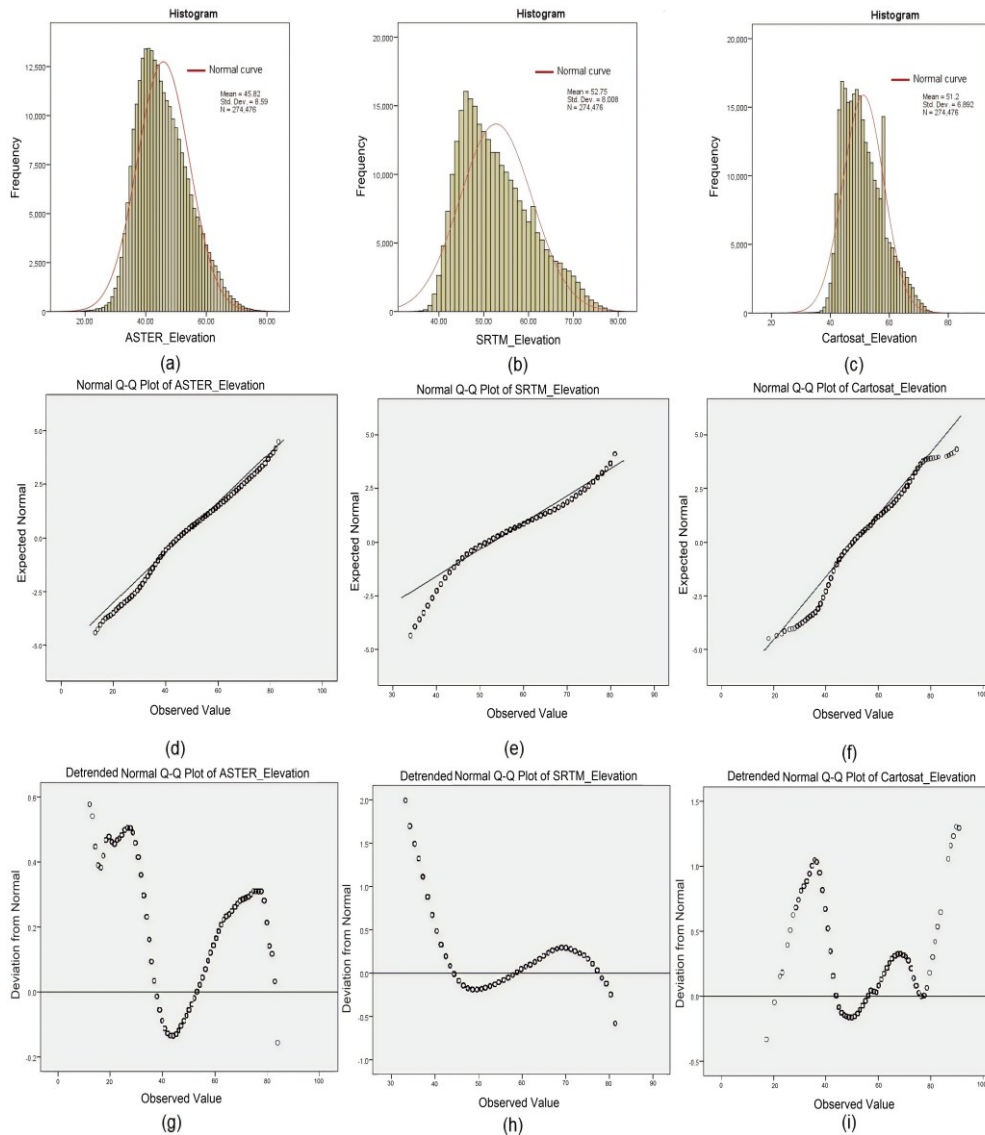


Figure 9:(a) Histogram of ASTER data (b) Histogram of SRTM data (c) histogram of Cartosat data (d) Quantile-Quantile Plot of ASTER data (e) Quantile-Quantile Plot of SRTM data (f) Quantile-Quantile Plot of Cartosat data (g) Detrended Normal Q-Q Plot of ASTER data (h) Detrended Normal Q-Q Plot of SRTM data (i) Detrended Normal Q-Q Plot of Cartosat data

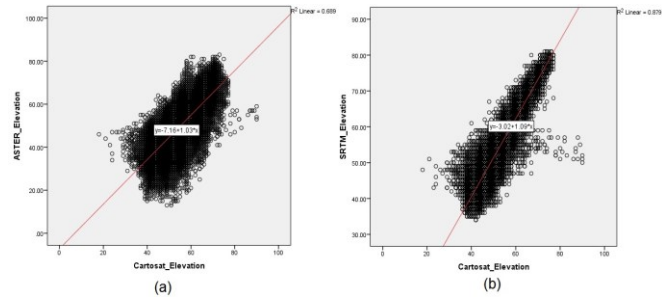


Figure 10: (a) Scatterplot showing linear regression of ASTER derived elevation vs Cartosat derived elevation (b) Scatterplot showing linear regression of SRTM derived elevation vs Cartosat derived elevation

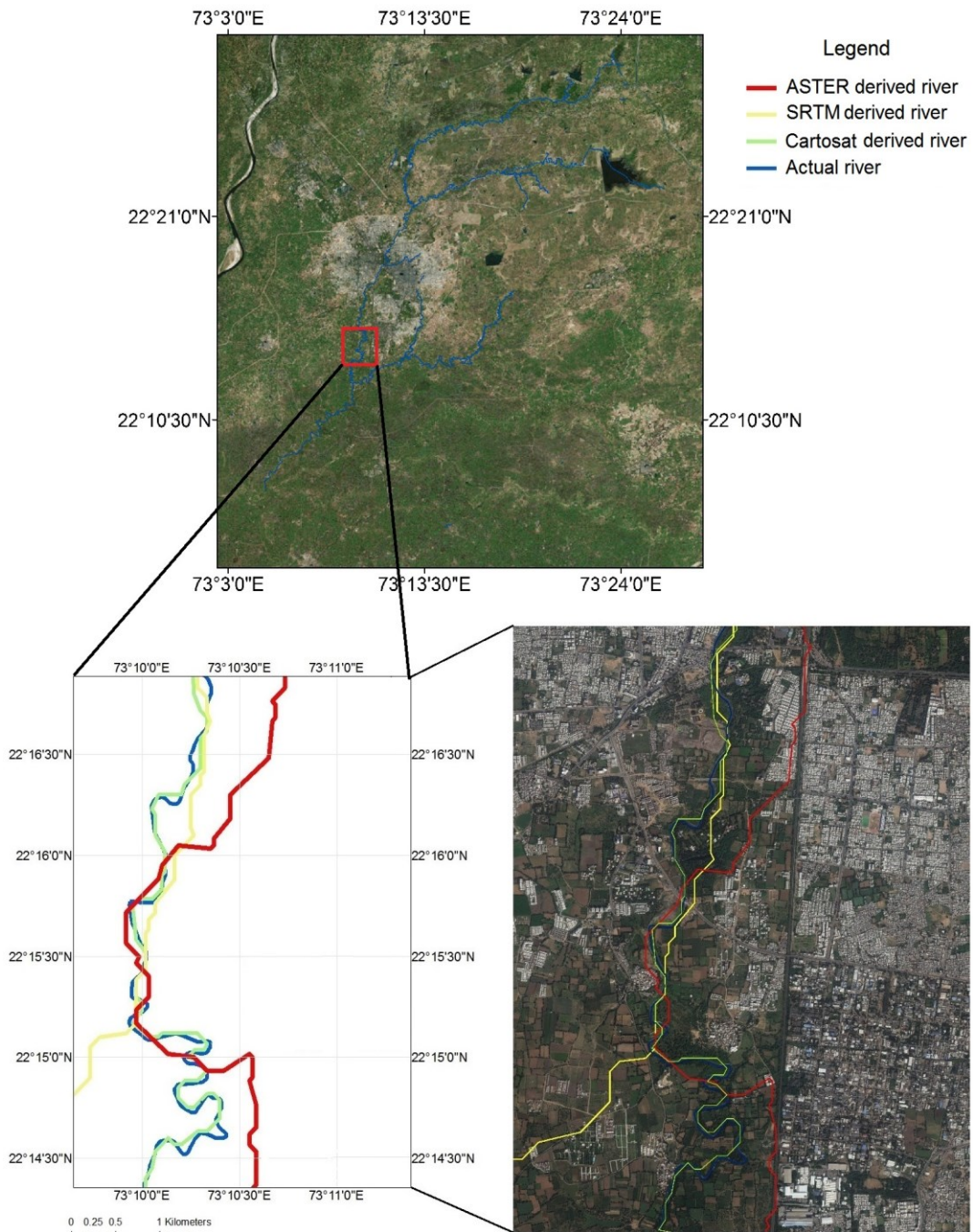


Figure 11: Map showing ASTER, SRTM, and Cartosat derived river deviation from the actual river

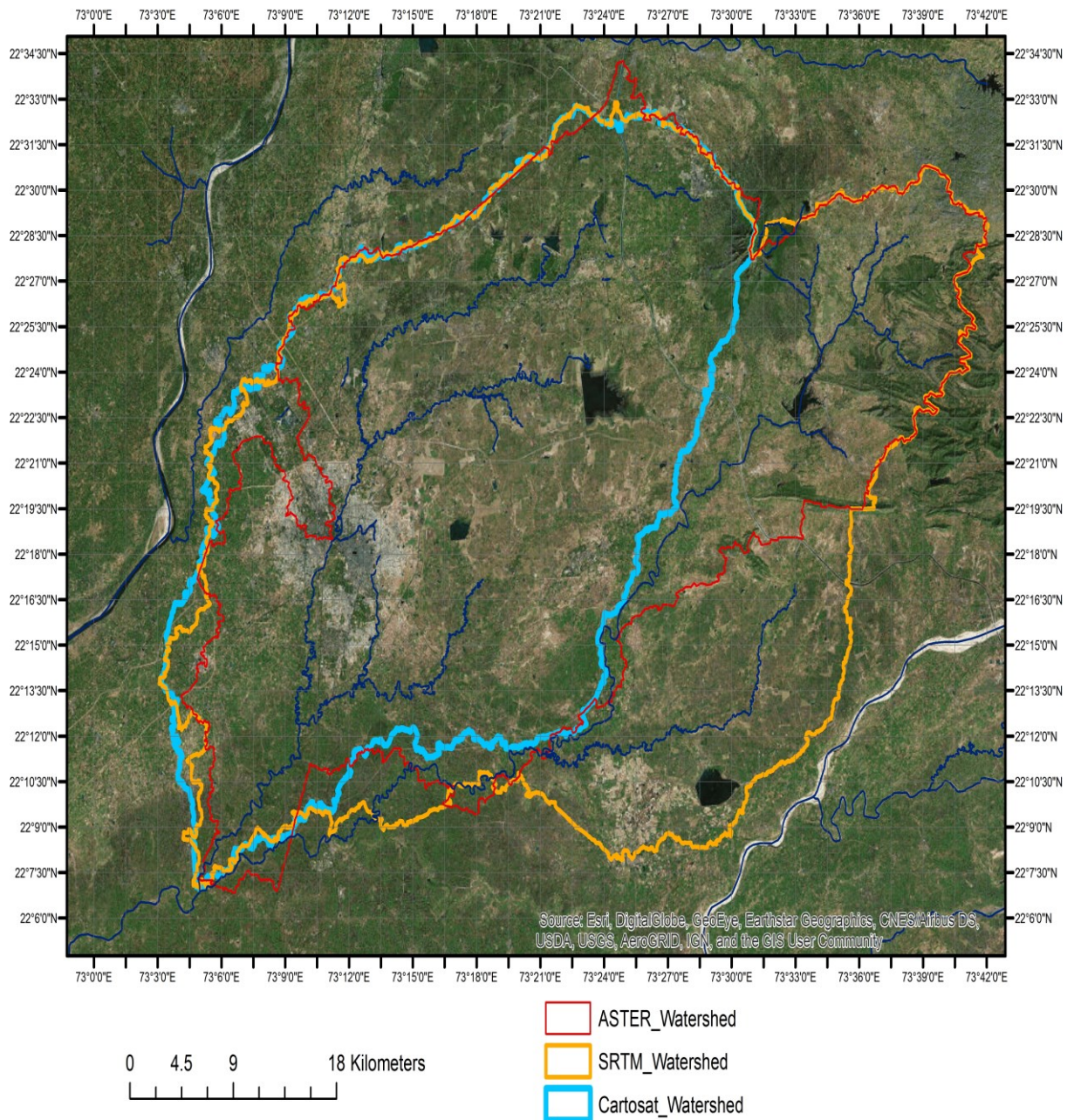


Figure 12: Delineated watershed boundaries from ASTER, SRTM and Cartosat data

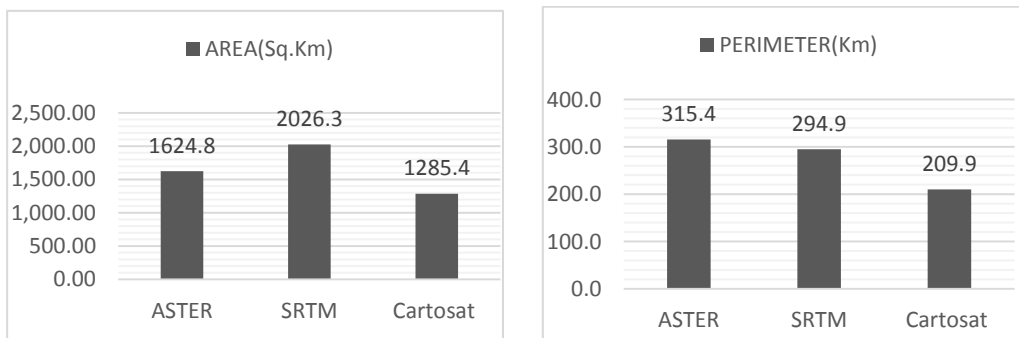


Figure 13: Area and perimeter of delineated watersheds

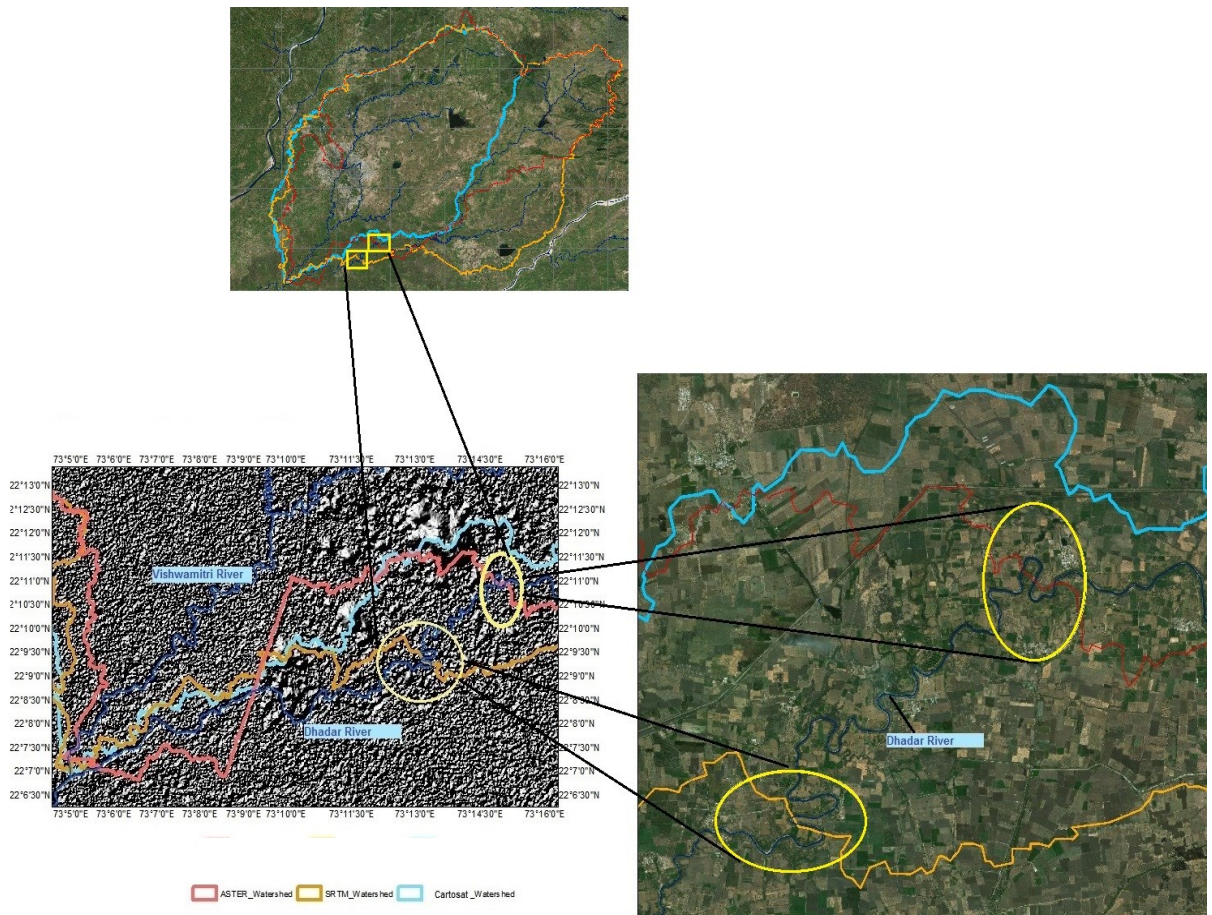


Figure 14: Visual Inspection of Watersheds derived from ASTER, SRTM, and Cartosat over the Shaded Relief map and Satellite imagery

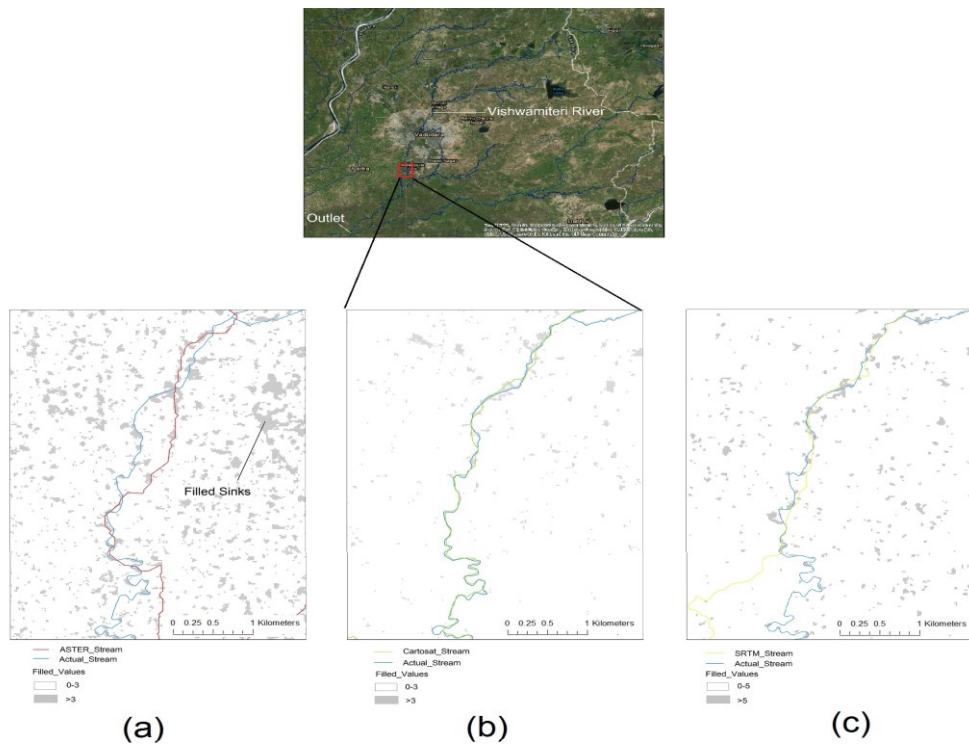


Figure 15: (a) Filled sinks in ASTER (b) Filled sinks in Cartosat (c) Filled sinks in SRTM

2. **Objective:** To develop an approach to analyze Sentinel–2 satellite images using traditional and principal component analysis based approaches to create land use and land cover map, which is a prerequisite for developing the curve number.

Principal component analysis was used for data compression of Sentinel-2 multispectral data to statistically maximise the amount of information from the original data (bands) to a smaller number of components, called principal components. The first few principal components possess most of the variability of the data. The first principal component band derived from the first eigenvector had the maximum amount of the total variance of the Sentinel–2 data set containing bands 2–8, 8A, 11 and 12. The first three principal component bands accounted for 97.92% of eigenvalues. The variances percentage of the remaining principal component bands decreased in order of the corresponding eigenvalues. The variance of the PCA bands 4 to 10 is small and mostly had noises; thus the bands were removed from the analysis. A loading plot shows how strongly each band influences a principal component. It ranges from -1 to 1. Loadings close to -1 or 1 indicate that the band strongly influences the component. Loadings close to 0 indicate that the band has a weak influence on the component. [Figure 15](#) shows the loading plot of the bands. It can be seen that bands 6-8A have large positive loadings on component 1. While, bands 2-5 and 11-12 have large positive loadings on component 2. Factor loading shows how much each band has contributed to the factor. Bands 6-8A (Vegetation Red Edge and near infrared bands are highly correlated, ([Table 8](#)) loaded highly in the first principal component, bands 2-5 and 11-12 (highly correlated), loaded highly (positively) in principal component 2 and Band 2-5 marginally loaded onto principal component 3. Principal component 4-10 can be termed as noise components since no factor loading is prominent. It has been observed that deciduous plants have a sharp order-of-magnitude increase in leaf reflectance between approximately 700 to 750 nm wavelength and healthy vegetation reflects highly in near infrared band. Principal component 1 can be called as healthy vegetation component as it has the highest factor loading of 0.99 from band 7 and band 8A. However, principal component 2 and principal component 3 can't be generalised as loading is scattered across the spectrum. PCA transformed the correlated Sentinel–2 dataset into a substantially smaller set of uncorrelated variables representing most of the information present in the original dataset. [Figure 16 \(a–c\)](#) shows the PCA bands derived from the Sentinel–2 data and [Figure 16 \(d–f\)](#) show the frequency distribution of corresponding principal component bands. The total range (maximum value - minimum value) of PCA band 3 is greater than the PCA band 1 and PCA band 2. However, most of the pixels fall in a small range around the mean of 6486.13, which shows information loss in PCA band 3. The frequency distribution reveal that the variance of the first principal component is the highest, followed by the second and then by the third. The calculated values of variance for PCA bands 1, 2 and 3 were 395879.55, 284229.30, and 45254.05, respectively. The image produced from PCA band 1 data resembles original image and it contains most of the pertinent information inherent to the scene due to high variance. Adjacent bands in a multispectral remotely sensed image are often highly correlated and often convey almost the same information about the object. A high correlation meaning thereby that the bands are not statistically independent. A low degree of correlation was observed among the PCA bands 1, 2, and 3. The correlation values between PCA bands 1 and 2, 1 and 3, and 3 and 2 were 0.01, -0.01, and 0.25, respectively. Non-structured appearance of the scatter plots and low correlation values confirm that there is no relationship among the PCA bands. High Correlation in stack 1 shows ([Table 8](#)) that there is redundancy of information and if this redundancy can be reduced, then information can be compressed. The correlation between the bands which exist in the original data has

disappeared in the principal components. So, the PCA was able to reduce correlation significantly. The principal components are new uncorrelated bands obtained by linear combination of original data, retaining as maximum as possible the information present on the original data. Prediction performances of the three classifier algorithms, MLE, RF, and SVM, were evaluated to reveal the efficiency of two different land use and land cover classification approaches with training data of less than 1000 pixels per class. Training data for each land use and land cover class were collected as a group of pixels. Stratified random sampling was used to obtain the testing data. The classification performed on the original Sentinel–2 bands led to an unacceptable outcome with a classification overall accuracy of 22% for MLE. However, 60% and 64% classification overall accuracy was achieved with RF and SVM classifiers, respectively. The classification results of RF and SVM are acceptable as the training data were limited to less than 1000 pixel per class. In the PCA-based classification approach, the same training polygons were used to avoid the optimistic bias in classification. PCA based approach significantly improved the overall classification accuracy of all the three classifiers. The overall classification accuracy varied considerably among the classifiers. The overall classification accuracy of MLE classifier was increased from 22% to 41% (19% increase) in the PCA based approach. The overall accuracy RF classifier was increased by 10% reaching 70%, whereas SVM classifier outperformed both the classifiers with 76% overall accuracy (increased by 12%). Hec-GeoHMS was used to create the Curve Number with the help of the SVM classified land use and land cover map using PCA based approach and soil map containing hydrological soil groups. The Curve Number value varied from 36 to 100 for the study area, lower numbers indicate low runoff potential while larger numbers indicate an increased runoff potential. The calculated Curve Number is also termed as CN II or AMC II (Antecedent Moisture Condition II). The calculated Curve Number can be adjusted to dry moisture conditions (called as AMC I) and high moisture conditions (called as AMC III) by using adjusting factors. [Figure 17](#) shows the Curve Number maps, for the antecedent moisture condition II generated using traditional approach and PCA based approach. It is evident from the results that land use and land cover map influence the Curve Number Map significantly.

Table 8: Covariance (Correlation) matrix of sentinel–2 bands

Sentinel-2 Bands	Band 2	Band 3	Band 4	Band 5	Band 6	Band 7	Band 8	Band 8A	Band 11	Band 12
Band 2	40426.8 (1.00)	43694.4 (0.98)	63465.1 (0.95)	45236.1 (0.88)	6071.1 (0.08)	-8485.5 (- 0.08)	-9932.3 (- 0.10)	-14377.9 (-0.12)	42030.1 (0.53)	55946.5 (0.68)
Band 3	43694.4 (0.98)	49362.7 (1.00)	70250.5 (0.95)	52331.9 (0.92)	15490.6 (0.19)	1389.2 (0.01)	360.7 (0.00)	-3597.5 (- 0.03)	52797.9 (0.60)	63910.7 (0.71)
Band 4	63465.1 (0.95)	70250.5 (0.95)	111007.2 (1.00)	78097.1 (0.92)	-1973.4 (- 0.01)	-32521.7 (-0.19)	-35057.0 (-0.20)	-42296.8 (-0.22)	84124.7 (0.64)	111431.2 (0.82)
Band 5	45236.1 (0.88)	52331.9 (0.92)	78097.1 (0.92)	65216.5 (1.00)	23153.8 (0.24)	6455.0 (0.05)	3933.8 (0.03)	3102.1 (0.02)	77195.9 (0.76)	86156.7 (0.83)
Band 6	6071.1 (0.08)	15490.6 (0.19)	-1973.4 (- 0.01)	23153.8 (0.24)	141140.0 (1.00)	189019.7 (0.97)	179641.9 (0.93)	209046.3 (0.96)	55332.7 (0.37)	-1619.9 (- 0.01)
Band 7	-8485.5 (-0.08)	1389.2 (0.01)	-32521.7 (-0.19)	6455.0 (0.05)	189019.7 (0.97)	270417.6 (1.00)	256318.7 (0.96)	298626.5 (0.99)	47352.7 (0.23)	-34947.6 (-0.16)
Band 8	-9932.3 (-0.09)	360.7 (0.01)	-35057.0 (-0.20)	3933.8 (- 0.20)	179641.9 (0.93)	256318.7 (0.96)	265932.9 (1.00)	286099.6 (0.96)	47354.6 (0.23)	-33365.4 (-0.16)
Band 8A	-14377.9 (-0.12)	-3597.5 (-0.03)	-42296.8 (-0.22)	3102.1 (- 0.22)	209046.3 (0.96)	298626.5 (0.99)	286099.6 (0.96)	336385.7 (1.00)	58667.2 (0.26)	-37889.3 (-0.16)
Band 11	42030.1 (0.53)	52797.9 (0.60)	84124.7 (0.64)	77195.9 (0.64)	55332.7 (0.37)	47352.7 (0.23)	47354.6 (0.23)	58667.2 (0.25)	157985.6 (1.00)	142013.0 (0.88)
Band 12	55946.5 (0.69)	63910.7 (0.71)	111431.2 (0.83)	86156.7 (0.83)	-1619.9 (- 0.01)	-34947.6 (-0.16)	-33365.4 (-0.16)	-37889.3 (-0.16)	142013.0 (0.88)	166130.1 (1.00)

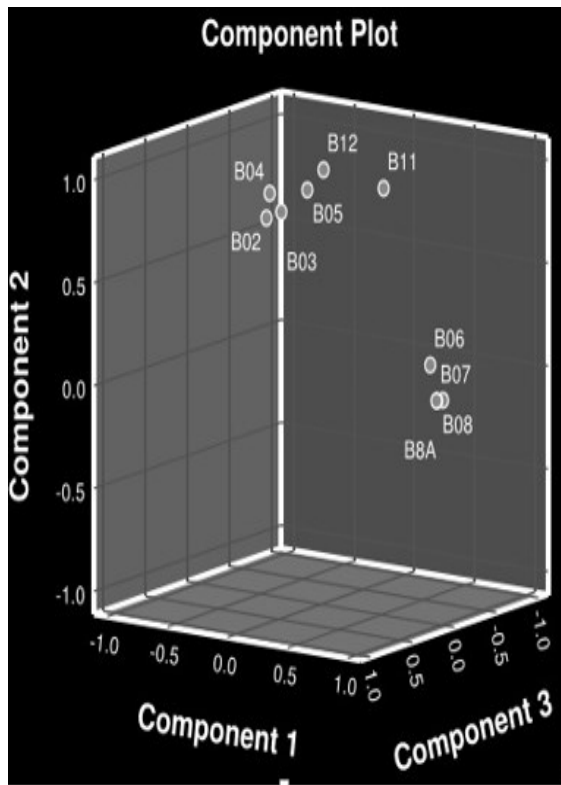


Figure 15

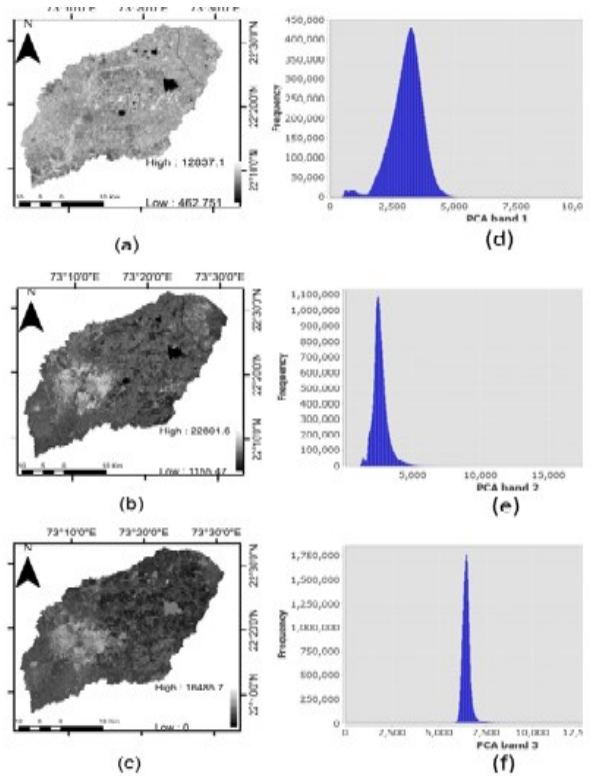


Figure 16

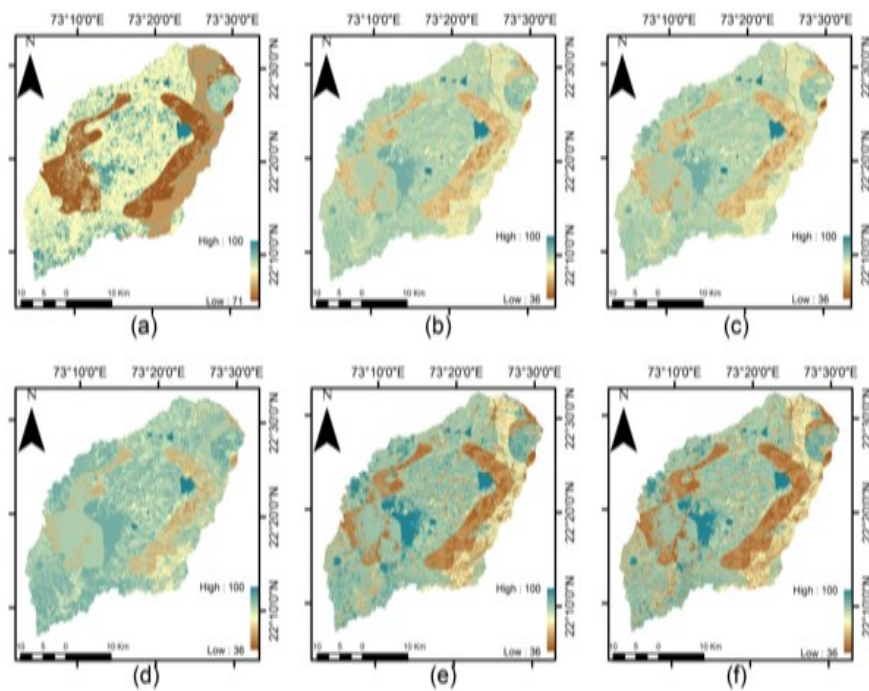


Figure-17

Figure 16: Loading plot of component 1, 2 and 3; Figure 17: Visual comparison of the principal component bands derived from the Sentinel-2 data (a) PCA band 1 (b) PCA band 2 (c) PCA band 3 and (d) Frequency distribution of principal component band 1 (e) Frequency distribution of principal component band 2 (f) Frequency distribution of principal component band 3; Figure 187: Curve number for antecedent moisture condition II generated from traditional approach (a) MLE (b) RF (c) SVM classifiers and PCA based approach in (d) MLE (e) RF (f) SVM classifiers

3. **Objective:** To perform Morphometrical analysis of Vishwamitri watershed and prioritization of sub-watersheds for assessing the flood influencing characteristics of the five sub-watersheds of the Vishwamitri watershed

**Basin length ( $L_b$ ):** The basin length ( $L_b$ ) is the longest length of the basin from the head waters to the point of confluence. The basin length determines the shape of the basin. High basin length indicates elongated basin. The computed  $L_b$  for the basin using Arc-hydro tool is 66.232 km.

**Area of watershed (A):** Another significant parameter, such as the length of stream drainage, is the area of the river basin. An interesting relationship between the total basin areas and the total stream lengths, which are supported by the contributing areas. The Vishwamitri watershed area is 1289.39 km<sup>2</sup>, computed with the help of GIS software.

**Perimeter of watershed (P):** It is the outer boundary of the watershed that enclosed its area and used as an indicator of watershed size and shape. The computed perimeter for the Vishwamitri watershed using GIS software is 279.44 km.

**Stream order ( $S_u$ ):** Stream ordering is a method of assigning a numeric order to links in a stream network. Stream ordering is defined as a measure of the position of a stream in the hierarchy of tributaries. There are different systems available for ordering streams. In the present investigation, maximum frequency is observed in the first-order streams (Table 9). More number of first-order streams is observed in the hilly region of the study area, which point towards terrain density and compacted nature of the bedrock lithology.

**Stream Length ( $L_u$ ):** The total length of individual stream segments of each order is the stream length of that order. Generally, the total length of stream segments is the maximum in first-order streams and decreases with an increase in the stream order. Streams with relatively short lengths are representative of areas with steep slopes and finer texture, whereas longer lengths of stream are generally indicative of low gradients. The mean and total stream length of each stream order is tabulated in Table 9.

**Bifurcation Ratio ( $R_b$ ):** The bifurcation ratio is the ratio of the number of the stream segments of given order  $N_u$  to the number of streams in the next higher order ( $N_{u+1}$ ).  $R_b$  is an important parameter to affect peak of the runoff hydrograph). High  $R_b$  values indicate instantaneous discharge and possibility of flash flooding during extended rainy hours. However,  $R_b$  does not precisely remain constant between stream orders because of variations in basin geometry, lithology, and tectonics. The flat terrains have low  $R_b$  values, whereas mountainous or highly dissected terrains have values from 3 to 5. In the present study, mean bifurcation ratio ( $R_{bm}$ ) for overall watershed is 2.12. The low  $R_b$  value for Vishwamitri watershed suggest delayed hydrograph peak. The lower values of  $R_b$  are characteristics of the watersheds, which have suffered less structural disturbances and the drainage pattern has not been distorted because of the structural disturbances. The higher value of  $R_b$  indicates highly dissected terrain, mature topography with a higher degree of drainage integration, and higher discharge potential. In particular, high  $R_b$  value of sub-watershed SW I suggests the early hydrograph peak with high potential for flash flooding during the storm events among all the sub-watersheds. It is usual to use the weighted mean  $R_b$  value to characterize a watershed using more representative value in situation when the values of  $R_b$  differs for sequential stream orders. For this reason, the weighted mean  $R_b$  of the study watershed was calculated as follow.

$$\text{Weighted mean bifurcation ratio (WRB)} = \frac{R_{b1}N(u_1) + R_{b2}N(u_2) + R_{b3}N(u_3) + R_{b4}N(u_4)}{\text{total number of stream segments}}$$

The weighted mean bifurcation ratio (WRB) for the watershed of Vishwamitri is 3 indicates that geological structures (tectonic activity) exert very low influence on the pattern of streams.

**Drainage density ( $D_d$ ):** The measurement of drainage density provides a numerical measurement of landscape dissection and runoff potential. The  $D_d$  of Vishwamitri watershed is 0.43 km/km<sup>2</sup>. The  $D_d$  of sub-watersheds range from 0.35-0.5. There are five classes of drainage density with the following value ranges (km/km<sup>2</sup>), i.e., very coarse (<2), coarse (2-4), moderate (4-6), fine (6-8), and very fine (>8). A high value of  $D_d$  indicates a relatively high density of streams, high runoff, a quick stream response, and consequently, a low infiltration rate. By contrast, low drainage density of a watershed implies low runoff and takes longer time to peak. Low class of  $D_d$  shows a poorly drained basin with a slow hydrologic response. Besides, low class of  $D_d$  has a resistant permeable subsurface material, dense vegetation cover and low relief.

**Drainage frequency ( $F_s$ ):** Stream frequency is the total number of streams of all orders per unit area. The analysis of the results show that  $F_s$  is maximum in sub-watershed SW III (0.19/km<sup>2</sup>), followed by SW II and SW V (0.15/km<sup>2</sup>), SW IV (0.14/km<sup>2</sup>) and SW I (0.10/km<sup>2</sup>). Overall, the results of  $F_s$  reflect early peak discharge for sub-watersheds in order of their decreasing  $F_s$  resulting in flash floods, while the discharge from SW I takes longer time to peak because of low runoff rates due to lesser number of streams.  $F_s$  for Vishwamitri watershed is 0.13/km<sup>2</sup>.

**Drainage Texture ( $R_r$ ):** Drainage texture is the total number of stream segments of all order in a river basin to the perimeter of the basin. Unit of drainage texture is km<sup>-1</sup>. There are five different texture classes: very coarse (<2), coarse (2-4), moderate (4-6), fine (6-8), and very fine (>8). According to this classification, Vishwamitri watershed has very coarse drainage texture (0.6 km<sup>-1</sup>). The  $R_r$  value for sub-watersheds range from 0.14-0.35. Hydrologically very coarse texture watersheds have large basin lag time periods.

**Relief ratio ( $R_r$ ):** The high  $R_r$  implies on shorter lag time and attains higher peak discharge and flow velocities. With increasing relief, steeper hill slopes and higher stream gradients, time of concentration of runoff decreases, thereby increasing flood peaks. The  $R_r$  for Vishwamitri watershed is 0.01, indicating overall nearly flat terrain or lower slope values. The  $R_r$  values for sub-watersheds range between 0.00-0.02. The SW III, SW IV and SW V having 0  $R_r$  indicating a flat terrain with longer basin length and their influence on flood is very less. While, sub-watersheds SW I and SW II have relatively high values of  $R_r$  and contribute more water in a short period of time and cause floods in the lower region of the basin.

**Ruggedness number ( $R_n$ ):** The ruggedness number is expressed as the product of basin relief and drainage density. High  $R_n$  occur in those basins which have steep and long slopes and fine texture, thus, is highly susceptible to erosion and increased peak discharge. Slope is another important indicator of runoff, which provides general representation of relief ruggedness within the drainage basin. The calculated  $R_n$  value of Vishwamitri watershed is 0.32. The low  $R_n$  value of Vishwamitri watershed due to low relief and lesser degree of terrain complexity, causing less water flow. In the upper Vishwamitri watershed, SW I and SW II have relatively high  $R_n$  values, indicating that they have high relief, fine texture, and possibilities of high surface flow. Moreover, these sub-basins are susceptible to erosion and producing increased peak discharge. The SW III, SW IV and SW V have the lowest  $R_n$  values because of low relief and lesser degree of terrain complexity causing less water flow.

**Form factor ( $F_f$ ):** High  $F_f$  values occur in the basins having potential to produce high peak flows in short duration and low  $F_f$  values are vice versa. The value of form factor would always be greater than 0.78 for perfectly circular basin. Smaller the value of form factor, more elongated will be the basin. The low  $F_f$  value of 0.29 of Vishwamitri watershed reveals that the shape of the study watershed is elongated, it has less side flow for shorter duration and high main flow for longer duration. The  $F_f$  values for sub-watersheds range between 0.1-0.3, indicate elongated shape of sub-watersheds.

**Circularity ratio ( $R_c$ ):** The  $R_c$  values can attain a maximum of 1.0 where the outline of the watershed is approaching near circularity. A numerically low  $R_c$  indicates an elongated shape, while higher values are expression of approach to near circularity. Elongated drainage basins are characterised by longer lag times and lower peak discharge. In study area, the overall  $R_c$  value of Vishwamitri watershed is 0.21 and, for sub-watersheds it range from 0.07-0.2. The  $R_c$  values suggest the elongated shape of the Vishwamitri watershed and its sub watersheds.

**Elongation ratio ( $R_e$ ):** It is defined as the ratio of diameter of a circle with the same area as that of the basin to the maximum basin length. The  $R_e$  values vary from 1 for circular basins and 0 for elongate basins. High  $R_e$  values occur for circular basins, considered as highly hazardous, because they yield peak flow in short period of time compared to low  $R_e$  in elongated basins. These values can be grouped into three categories, namely, circular ( $>0.9$ ), oval ( $0.9-0.8$ ), less elongated  $0.8-0.7$ ) and elongated ( $<0.7$ ). The overall  $R_e$  value of Vishwamitri watershed is 0.61 and, for sub-watersheds it ranges from 0.37-0.62.

**Length of Overland Flow ( $L_g$ ):** Length of overland flow is a length of water over the ground before it gets concentrated into certain stream channels. There are three classes of  $L_g$  i.e., low value ( $< 0.2$ ), moderate value ( $0.2 - 0.3$ ), and high value ( $>0.3$ ). Low value of  $L_g$  indicates high relief and short flow paths which leads to more vulnerable to the flash flooding. Meanwhile, a high value of  $L_g$  means gentle slopes and long flow paths.  $L_g$  value for overall watershed is 1.43 and, for sub-watersheds it ranges from 1-1.43.

#### **Hypsometry Analysis**

The relative area is obtained as a ratio of the area above a particular contour to the total area of the watershed encompassing the outlet. Considering the watershed area to be bounded by vertical sides and a horizontal base plane passing through the outlet, the relative elevation is calculated as the ratio of the height of a given contour ( $h$ ) from the base plane to the maximum basin elevation ( $H$ ) (up to the remote point of the watershed from the outlet. This provided a measure of the distribution of landmass volume remaining beneath or above a basal reference plane. The area under the hypsometric curve (Hypsometric integral (HI)) indicates the erosion process dynamics in a watershed. Actually, the shape of the hypsometry curve shows the evolutionary stage of a basin. Hypsometric Integral (HI):

$$HI = \frac{[Elev_{mean} - Elev_{min}]}{[Elev_{max} - Elev_{min}]}$$

$$= \frac{[(-8.2) - (-40.0)]}{[(738) - (-40.0)]}$$

$$= 0.04$$

Where,  $Elev_{mean}$  is the average elevation of the catchment;  $Elev_{min}$  and  $Elev_{max}$  are the minimum and maximum elevations within the catchment.

The hypsometry and the HI are used in classical conceptual geomorphometric models of landscape evolution as follows: i) for HI above 0.60 the area is considered young; ii) for HI ranging between 0.35 - 0.60 the area is in a steady state balance or mature phase and iii) HI below 0.35 characterizes a Monadnock phase in landscape evolution. Vishwamitri watershed is certainly indicative of a marked old stage in the basin's evolution [Figure 18](#), meaning that the watershed has reached the equilibrium in the longitudinal profiles of the river. This is further attested by very low hypsometric integral (HI = 0.04). Low value of HI occurs in terrains characterized by isolated relief feature standing above extensive level surfaces.

**Compound value and weightage:** Single or limited parameters cannot present the comprehensive picture of the flood hazard potential of any sub-watershed, and hence, each of the linear, aerial, and relief morphometric parameters along with CN is taken into consideration for assessing the

flood influencing characteristics of the five sub-watersheds (Figure 19) of the Vishwamitri watershed, as these parameters have a direct but variable relationship with flood runoff. Therefore, influencing value or rank (highest weightage 5 and least 1) is given to each sub-watershed based on the nature of the selected parameter (Table 10).The prioritization was carried out by assigning ranks to the individual indicators contributing to flood runoff and a compound value ( $C_v$ ) was calculated for final prioritization.  $C_v$  is derived by calculating the average of ranks assigned to the individual parameters. The sub-watershed with highest  $C_v$  is contributing most to flood runoff as a result needs highest priority for flood mitigation measures, whereas sub-watershed with lowest  $C_v$  is contributing least to flood runoff thereby in low priority. Thus an index of high, medium and low priority was produced.

Table 9: Calculated bifurcation ratio, stream length, stream number and stream order

Stream order ( $S_u$ )	Stream number ( $N_u$ )	Stream Length ( $L_u$ )	Bifurcation Ratio
1	85	294.5	2.1
2	39	124.7	1.3
3	30	88.1	3
4	10	33.0	2
5	5	16.7	
Total	169	557.1	Mean 2.1

Table 10: Computed compound value

Sub-watershed ID	$F_f$	$R_c$	$R_e$	$D_d$	$R_t$	$R_r$	$R_n$	WRB	$L_g$	$F_s$	CN	sum	$C_v$
I	3	4	3	5	2	4	5	5	5	1	3	40	3.64
II	2	3	2	2	4	5	4	1	2	3	4	32	2.91
III	1	1	1	4	1	2	2	2	4	5	1	24	2.18
IV	5	5	5	3	5	3	3	4	3	2	2	40	3.64
V	4	2	4	1	3	1	1	3	1	4	5	29	2.64

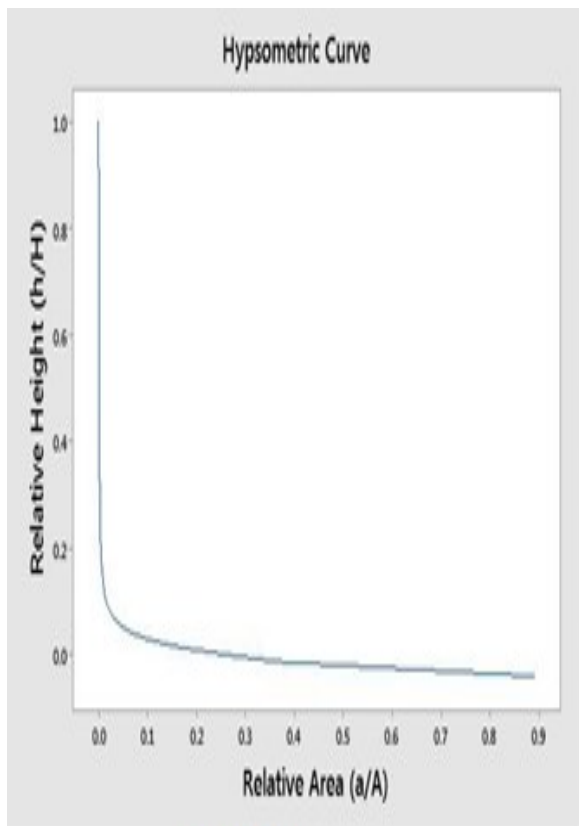


Figure 18

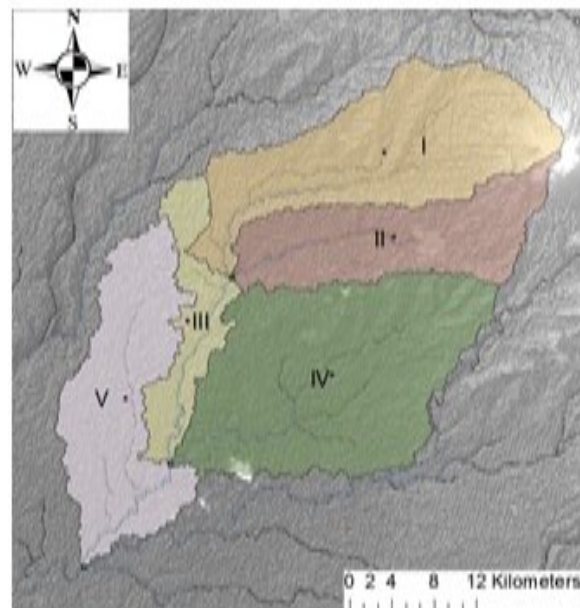


Figure 19

Figure 19: Hypsometric curve of Vishwamitri watershed; Figure 19: Sub watersheds of Vishwamitri watershed

4. **Objective:** To identify potential runoff storage zones based on the various physical characteristics of the Vishwamitri watershed using a GIS-based conceptual framework that combines through analytic hierarchy process using multi criteria decision-making method.

**Weighted Overlay Process (WOP) within GIS:** Potential runoff storage zones of the study area (Figure 20) was generated by integrating the thematic layers of slope, LULC, curve number, HAND, stream order and TWI using weighted overlay process (WOP) within GIS. Resulted raster was classified into four classes namely (a) Not suitable (b) Marginally Suitable (c) Moderately Suitable (d) Optimally Suitable. Result shows that 17 % of the area is optimally suitable, 33.2% of the area is moderately suitable, 33.1 % of the area is marginally suitable and 18.7% of the area is not suitable for water storage zones/structures. Sixteen suitable sites on such zones (optimally suitable class) have also been identified for water storage structures, as shown in Figure 21. Criteria of selection of these sites are: first, proximity of the sites to the agricultural fields. Second, sites should be on unused or barren land. Third, narrow cross-section of the valley with high shoulders to minimise the amount of construction material needed for building the small dams or check dams, nala bunds, gully plug and bundhis. Results are also confirmed by the already built water storage structures in derived potential runoff storage zones which are in optimally suitable class (Figure 22).

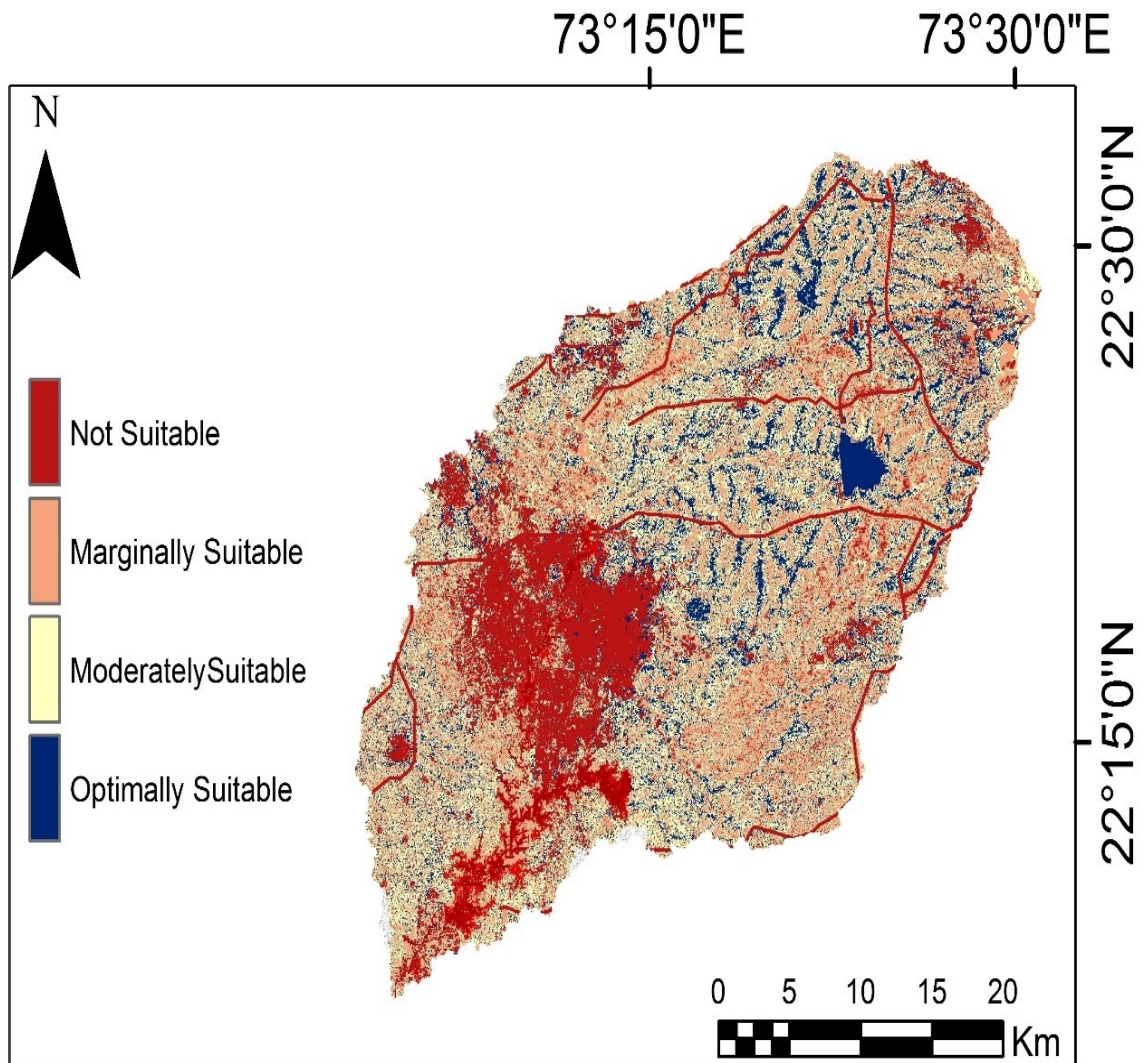


Figure 20: Potential runoff storage zones of the study area

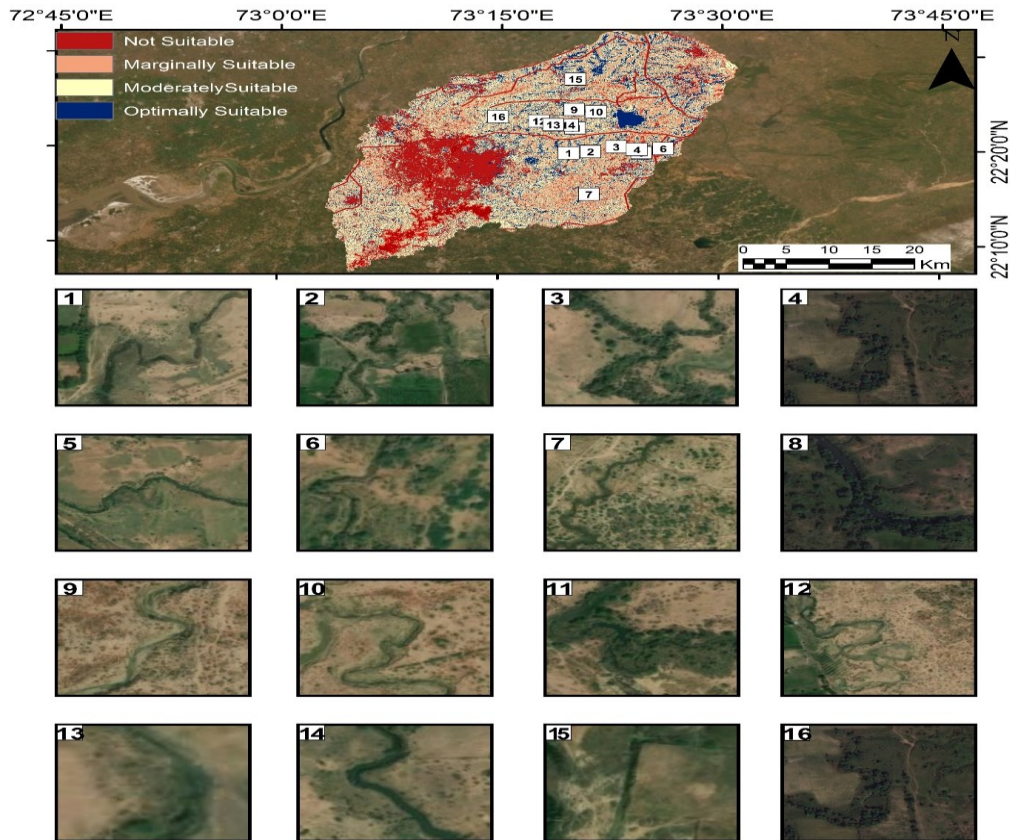


Figure 21: Identified sites for water storage structures on potential runoff storage zones.

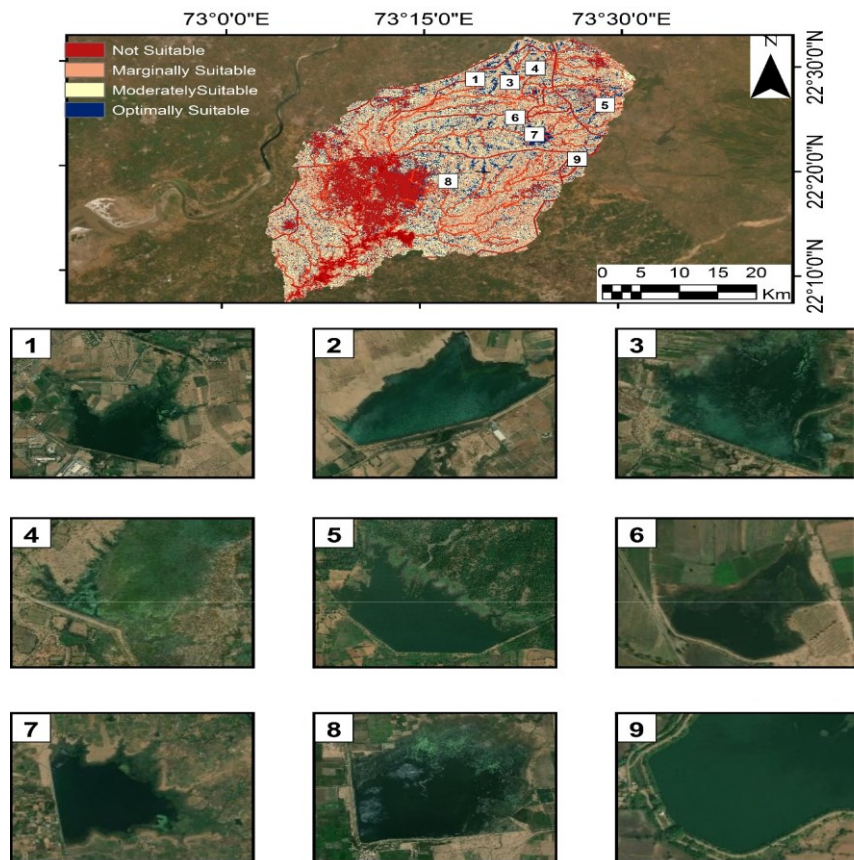


Figure 22: Already built water storage structures on the derived potential runoff storage zones.

5. **Objective:** To develop an approach for operational flood extent mapping using Synthetic Aperture Radar (SAR) and preparation of flood inundation map for data scarce region using 2D flow modelling using rain on grid model.
- Multi-looked, calibrated, filtered (Lee) SAR data were not projected on the map coordinates of each pixel. The pixel was in the original coordinate position of data (rows/columns) in the field of ground range. In the orthorectified imageries, each of the pixels that were corrected and projected using the Range-Doppler terrain correction appeared at the actual position. [Table 9](#) and [10](#), and [Figure 23](#) and [24](#) show the comparison of classification results of random forest classifier and support vector machine classifier for VV and VH polarization. The training data were kept the same for both the classifiers to avoid optimistic bias in the classification. For the study area Kerala, the random forest classifier exhibited maximum overall accuracy of 88.80% with the kappa coefficient value of 0.72. Both the classifiers obtained better accuracy results in VV polarization compared to the VH polarization. The least overall accuracy of 82.60% and a kappa coefficient value of 0.63 were observed with random forest in VH polarization, which was followed by the support vector machine in VV polarization. RF achieved higher classification accuracy than SVM by about 5% in VV polarization. However, both the classifiers produced comparable overall accuracies in VH polarization (SVM achieved higher classification accuracy than RF by about 1%). The NDWI calculated for the cloud-free extent is shown in [Figure 25 \(d\)](#). The inundated area in the calculated NDWI over the cloud-free extent is 73.88%, which is 41.78 km<sup>2</sup>. However, it has also been observed ([Table 11](#)) that the inundated area using random forest classification on filtered VV data over the cloud-free extent is 71.18%, which is 40.25 Km<sup>2</sup>. For the study area Assam, the SVM classifier exhibited maximum overall accuracy of 92% with the kappa coefficient value of 0.81. Both the classifiers obtained better accuracy results in VH polarization compared to the VV polarization. The least overall accuracy of 83.60% and a kappa coefficient value of 0.65 were observed with random forest in VV polarization, which was followed by the RF in VH polarization. SVM achieved higher classification accuracy than RF by about 5.38% in VH polarization. The NDWI calculated for the cloud-free extent is shown in [Figure 26 \(d\)](#). The inundated area in the calculated NDWI over the cloud-free extent is 74.09%, which is 491.47 km<sup>2</sup>. However, it has also been observed ([Table 12](#)) that the inundated area using SVM classification on filtered VH data over the cloud-free extent is 62.76%, which is 416.99Km<sup>2</sup>.

Table 9: Comparison of user's accuracy (UA), producer's accuracy (PA), overall accuracy (%), and kappa coefficient using random forest tree and support vector machine algorithms for VV and VH polarization over Kerala region

	VV Polarization				VH Polarization			
	RF		SVM		RF		SVM	
	PA	UA	PA	UA	PA	UA	PA	UA
Inundation	0.89	0.96	0.79	0.99	0.78	0.99	0.79	0.99
Rest	0.88	0.72	0.98	0.60	0.98	0.58	0.98	0.60
Kappa coefficient	0.72		0.64		0.61		0.63	
Overall Accuracy (%)	88.80%		83.80%		82.60%		83.60%	

Note: UA - User's accuracy, PA - Producer's accuracy VV - Vertical-Vertical, VH - Vertical-Horizontal, RF - Random Forest, SVM -Support Vector Machine

Table 10: Inundated area statistics of RF and SVM over cloud-free optical data for Kerala region

	VV Polarization		VH Polarization		NDWI
	RF	SVM	RF	SVM	-
Inundated area (Km <sup>2</sup> )	40.25	34.82	34.17	35.19	41.78
Rest (Km <sup>2</sup> )	16.29	21.72	22.38	21.36	14.77

Table 11: Comparison of user's accuracy (UA), producer's accuracy (PA), overall accuracy (%), and kappa coefficient using random forest tree and support vector machine algorithms for VV and VH polarization over Assam region

	VV Polarization				VH Polarization			
	RF		SVM		RF		SVM	
	PA	UA	PA	UA	PA	UA	PA	UA
Inundation	0.77	1.0	0.82	1.0	0.81	0.99	0.89	0.99
Rest	1.0	0.62	1	0.69	0.99	0.67	0.99	0.77
Kappa coefficient	0.65		0.72		0.70		0.81	
Overall Accuracy (%)	83.60%		87.60%		86.60%		92.00%	

Note: UA - User's accuracy, PA - Producer's accuracy VV - Vertical-Vertical, VH - Vertical-Horizontal, RF - Random Forest, SVM -Support Vector Machine

Table 12: Inundated area statistics of RF and SVM over cloud-free optical data for Assam region

	VV Polarization		VH Polarization		NDWI
	RF	SVM	RF	SVM	-
Inundated area (Km <sup>2</sup> )	363.92	389.21	387.62	416.99	491.47
Rest (Km <sup>2</sup> )	300.41	275.12	276.70	247.34	171.86

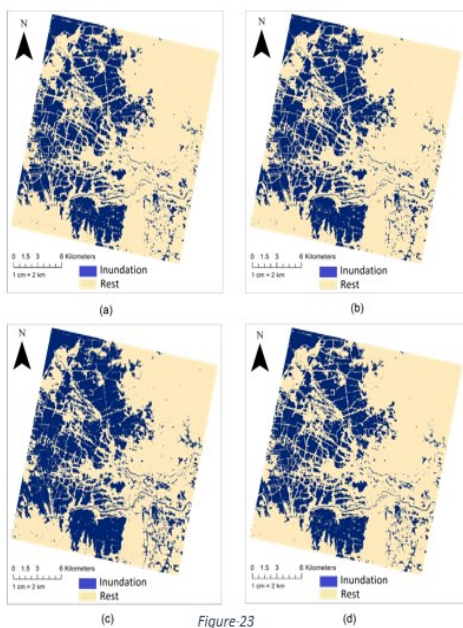


Figure 23

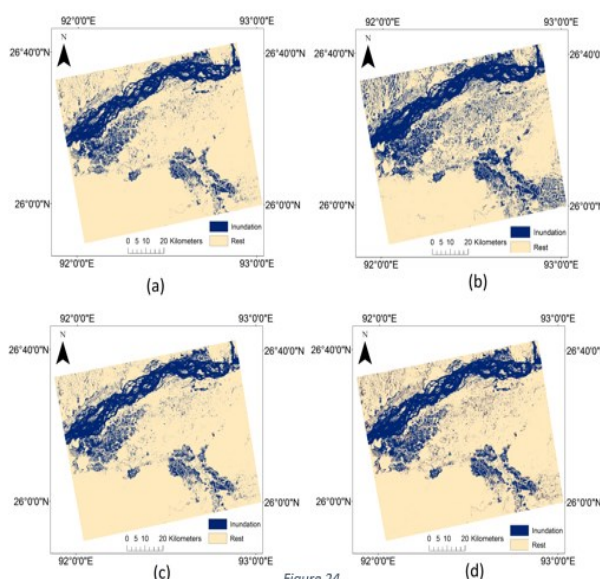


Figure 24

Figure 23: Kerala (a) Random forest tree classification on filtered VH; (b) Support vector machine classification on VH; (c) Random forest tree classification on filtered VV; (d) Support vector machine classification on VV; Figure 24: Assam (a) Random forest tree classification on filtered VH; (b) Support vector machine classification on VH; (c) Random forest tree classification on filtered VV; (d) Support vector machine classification on VV

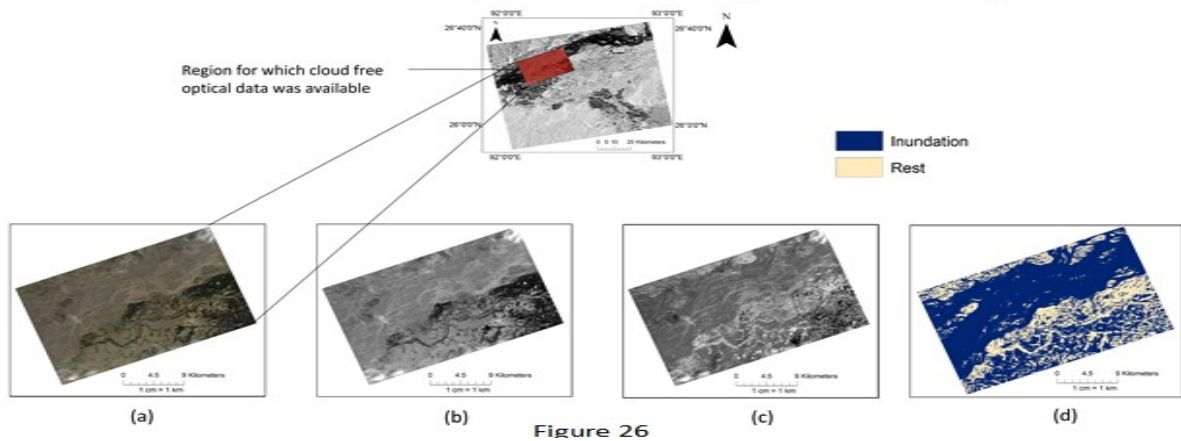
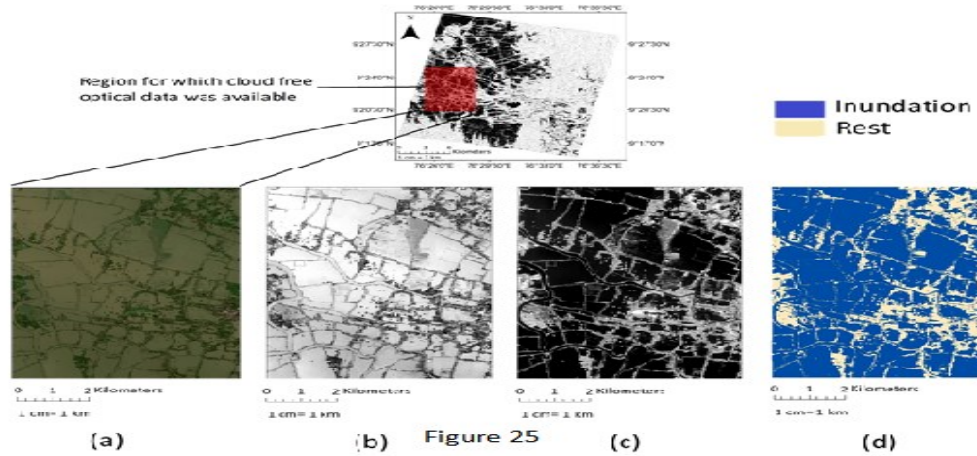


Figure 25: (a) Natural colour composite R-B04 G-B03 B-B02, (b) Green band (c) Near-infrared (d) Calculated NDWI over cloud-free extent for Kerala region; Figure 26: (a) Natural colour composite R-B04 G-B03 B-B02, (b) Green band (c) Near-infrared (d) Calculated NDWI over cloud-free extent for Assam region

**2D hydraulic modelling for inundation:**

Thiessen polygon method for calculating the average precipitation over Vishwamitri watershed for storm event (30-07-2019 to 03-08-2019).

For M stations, the average precipitation  $\bar{P}$  is calculated as

$$\bar{P} = \sum_{i=1}^M P_i \frac{A_i}{A}$$

The ratio  $\frac{A_i}{A}$  is called weightage factor for each station.

**Calculation for runoff estimation:**

The potential maximum soil retention is calculated using following formula:

$$S = \frac{25400}{CN} - 254$$

where S is in mm, and CN is the curve number (dimensionless).

The assumption of SCS-CN is that, for a single storm event, potential maximum soil retention is equal to the ratio of direct run-off to available rainfall. This relationship, after algebraic manipulation and inclusion of simplifying assumptions, results the following expression:

$$\text{Daily Runoff (mm) } Q = \frac{(P - I_a)^2}{(P + S - I_a)} = \frac{(P - \lambda S)^2}{P + (1 - \lambda)S} \text{ for } P > \lambda S$$

- Q = direct run-off depth  
P = total rainfall  
 $I_a$  = initial abstraction

$I_a$  and S can be related using the following equation:

$$I_a = \lambda S$$

$\lambda = 0.2$  was assumed in original SCS-CN model

Calculated weighted curve number of AMC I, AMC II and AMC III are 68.99, 84.04 and 92.50 for the Vishwamitri watershed.

Empirical equations of daily runoff for Vishwamitri watershed for AMC I, AMC II and AMC III conditions:

$$Q(\text{mm}) = \frac{(P - 22.83)^2}{(P + 114.16 - 22.83)} \text{ for AMC I}$$

$$Q(\text{mm}) = \frac{(P - 9.64)^2}{(P + 48.23 - 9.64)} \text{ for AMC II}$$

$$Q(\text{mm}) = \frac{(P - 4.11)^2}{(P + 20.59 - 4.11)} \text{ for AMC III}$$

Table 13: Estimated Daily runoff for the period 30-07-2019 to 03-08-2019 using weighted CN

Date	Cumulative time in Hrs	$\Delta t$ in Hrs	Incremental rainfall (mm)	Maximum potential retention (S) in mm	Initial abstraction $I_a = \lambda S$ (0.2S)	Daily runoff (Q) in mm
30-07-2019	24	24	20.06	48.24	9.65	1.85
31-07-2019	48	24	256.46	48.24	9.65	206.46
01-08-2019	72	24	28.97	20.60	4.12	13.59
02-08-2019	96	24	23.93	20.60	4.12	9.71
03-08-2019	120	24	79.59	20.60	4.12	59.29

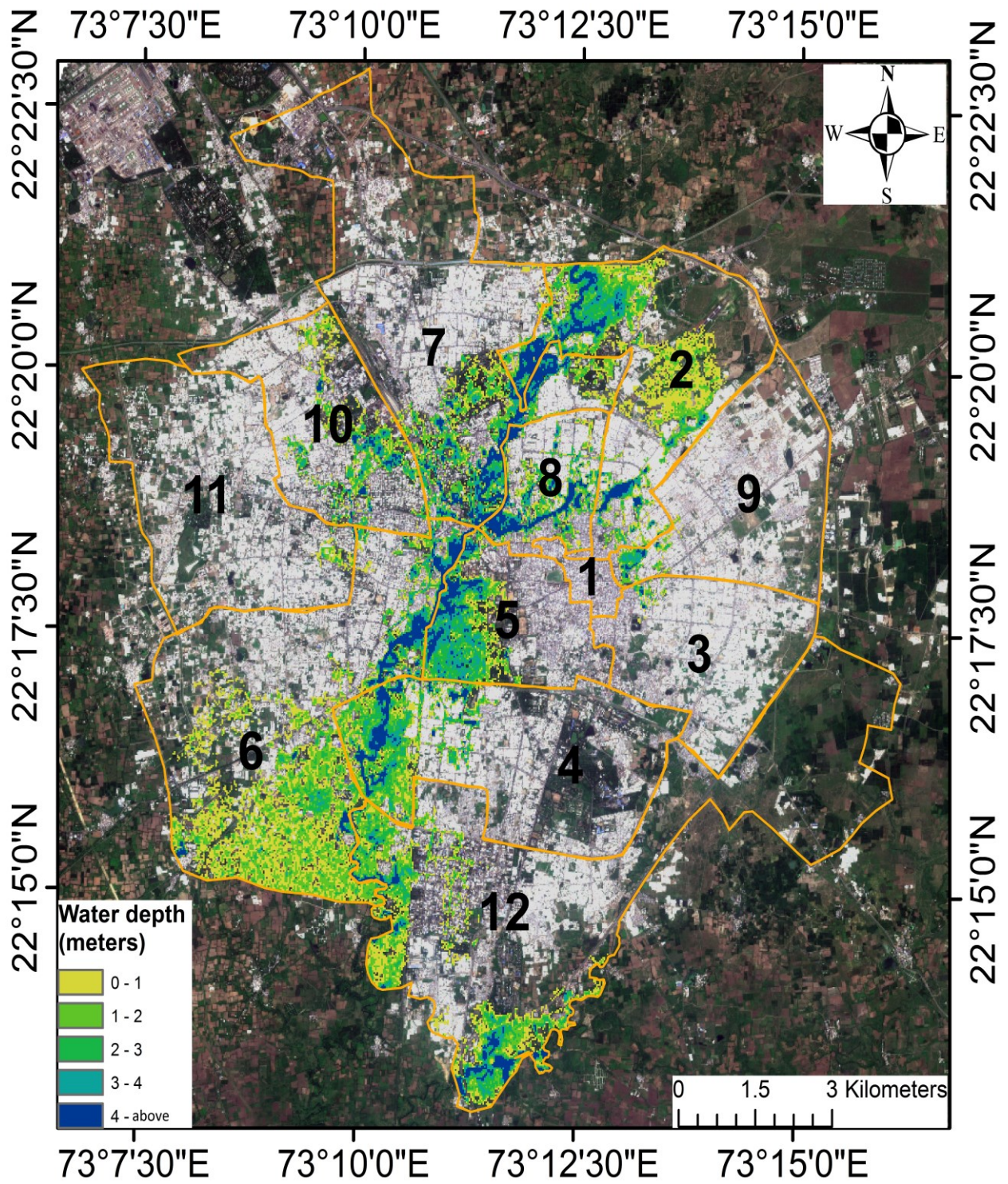


Figure 27: Inundation map of Vadodara city using 2D modelling

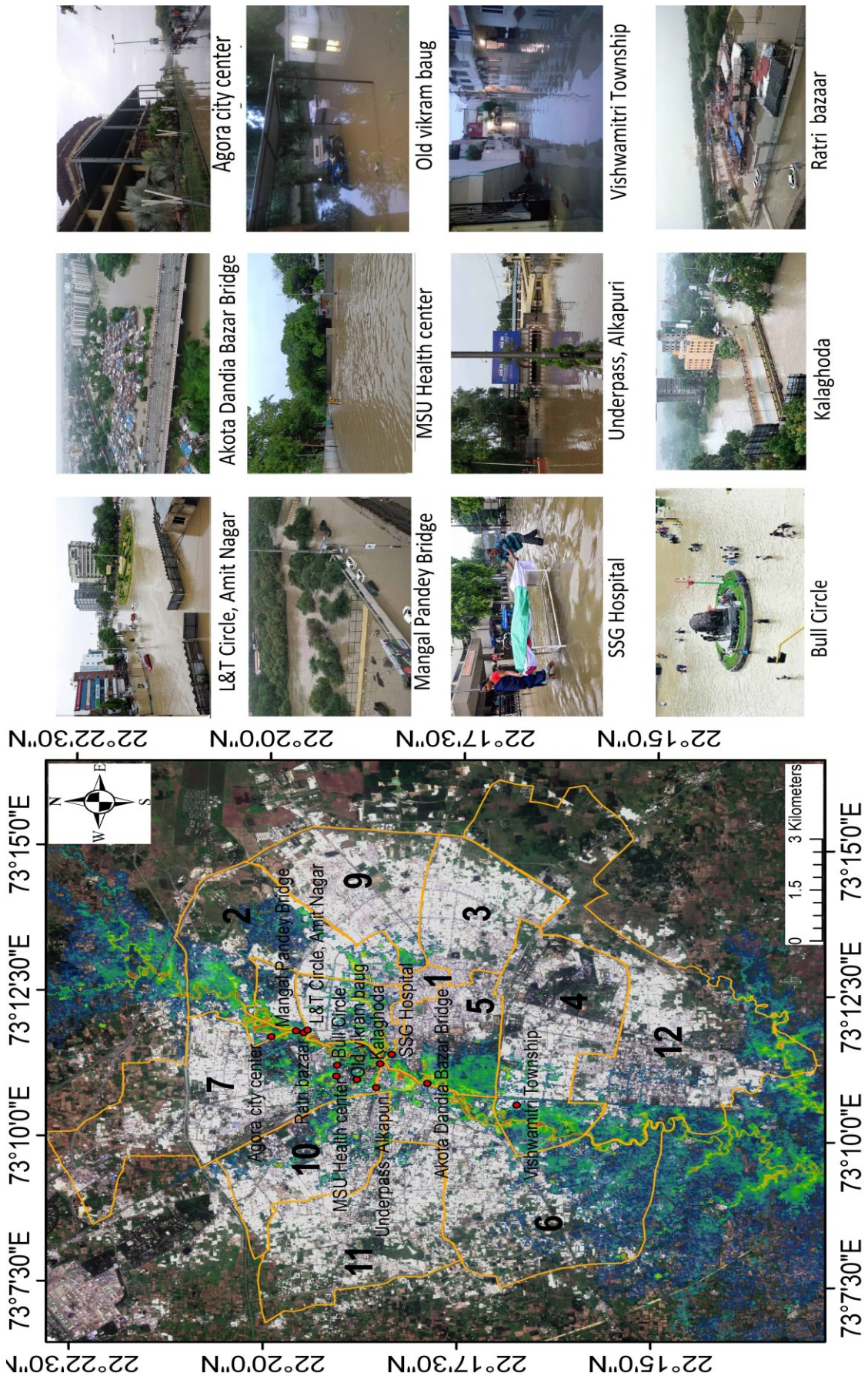


Figure 28: Map validation using sites visit

6. **Objective:** To quantify the effects of urban land forms on land surface temperature and modeling the spatial variation using machine learning. The models can help to predict land surface temperature under temporary cloud cover spots, which are present in the data at the time of the acquisition, using neighboring biophysical (cloud-free) independent variables relationship with land surface temperature.

**LST distribution over the study area:** The estimated land surface temperatures for the summer and winter seasons are shown in [Figure 29](#). The urban heat in Vadodara city in the summer and winter is significant because the high temperature zones are generally consistent with the urban built-up areas near the ward numbers 3, 9 and northeast of ward number 12, and the densely built-up areas in the ward numbers 3, 5, 6 and 12. However, the intensity of land surface temperature in winter is relatively low. In summer, the high temperature zone and the extremely high temperature zone occupy approximately 13.41% and 16.16% ([Table 14](#)) of the total study area, respectively. Furthermore, in winter, areas with high and extremely high temperatures are approximately 13.39% and 15.68% of the total study area, respectively. These two temperature classes show a 0.5% increase in area from winter to summer.

**Temperature Variations for Different Land Cover Types:** To understand the relationship between land surface temperature and land use/land cover, the investigation of the thermal signature of each land use/land cover form is important. A comparison was therefore carried out between land use/land cover and land surface temperature. The mean temperature of each landform category was calculated by averaging all consistent pixels of a given landform category. The average LST at 11:02:51.19 AM in summer reached up to 41.00 °C, whereas in winter it was 30.97 °C. [Figure 5](#) shows the spatial distribution of land surface temperature in both summer and winter. In addition, LST in summer had an almost similar coefficient of variation (CV) than in winter, which indicated that temperature fluctuation in winter and summer are not dramatic. The average land surface temperature values of four land use/land cover types from high to low are baresoil > builtup > vegetation > water. The results indicated the highest land surface temperature was recorded for baresoil while the lowest was recorded for water bodies for both the seasons. In the study period, the city of Vadodara showed lower surface temperatures in residential urban areas as compared to the outskirts of the city. It is caused by heat from the sun in the surrounding areas that is directly absorbed into the ground, causing it to heat up faster than other ground cover ranges. This could be because of the different values of the surface albedo and land surface temperature on residential urban areas and baresoil. The residential areas in the city are generally painted with light colors which increases the albedo value than the baresoil land. In contrast, asphalt roads, pavements, buildings, concrete and other features that make up the urban surfaces tend to slowly release the heat absorbed. A high albedo means the surface reflects the majority of the radiation that hits it and absorbs the rest. However, black asphalt or roads in the urban areas tend to have high land surface temperature and low albedo value due to its thermal characteristic. Black asphalt or roads have a high tendency to absorb solar radiation. In other words, builtup areas tend to retain heat longer than other classes, such as barren land in the city areas, which does not retain heat for as long. The results of this study suggest that the wastelands / barren lands have higher temperatures than residential urban areas. To investigate the connection of LST with biophysical variables, indices such as NDVI, NDWI and DBSI were derived from Landsat 8. The NDVI has been used extensively to define the overall vegetation and green area conditions. A higher NDVI shows a higher vegetation likelihood. The DBSI can reveal the builtup and barren land of urban areas. High DBSI values generally signify areas with baresoil while mid-range values signify intensive urban development. Based on reflected near-infrared radiation and visible green light, NDWI enhances the open water features. A higher NDWI shows a higher water body likelihood. The relationship between land surface temperature and urban surface characteristics was examined using the Pearson correlation coefficient. The overall results indicated a statistically significant correlation (significant at the 0.01 level (2-tailed)). The NDVI map of Vadodara city is illustrated in [Figure 30-A](#). The value of the NDVI ranged between -0.169 and 0.519, the areas with high NDVI values can be

identified with dark green color. The strong negative correlation ( $r=-0.650$ ) with LST and NDVI, shows that high areas of vegetation are the most likely to regulate the surface heating effect. Results describe the high temperature in less dense vegetative areas and low temperature in highly vegetated areas. Lower temperatures in vegetation areas are due to processes like transpiration and evapotranspiration. DBSI values ranged between  $-0.052$  and  $0.255$ , the DBSI value over baresoil and builtup classes showed a positive correlation with LST. It was found that the baresoil and builtup areas have a noticeable effect on the surface urban heat. Water bodies have a little thermal response and are known to be an efficient absorbent of radiation. The result presented in [Figure 30-B](#) indicates the NDWI spatial distribution of water, the NDWI values ranged from  $-0.458$  to  $-0.166$ . A negative correlation was observed between LST and NDWI over water bodies. Surface water characteristics reflect the pattern of heat flow and can be used to minimize the impact of urban heat.

**Land Contribution Index (CI) and Landscape index (LI):** To accurately identify the connection between the surface parameters and the trajectory of the land surface temperature in the area under study, a contribution index for each type of land cover was calculated for the summer and winter seasons. Here each of the selected land use/land cover type's impact on the land surface temperature of the study area was analyzed. The results of the calculated contribution indexes of the land use/land cover types show the dominance of the baresoil surface in relation to the impact on the overall land surface temperature regime of the study area. This development may result from the baresoil land cover type being one of the two classes with a positive net contribution index. Secondly, this contribution index is higher than all the others combined for both the seasons, indicating that the area covered by the baresoil contributes to more surface heating than any other form of land use/land cover in the study area or has the highest heat generation capacity on the surface. Among the four types, vegetation provided maximum heat mitigating impact in the study area. The contribution index value of water remained the same for both the seasons, indicating that temperature variation over water tends to be less variable due to its high thermal capacity. As expected, baresoil and builtup land had high contribution index in summer, which was significantly lower in winter due to lower solar radiation. Apart from baresoil and builtup land, the other types also provided less heat contribution in winter. These observations can be explained by the rainfall season prior to winter season which leads to more vibrant urban green space and therefore more heat sinking. To identify administrative wards with green spaces requirements (such as woodlands, parks, street trees, green roofs and facades), values were assigned on the scale of 1 (low temperature zone) to 6 (extremely high temperature zone) on land surface temperature rasters of both the seasons. A combined score value was later used to divide the administrative wards into low, medium and high green spaces requirement wards. [Figure 31](#) and [Table 15](#) show that ward numbers 2, 9 and 12 belong to high green spaces requirement wards. Strategically planting vegetation in such heat-exposed areas will be more effective than merely selecting a large percentage of the green cover. This strategy will moderate the city climate because shading and evapotranspiration reduce the thermal load outdoors during hot weather conditions.

**Model fitting and evaluation:** To evaluate the machine learning models' performances for K-Nearest Neighbor (K-NN) regression, Neural Networks (NN), Random Trees (RT) regression and Support Vector Machine (SVM) regression with the mean moving kernel (observation grid) of  $2 \times 2$  and  $5 \times 5$  for each explanatory variable (NDVI, NDWI and DBSI). Three measures, namely, coefficient of determination, bias and RMSE were used. When considering both the scenarios ( $2 \times 2$  and  $5 \times 5$ ), more than 60% of the land surface temperature variation was explained by explanatory variables in each model except RT ( $2 \times 2$  and  $5 \times 5$ ), which was nearly about 20% only. Maximum land surface temperature variation was explained in NN  $5 \times 5$  (about 64.1%), followed by, KNN  $5 \times 5$  (62.6%), SVM

5×5 (62.1%), KNN 2×2 (61.7%). While, variation was explained equally in NN 5×5 and SVM 2×2 (61.3%). For KNN 2×2, KNN 5×5, RT 2×2, SVM 2×2 and SVM 5×5 the land surface temperature absolute error map (|predicted LST– actual LST|) are shown in Figure 32-A1,E1,C1,D1 and H1, the mean value of error map (predicted LST– actual LST) or Bias (°C) and standard deviation were found to be -0.0076 °C, -0.0097 °C, -0.0006 °C, -0.0622 °C and -0.0642 °C, and 0.561 °C, 0.549 °C, 0.889 °C, 0.621 °C and 0.612 °C, respectively (Table 16). The corresponding frequency histograms of error (Figure 32-A2, E2, C2, D2 and H2) indicate that the above mentioned models underestimated the predicted LST. For NN 2×2, NN 5×5 and RT 5×5 the land surface temperature absolute error maps are shown in Figure 32-B1, F1, and G1, the mean value of error map or Bias (°C) and standard deviation were found to be 0.0047 °C, 0.0011 °C and 0.0034 °C, and 0.617 °C, 0.595 °C and 0.890 °C, respectively (Table 16). The corresponding frequency histograms of error (Figure 32-B2, F2, and G2) indicate that the models slightly overestimated the predicted LST. The comparative results revealed that the K-NN algorithm outperformed the other models. The lowest overall RMSE was calculated at a value of 0.549 °C for KNN 5×5, followed by, KNN 2×2 (0.561°C). The worst performances were observed by RT models (2×2 and 5×5) (Figure 33-E and F). However, NN 2×2, NN 5×5, SVM 2×2 and SVM 5×5 models performed moderately good with overall RMSE of 0.617, 0.594,0.623 and 0.615, respectively.

Table 14: Calculated area and percentage of each temperature class for summer and winter.

Temperature classes	Summer	Winter
	Area km <sup>2</sup> (%)	Area km <sup>2</sup> (%)
Low temperature zone	20.03 (12.49)	21.42 (13.35)
Secondary low temperature zone	29.10 (18.14)	26.77 (16.69)
Medium temperature zone	34.29 (21.38)	34.82 (21.71)
Secondary high temperature zone	29.55 (18.42)	30.74 (19.17)
High temperature zone	21.51 (13.41)	21.48 (13.39)
Extremely high temperature zone	25.92 (16.16)	25.15 (15.68)

Table 15: Administrative wards with green spaces requirement.

Ward no.	Summer		Winter		Combined score	Green spaces requirement
	Majority class	Individual score	Majority class	Individual score		
1	Secondary high temperature zone	4	Secondary high temperature zone	4	8	Medium
2	Extremely high temperature zone	6	Extremely high temperature zone	6	12	High
3	Medium temperature zone	3	Secondary high temperature zone	4	7	Medium
4	Medium temperature zone	3	Medium temperature zone	3	6	Medium
5	Medium temperature zone	3	Low temperature zone	1	4	low
6	Secondary high temperature zone	4	Medium temperature zone	3	7	Medium
7	Medium temperature zone	3	Medium temperature zone	3	6	Medium
8	Medium temperature zone	3	Medium temperature zone	3	6	Medium
9	Medium temperature zone	3	Extremely high temperature zone	6	9	High
10	Secondary low temperature zone	2	Medium temperature zone	3	5	Medium
11	Secondary low temperature zone	2	Medium temperature zone	3	5	Medium
12	Extremely high temperature zone	6	Extremely high temperature zone	6	12	High

Table 16: Calculated bias and RMSE of the predictive models.

	Bias(°C)		RMSE(°C)	
	2X2	5X5	2X2	5X5
KNN	-0.0076	-0.0097	0.561	0.549
NN	0.0047	0.0011	0.617	0.594
RT	-0.0006	0.0034	0.888	0.890
SVM	-0.0622	-0.0642	0.623	0.615

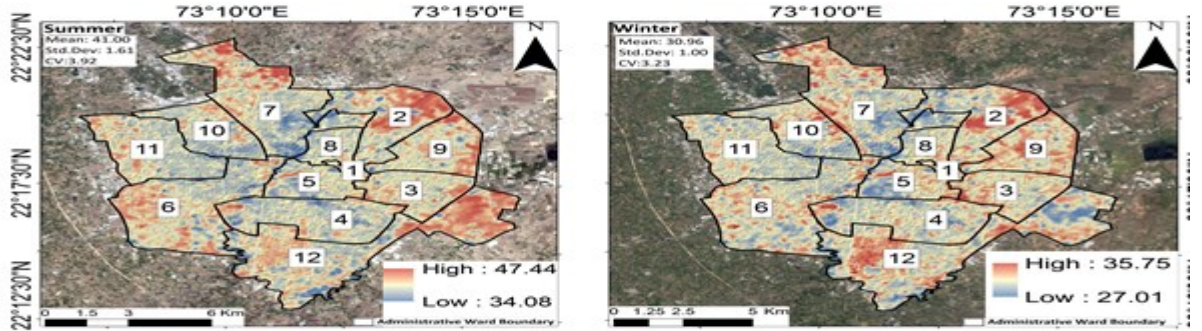


Figure 29

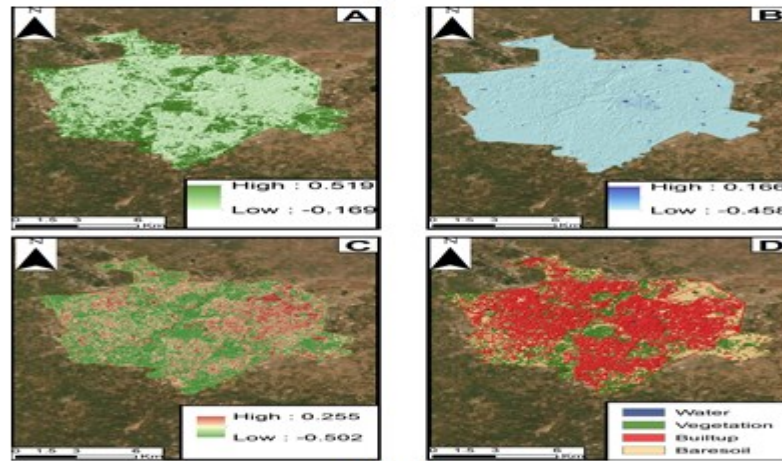


Figure 30

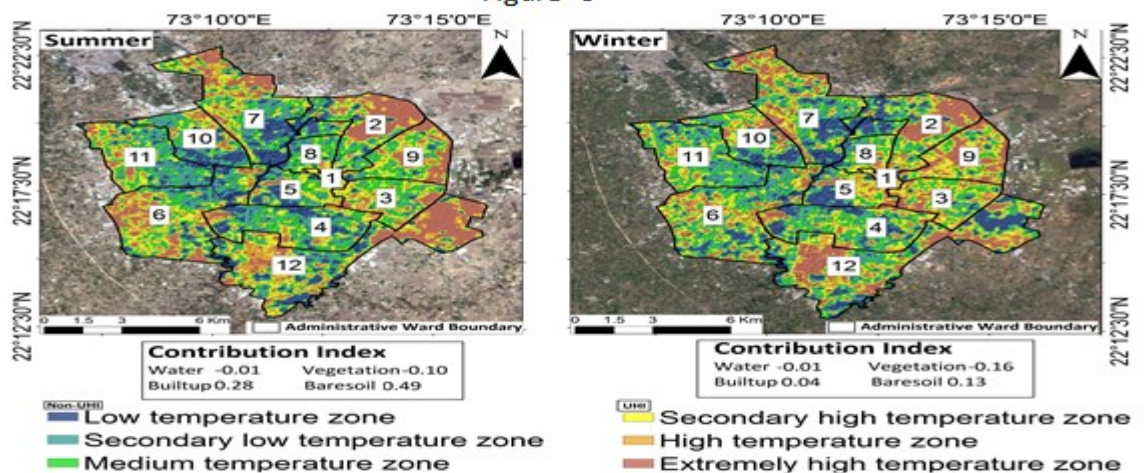


Figure 31

Figure 29: Estimated land surface temperatures for the summer and winter seasons using Landsat 8 data; Figure 30: Spatial distribution of (A) NDVI, (B) NDWI, (C) DBSI and (D) Land use/land cover over Vadodara city; Figure 31: Classification of heat zones into UHI and non-UHI zones, and contribution index of land use/land cover classes in summer and winter seasons.

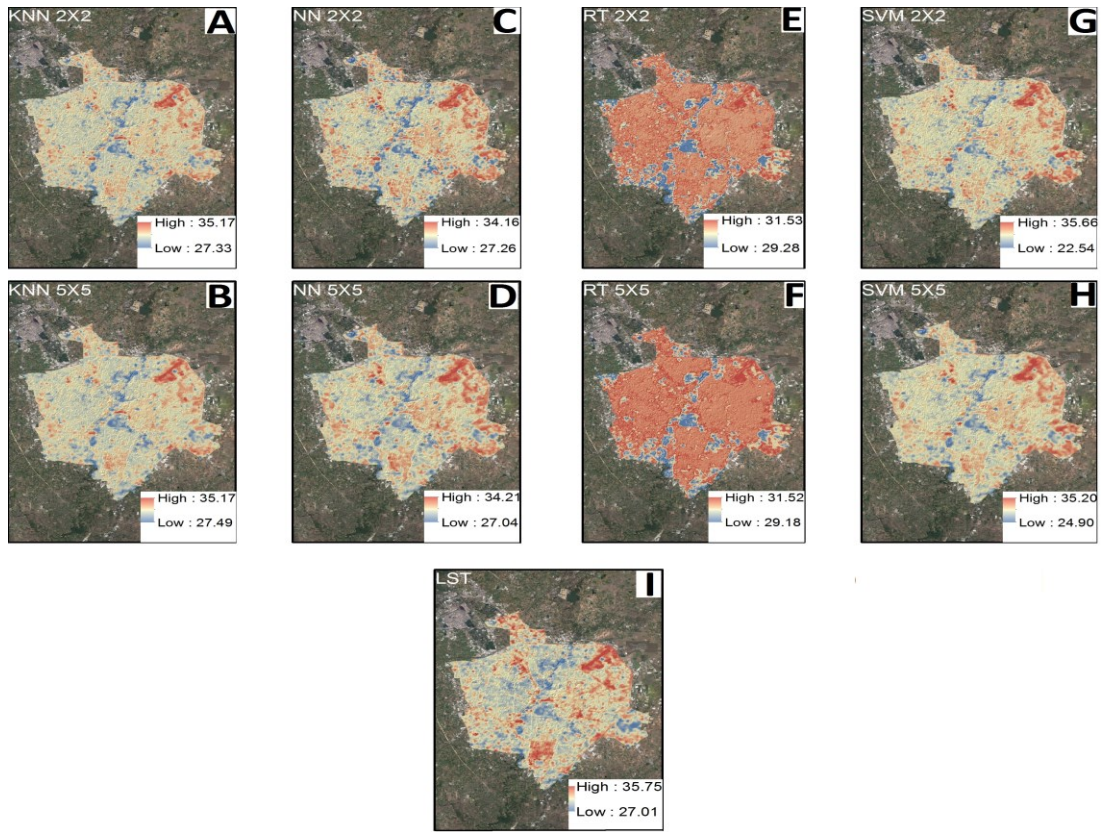


Figure 32: Maps A,B, C, D,E,F,G and H show the predicted LST using the K-NN (2x2), K-NN (5x5), NN (2x2), NN(5x5), RT (2x2), RT (5x5), SVM (2x2) and SVM (5x5) models, respectively. Map I shows the observed LST estimated using Landsat 8.

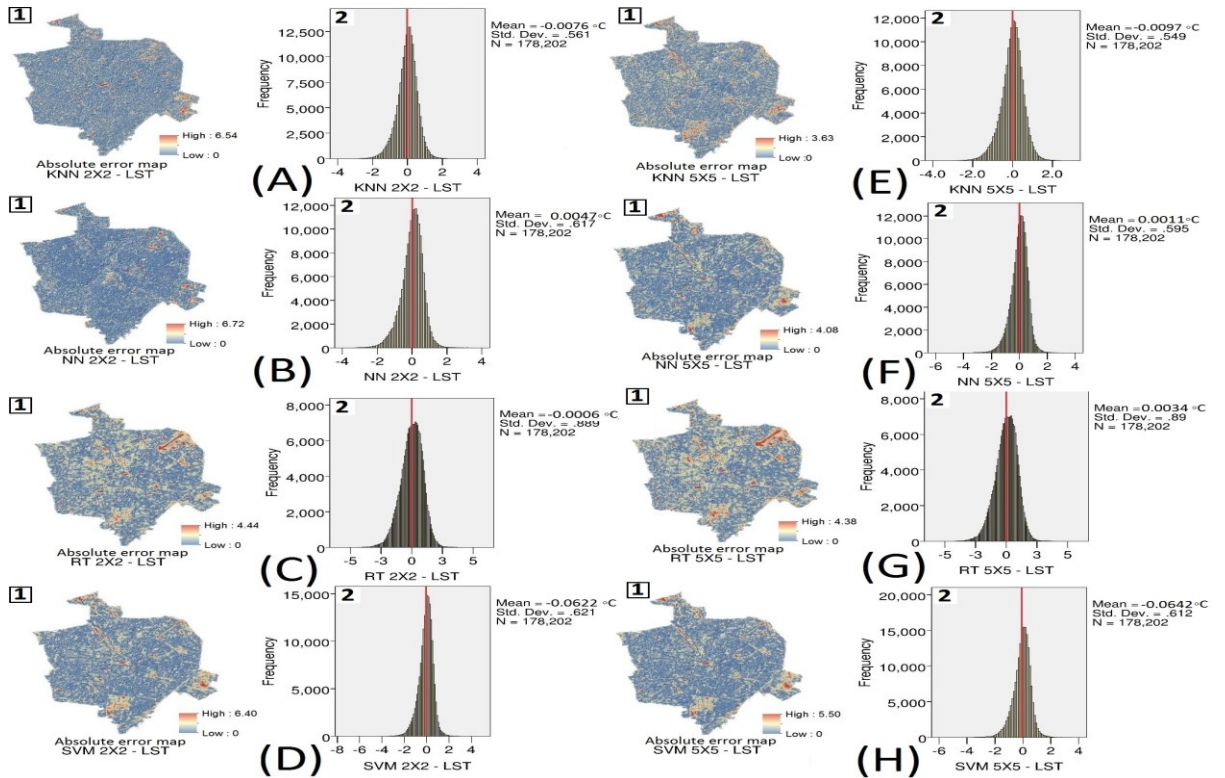


Figure 33: Absolute error maps A1-H1 and corresponding frequency histogram of error A2-H2 of predictive models

## 6. Conclusions and Recommendations

### 6.1 General

This chapter briefly shows the conclusions obtained for the individual objective. Based on the conclusion few recommendations have been given.

### 6.2 Conclusions

1. All the DEMs have imperfections for the delineation of the small river like Vishwamitri. Moreover, a comparison shows that SRTM 30 m and ASTER 30 m failed to delineate proper main drainage for the Vishwamitri river. However, Cartosat 30 m DEM exhibited better results.
2. It can be concluded that for hydrological studies the Cartosat DEM should be given first preference followed by the SRTM DEM for the areas where the relief class belongs to a flat relief.
3. PCA based approach is far superior to the traditional approach. Highest classification accuracy was achieved with SVM classifier.
4. SVM outperformed the MLE and RF classifiers in both traditional as well as PCA based approach even with a small training dataset. The uncorrelated principal component bands enhanced the classification accuracy as compared to the use of Sentinel-2 original bands. This confirms the feasibility of PCA in remote sensing to extract land use and land cover information and enhance the classification.
5. Proposed suitability map for potential water storage zones developed by the GIS technique for the study area may be implemented in the future to overcome growing water scarcity due to global/regional climate change. Since the approach and the analysis showed in this research have non-exclusive relevance, they are exceptionally valuable for other parts of the world, especially for developing countries, despite hydrological and agro-climatic variations.
6. The proposed approaches for flood inundation mapping show the potential for monitoring damages caused by floods, providing basic information that can help local communities manage water-related risk, planning land and water management as well as other flood control programs.
7. Spatial distribution of land surface temperature provides critical information for the understanding of local climatic conditions in the cities and can be used as a potential measure to introduce necessary steps to minimize the adverse effects of high land surface temperature. The results indicated the highest land surface temperature was recorded for bare soil while the lowest was recorded for water bodies. Based on research results, this study suggested that a new urban heat mitigation strategy is an important element in the spatial arrangement of impermeable surfaces and green areas as well as water bodies that manage urban heating and cooling.
8. The evaluation of the prediction models shows that the K-NN, NN and SVM models, are the optimum models for predicting the land surface temperature in Vadodara city using neighboring biophysical independent variables relationship with land surface temperature. In addition, it is shown that the K-NN (5×5 observation grid) model exhibits good performance with RMSE of 0.549 °C. The model can help to predict land surface temperature under temporary cloud cover spots, which are present in the data at the time of the acquisition using neighboring biophysical (cloud free) independent variables relationship with land surface temperature.

### 6.3 Recommendations

1. High spatial resolution DEM data must be used.
2. The sub-watersheds I and IV having more flood influencing characteristics as a result needs highest priority for flood mitigation measures.
3. To overcome growing water scarcity due to global/regional climate change, water storage structures must be made on potential water storage zones.
4. To reduce floods, we suggest that there is dire need to construct flood spill channel.

## 7. References

1. Ahmed, S. A., Chandrashekarappa, K. N., Raj, S. K., Nischitha, V., & Kavitha, G. (2010). Evaluation of morphometric parameters derived from ASTER and SRTM DEM—a study on Bandihole sub-watershed basin in Karnataka. *Journal of the Indian society of remote sensing*, 38(2), 227-238.
2. Altaf, F., Meraj, G., & Romshoo, S. A. (2013). Morphometric analysis to infer hydrological behaviour of Lidder watershed, Western Himalaya, India. *Geography Journal*, 2013.
3. Astola, H., Häme, T., Sirro, L., Molinier, M., & Kilpi, J. (2019). Comparison of Sentinel-2 and Landsat 8 imagery for forest variable prediction in boreal region. *Remote Sensing of Environment*, 223, 257-273.
4. Avdan, U., & Jovanovska, G. (2016). Algorithm for automated mapping of land surface temperature using LANDSAT 8 satellite data. *Journal of Sensors*, 2016
5. Bhat, M. S., Alam, A., Ahmad, S., Farooq, H., & Ahmad, B. (2019). Flood hazard assessment of upper Jhelum basin using morphometric parameters. *Environmental Earth Sciences*, 78(2), 54.
6. Bhat, M. S., Alam, A., Ahmad, S., Farooq, H., & Ahmad, B. (2019). Flood hazard assessment of upper Jhelum basin using morphometric parameters. *Environmental Earth Sciences*, 78(2), 54.
7. Chaplot, V. (2014). Impact of spatial input data resolution on hydrological and erosion modeling: Recommendations from a global assessment. *Physics and Chemistry of the Earth*, 67–69, 23–35. <https://doi.org/10.1016/j.pce.2013.09.020>
8. Cheng, G., Han, J., Guo, L., Liu, Z., Bu, S., & Ren, J. (2015). Effective and Efficient Midlevel Visual Elements-Oriented Land-Use Classification Using VHR Remote Sensing Images. *IEEE Transactions on Geoscience and Remote Sensing*, 53(8), 4238–4249. <https://doi.org/10.1109/TGRS.2015.2393857>
9. Durand, J. M., Gimonet, B. J., & Perbos, J. R. (1987). SAR Data Filtering for Classification. *IEEE Transactions on Geoscience and Remote Sensing*, GE-25(5), 629–637. <https://doi.org/10.1109/TGRS.1987.289842>
10. Ficklin, D. L., Tan, M. L., Chaplot, V., Dixon, B., Ibrahim, A. L., & Yusop, Z. (2015). Impacts of DEM resolution, source, and resampling technique on SWAT-simulated streamflow. *Applied Geography*, 63, 357–368. <https://doi.org/10.1016/j.apgeog.2015.07.014>
11. Goodman, J. W. (1976). Some fundamental properties of speckle. *JOSA*, 66(11), 1145-1150
12. Guth, P. L. (2010, November). Geomorphometric comparison of ASTER GDEM and SRTM. In A special joint symposium of ISPRS Technical Commission IV & AutoCarto in conjunction with ASPRS/CaGIS.
13. Haashemi, S., Weng, Q., Darvishi, A., & Alavipanah, S. K. (2016). Seasonal variations of the surface urban heat island in a semi-arid city. *Remote Sensing*, 8(4), 352
14. Han, J., Zhang, D., Cheng, G., Guo, L., & Ren, J. (2015). Object detection in optical remote sensing images based on weakly supervised learning and high-level feature learning. *IEEE Transactions on Geoscience and Remote Sensing*, 53(6), 3325–3337. <https://doi.org/10.1109/TGRS.2014.2374218>
15. Jarihani, A. A., Callow, J. N., Mcvigar, T. R., Niel, T. G. Van, & Larsen, J. R. (2015). Satellite-derived Digital Elevation Model ( DEM ) selection , preparation and correction for hydrodynamic modelling in large , low-gradient and data-sparse catchments. *JOURNAL OF HYDROLOGY*, 524, 489–506. <https://doi.org/10.1016/j.jhydrol.2015.02.049>
16. Khatami, R.; Mountrakis, G.; Stehman, S.V. A meta-analysis of remote sensing research on supervised pixel-based land-cover image classification processes: General guidelines for practitioners and future research. *Remote Sens. Environ.* 2016, 177, 89–100.
17. Laforteza, R., Carrus, G., Sanesi, G., Davies, C., 2009. Benefits and well-being perceived by people visiting green spaces in periods of heat stress. *Urban Forestry & Urban Greening* 8, 97–108, <http://dx.doi.org/10.1016/j.ufug.2009.02.003>.
18. Lee, J. S., & Pottier, E. (2009). *Polarimetric radar imaging: from basics to applications*. CRC press.
19. Ma, Y., Kuang, Y., & Huang, N. (2010). Coupling urbanization analyses for studying urban thermal environment and its interplay with biophysical parameters based on TM/ETM+ imagery. *International Journal of Applied Earth Observation and Geoinformation*, 12(2), 110–118.
20. Magesh, N. S., & Chandrasekar, N. (2014). GIS model-based morphometric evaluation of Tamiraparani subbasin, Tirunelveli district, Tamil Nadu, India. *Arabian Journal of Geosciences*, 7(1), 131-141.
21. Mallick, J., Atzberger, C., & Kerle, N. (2009). Satellite-based analysis of the role of land use/land cover and vegetation density on surface temperature regime of Delhi, India. *Journal of the Indian Society of Remote Sensing*, 37(2), 201-214.
22. Mallick, J., Kant, Y., & Bharath, B. D. (2008). Estimation of land surface temperature over Delhi using

- Landsat-7 ETM+. *J. Ind. Geophys. Union*, 12(3), 131-140.
23. Manandhar, R., Odehi, I. O. A., & Ancevt, T. (2009). Improving the accuracy of land use and land cover classification of landsat data using post-classification enhancement. *Remote Sensing*, 1(3), 330–344. <https://doi.org/10.3390/rs1030330>
  24. Masoud, M. H. (2016). Geoinformatics application for assessing the morphometric characteristics' effect on hydrological response at watershed (case study of Wadi Qanunah, Saudi Arabia). *Arabian Journal of Geosciences*, 9(4), 280.
  25. Ozdemir, H., & Bird, D. (2009). Evaluation of morphometric parameters of drainage networks derived from topographic maps and DEM in point of floods. *Environmental geology*, 56(7), 1405-1415.
  26. Ozesmi, S. L., & Bauer, M. E. (2002). Satellite remote sensing of wetlands. *Wetlands Ecology and Management*, 10(5), 381–402. <https://doi.org/10.1023/A:1020908432489>
  27. Persendt, F. C., & Gomez, C. (2016). Assessment of drainage network extractions in a low-relief area of the Cuvelai Basin (Namibia) from multiple sources: LiDAR, topographic maps, and digital aerial orthophotographs. *Geomorphology*, 260, 32–50. <https://doi.org/10.1016/j.geomorph.2015.06.047>
  28. Romshoo, S. A., Bhat, S. A., & Rashid, I. (2012). Geoinformatics for assessing the morphometric control on hydrological response at watershed scale in the Upper Indus Basin. *Journal of Earth System Science*, 121(3), 659-686.
  29. Shafizadeh-Moghadam, H., Weng, Q., Liu, H., & Valavi, R. (2020). Modeling the spatial variation of urban land surface temperature in relation to environmental and anthropogenic factors: a case study of Tehran, Iran. *GIScience & Remote Sensing*, 1-14.
  30. Sharma, A., & Tiwari, K. N. (2014). A comparative appraisal of hydrological behavior of SRTM DEM at catchment level. *JOURNAL OF HYDROLOGY*, 519, 1394–1404. <https://doi.org/10.1016/j.jhydrol.2014.08.062>
  31. Tomlinson, C. J., Chapman, L., Thornes, J. E., & Baker, C. (2011). Remote sensing land surface temperature for meteorology and climatology: a review. *Meteorological Applications*, 18(3), 296-306.
  32. Wang, W., Yang, X., & Yao, T. (2012). Evaluation of ASTER GDEM and SRTM and their suitability in hydraulic modelling of a glacial lake outburst flood in southeast Tibet. *Hydrological Processes*, 26(2), 213–225. <https://doi.org/10.1002/hyp.8127>
  33. Wolock, D. M., & Price, C. V. (1994). Effects of digital elevation model map scale and data resolution on a topography-based watershed model. *Water Resources Research*, 30(11), 3041-3052.
  34. Zeng, C., Shen, H., Zhong, M., Zhang, L., & Wu, P. (2014). Reconstructing MODIS LST based on multitemporal classification and robust regression. *IEEE Geoscience and Remote Sensing Letters*, 12(3), 512-516.
  35. Zhao, M., Cai, H., Qiao, Z., & Xu, X. (2016). Influence of urban expansion on the urban heat island effect in Shanghai. *International Journal of Geographical Information Science*, 30(12), 2421-2441.



**THE MAHARAJA SAYAJIRAO UNIVERSITY OF BARODA**  
**DOCTOR OF PHILOSOPHY**

सत्यं शिवं सुन्दरम्

[Form fee : ₹. 5/- only]

[ Admisslon Fee : ₹. \_\_\_\_\_ only ]

To,  
The Registrar (Examinations),  
The Maharaja Sayajirao University of Baroda,  
Vadodara - 390 002.

Sir,

I offer myself as a candidate for the Degree of Doctor of Philosophy in the Faculty of Technology & Engineering  
in <sup>2</sup> Ph.D. in CIVIL Engineering

I submit herewith three typewritten copies of the Synopsis on my thesis embodying the results of my research on <sup>3</sup> \_\_\_\_\_  
REMOTE SENSING and GEOGRAPHIC INFORMATION SYSTEM APPROACH FOR  
HYDROLOGICAL, MORPHOMETRICAL and SPATIAL ANALYSIS OF VISHWAMITRI WATSHED<sup>4</sup>

I append herewith a signed statement showing in what particulars the work is based on the discovery of new facts by me or of new relations of facts observed by others and how the work tends to the general advancement of knowledge.

I also append herewith a statement indicating the sources from which my information has been derived and the extent to which I have based my work on the work of others, and the portion or portions of my thesis which I claim as original.

I declare that for the thesis which I am submitting, no degree or diploma or distinction has been conferred on me before, either in this or in any other University.

<sup>5</sup> In further support of my application, I am submitting herewith copies of published original research work done by me on the subject of my thesis and/or on cognate subjects.

The fees of Rs. \_\_\_\_\_ is remitted in the Office of Dean, Faculty of \_\_\_\_\_  
vide Receipt No. \_\_\_\_\_

Yours faithfully,

*(Signature)*  
(Signature)

Dated :

**PERSONAL DETAILS**

<sup>6</sup> Name in full  
(In Block letters)

Surname : Shri/Smt./Kum. \_\_\_\_\_

Name : VIKAS KUMAR RANAFather's/Husband's Name GAGAN SINGH RANA

Sex : Male

Nationality : INDIANNo. and Date of Registration FOTE/95009/02/2018

<sup>7</sup> Date of passing the examination, Class obtained, optional subjects offered and the name of the University

Date : 16/10/2017Class : PET (2017) 2Subjects CIVIL ENGINEERINGName of the University The Maharaja Sayajirao University of Baroda

1. Insert the name of the Faculty.
2. Insert the name of the subject ( e.g. 'Economics', Physics, 'Biochemistry' Etc.)
3. Please enter in detail the title and the subject of the thesis.
4. If a candidate presents a jointwork, he/she shall clearly state which portion is his/her own contribution as distinguished for the portion contributed by his/her collaborator.
5. To be struck off when it is not necessary. The candidate may forward with his thesis three copies of any original contribution or contributions to the advancement of knowledge on the subject selected by him/her for his/her thesis or any cognate subject published by him independently or jointly with others, upon which he relies in support of his candidature.
6. The name in the degree certificate will be written according to this entry.
7. Insert the name of the Examination on the basis of which you were registered for Ph.D.

\* Date of taking the degree Master of Engineering in Water Resource Engineering (2017)  
 Name of the University The Maharaja Sayajirao University of Baroda  
 Residential Address in Vadodara K/2, old Vikram Baug, Vadodara-390002  
 Permanent Residential Address Nalehar, Thural, Palampur, Dist- KANARA  
 Himachal Pradesh - 176107.

**Certificate of guiding teacher to be submitted by the candidate (see Ordinance Ph.D. 8 (iii))**

I certify that the thesis presented by Shri/Smt./Kum. VIKAS KUMAR RANA represents his/her original work which was carried out by him/her at WREMI, Faculty of Tech & Engg. under my guidance and supervision during the period 09/02/2018 to til date. I further certify that the forgoing statements made by him/her in regard to his/her Thesis are correct and undergo the required admission procedure and earn the required credit.

T. m. v. S  
 Signature of the Guiding Teacher  
 under whom the candidate has worked  
 WATER RESOURCES ENGINEERING  
 AND MANAGEMENT INSTITUTE  
 FACULTY OF TECHNOLOGY AND ENGINEERING  
 Place: Vadodara  
 Date: 30/01/2021

T. m. v. S  
 Counter Signature  
 DIRECTOR  
 WATER RESOURCES ENGINEERING  
 AND MANAGEMENT INSTITUTE  
 FACULTY OF TECHNOLOGY AND ENGINEERING  
 THE M. S. UNIVERSITY OF BARODA  
 SAMIALA - 391 410.

Vadodara

Date: 30/01/2021

AP  
 Dean  
 Faculty of Tech. & Engg.  
 M. S. University of Baroda,  
 Baroda

8. Insert the name of the Degree viz M.A., M.Sc., M.Ed., M. Com. etc. last received.

20/05/20 No. and Date of Registration 1101/2017 Name of the University The Maharaja Sayajirao University of Baroda  
 Date of passing the examination 11/10/2017 Class PH.D. (2017)  
 Subject Water Resources Engineering

10.10.17

# THE MAHARAJA SAYAJIRAO UNIVERSITY OF BARODA

Vadodra

## O. Ph. D.: I

- (i) A candidate holding recognized Master's Degree or recognized equivalent to Master's Degrees with at least 50% marks or Equivalent grades be considered eligible for registration for the Degree of Doctor of Philosophy in the concerned subjects.

The cases of the candidates who have passed the qualifying examination from the Indira Gandhi National Open University and from other Open Universities recognized by UGC/AICTE/AIU be referred to the Council of Post-Graduate studies and Research for consideration on merit.

**Eligibility of Candidate with Professional Degrees such as MBBS for pursuing Ph.D. In Basic Sciences\* :**  
The candidate with MBBS degree be considered eligible for registering for Ph.D. in relevant subjects in Faculty of Science only.

**Note:** (a) The related / conjunct subjects shall be decided by the Board of Studies concerned and shall be approved by the Council of Post-Graduate Studies and Research and the Syndicate.

- (ii) Notwithstanding anything contained in (i) above, a candidate who has passed the Master's Degree Examination in any subject or with marks not less than 50% may be permitted on the recommendation of the Council of Post-Graduate Studies and Research to register for any other subject under the same or other Faculty for the Ph.D. Degree.

- (iii) A person working in a National Laboratory or an Institution outside the University area recognized by this University for purposes of giving guidance Research and intending to register himself for the Ph.D. Degree of this University shall forward his application in the prescribed form for admission, provided he is eligible for such admission by virtue of his having a qualifying degree of this/ or any University, or an equivalent qualification or a person deputed by this University. The application form duly completed and signed by the recognized guiding teacher shall be sent through the Head of the Laboratory or the Institution to the Dean of the Faculty concerned of this University. Such applicant before being registered for the Ph.D. Degree shall be required to satisfy a Board consisting of the guiding teacher, Head of the Department and the Dean of the Faculty concerned at an interview and/or written examination to be conducted in the Department concerned that he possesses adequate knowledge to pursue the course in his special field of study.

In the case of a student registered in this university working under a recognized guide, from recognized Institutions outside the university the Head will be responsible for establishing liaison between the candidate, the guide, the Department concerned and the University. The Head will also ensure that the candidate comes to university department at least twice a year to present the progress of work done by him during the year to the Department concerned. The candidate shall be required to pay full tuition fees prescribed for admission to the Ph.D., to the Dean of the Faculty and the prescribed registration fee to the Registrar of the University through the Dean of the Faculty.

A student has to pay full tuition fees prescribed for admission to this University required under relevant ordinances; he/she shall apply for admission to the University only after obtaining the certificate of eligibility on production of the required documents and the prescribed fee. On receipt of the completed application for registration and the fee prescribed, from the Dean of the Faculty after admission, the University will issue a Registration Certificate showing the name of the candidate, the date of registration, the problem of research and the year in which the candidate is entitled to submit his/her thesis.

- (a) Joint Ph.D. degree programmes can be offered subject to the Memorandum of Understanding with the collaborating Institution/University is approved by the Syndicate of the University\*.
- (b) The Departmental Research Committee, on the recommendation of the Supervisor/Guide, may appoint scholars of eminence who shall be residing in India or abroad, as Joint Supervisor(s)/Joint Guide(s). The student, if required, may be ordinarily permitted to do research for maximum of 12 months in the Institute of the Joint Supervisor. Any extension shall require the prior approval of Departmental Research Committee\*.

A candidate registered under a guide of any subject in any department may request permission to have a Co-Guide@ from any National Laboratory or Research Institution outside the University or from any other department/faculty within this university. Such request shall be considered by the Board of the respective area of the subject [Defined under O. Ph.D. 2 (i) consisting of Dean of the faculty, Head of the department and the Guiding teacher, to appoint a co-guide on the recommendation of the guide.

The recommendation of the Board shall be informed to this university.

**Note:**

@ Co-guide may be appointed only in any National laboratory, or research Institution outside the University area, or any other departments within this university, provided he/she is qualified for guiding candidates for Ph.D. degree as defined under O.Ph.D.5.

### O. Ph. D. : 2

- (i) A candidate before being registered for the Ph.D. degree, shall be required to submit a written Research proposal to the department research committee and subsequently present the proposal in an open Seminar. Subsequently, the candidate shall appear for an Interview before a committee chaired by the Dean of the Faculty\*. Where the guiding teacher is also the Head of the Department concerned, then a senior teacher of the Department concerned who is a recognized Ph.D. guide be included in the Board. Where the guiding teacher is both Head of the Department and Dean of the Faculty concerned, then two such teachers of the Department concerned is included in the Board. If the Department concerned does not have the required number of such teachers, then a senior recognized Ph.D. guide from "other related Department/s of the Faculty" concerned be included in the Board so that in any given situation, the Board consists of not less than two other such teachers in addition to the guiding teacher.
- Course work and qualifying examination for Ph.D. Candidate :** All Ph.D. scholars shall take the following core courses comprising 6 credits (90 hours) i.e. research methodology, computer applications, written analysis and communication. In addition, the Departmental Research Committee shall suggest courses related to the subject within and outside the department, equivalent to atleast 6 credits (1 credit = 15 hours teaching) in the relevant area. A candidate having M.Phil or having completed the Pre-Ph.D.. course work from another university and moves to M.S. University, shall be exempted from the course work and the credits so obtained shall be treated at par with this University. However, such a candidate will have to appear in the University Entrance Examination as applicable to Fresh Candidates directly joining Ph.D\*.
- (ii) In the Faculty of Family and Community Sciences, every candidate shall be required to pass candidacy examination within a year of the date of registration and subsequently pass the Comprehensive examination prior to submission of his/her Thesis.
  - (iii) In the Faculty of Social Work, the candidate after being registered shall decide, in consultation with the guiding teacher and the Dean, three areas of study- in the field of social work related to the area of his doctoral investigation; one of these areas of study should be Social Research Methodology and Statistics. Further, within one year of the date of registration, but not before six months, the candidate will be required to appear for written and oral test before the Board comprising of the guiding teacher, Head of the Department and Dean to prove his proficiency in the area of study undertaken.
  - (iv) For those faculties like the Faculty of Journalism and Communication and the Faculty of Law, where the number of recognized Ph.D. guides is three or less, the 'Board' be constituted of only Two (2) persons;( **Note:**This special arrangement will cease and normal board as per O.Ph.D-2 (i) will be constituted, as and when the number of recognized guiding teachers in the faculty is more than three) the Head of the Department and the Dean of the Faculty, where guiding teacher holds one of these positions. If the guiding teacher holds both these position then the Board will constitute guiding teacher and anyone of the Deans from other faculties.
- Admission Procedure\*:** The concerned teacher may inform about the availability of positions for Ph.D. students through the Dean to the University and the same shall be advertised half yearly and such announcement shall be posted on the University website.
- Candidates who have qualified in the National/State level competitive examinations such as UGC-CSIR/NET/SLET/GATE/DBT, ICMR, GA, JRF etc. shall be exempted from taking University Entrance Examination.

However, for others the University shall conduct University Entrance Examination at least twice in a year on the pattern of UGC-CSIR NET examination.

Candidate qualifying in the above examination shall be interviewed by a committee constituted for the purpose. The committee shall consist of the Dean of the Faculty, Head of the Department and at least 3 recognized Ph.D. supervisors of the department, including guiding teacher and one recognized teacher from the outside department within the University. In case the department is having less than 3 recognized Ph.D. supervisors, at least 2 members from outside the department may be included in the Interview committee.

### O. Ph. D.: 3

(i) A candidate for Ph.D. degree after his registration shall be required to work for a minimum period of two full years under the guidance of a recognized teacher - Every registrant for the Ph.D. Degree of this University except those permitted to work in recognized Laboratories/Institutions etc. shall be required to attend the Department regularly and work directly under the guiding teacher during at least the first two terms or two semesters or one calendar Year from the date of registration as the case may be.

(a) Permanent teachers/employees who are in service in any other recognized university/college/research Institute/industry/organization in India and have a minimum of three years teaching/research experience, will be considered for registration to Ph.D. degree only if they get study leave for a period of at least six months and they shall be allowed to submit their thesis only after they have fulfilled the residency requirements of the university\*.

(b) The candidate will be required to work for at least two hundred days (inclusive of Course work) directly under the guiding teacher, on campus, within the period of four years. However, in exceptional cases, a candidate may be granted exemption by the Vice-Chancellor, keeping in view the merits of a specific case\*.

Provided that the guiding teacher will certify while forwarding the thesis that the concerned Ph.D. student has observed the provisions regarding attendance as provided under O. Ph. D. 3 (i) along with the copy of the muster roll.

(ii) A permanent teacher working in this University and is having required eligibility for registration for the degree of Doctor of Philosophy as defined under O. Ph.D. 1 (i); and also having more than five research publications may apply to the council of Post-graduate studies and research through proper channel, for self-guidedness.

(iii) A candidate may be permitted by the Vice-chancellor to make a change in the title of the problem of his thesis on the recommendation of the Board provided that the problem of Research remains substantially the same.

(iv) The Council of Postgraduate Studies and Research shall be competent to cancel the registration of a candidate in the event of his not showing satisfactory progress, upon his guide reporting the same to the Registrar through proper channel recommending the cancellation of the registration.

(v) A candidate may be permitted by the Vice-chancellor on the recommendation of the guiding teacher, the Head of the department and the Dean of the Faculty to permit him to volunteer to withdraw his registration as Ph.D. student for whatsoever reason.

### O. Ph. D.: 4

The minimum time limit for submitting the thesis for the Ph. D. Degree shall be two years from the date of registration. The candidate registered for Ph.D. degree shall be required to present an open seminar in the department, at least once in a year to review the progress of work of the candidate\*.

The candidate registered for Ph. D. Degree shall be required to pay the tuition and other fees as prescribed from time to time for all the terms from the date of registration to the date of submission of thesis.

A doctoral advisory committee to oversee the progress of work and advise on matters related to submission of thesis may be formulated for each candidate. The committee shall include the supervisor and 2 or 3 senior

- recognized Ph.D. Guides, from the same or other department of the university relevant to the theme of the work. Head of the department where the candidate is registered shall be the chairperson of the committee (In case Head is not recognized Ph.D. guide, the Vice-Chancellor is authorized to nominate the Chairman)\*.
- i) A Candidate who after completing four years from the date of his registration intends to continue his work for Ph.D. Degree shall be required to renew his registration by paying the tuition fees for each additional term/s of extension under intimation to the Registrar through proper channel. A Candidate who has so renewed his Ph. D. registration shall submit his thesis within a period of not more than eight years from the date of his original registration. After **eight** years no re-registration will be allowed and the candidate will have to register himself with a new topic and a new guide.
- j) "Notwithstanding the provision contained in Clause (iii) above, the Vice-Chancellor in special cases may permit the candidate to submit his/her Ph.D. thesis late by granting necessary extension, subject to the condition that he/she shall have to pay the necessary additional tuition fees for each additional term or a part thereof. The action taken by the Vice-Chancellor in such cases be informed to the Syndicate through Council of Post-graduate Studies and Research".

### O. Ph.D.: 5

The following shall be the guidelines to which the Council of Post-Graduate Studies and Research will give due consideration while recognizing teachers as qualified for guiding candidates for Ph. D. Degree:

- i) "A Professor shall be deemed as recognized for guiding Ph.D. students provided that he/she holds a Doctoral Degree or Equivalent research publications, without referring their cases to Council Post-Graduate Studies and Research and Syndicate. However he/she shall be required to inform in writing their willingness to be recognized for guiding Ph.D. students to the University Authorities and only thereafter shall they be deemed recognized as Ph.D. Guides."
- ii) A Professor/Scientist/Teacher working under retired scientist schemes sponsored by R & D agencies or having projects from R & D agencies with a provision to appoint research fellows, shall be permitted to guide students for Ph.D.\*.

#### **1. Guidelines for Faculties other than Faculties of Medicine, Performing Arts and Fine Arts:**

##### **(a) For Teachers other than professors:**

"A Teacher appointed on a permanent position at the M. S. University of Baroda should have a Ph.D. Degree of a recognized University and a minimum of Three years Experience as a Teacher after Ph.D. and also having five Original Research Publications in peer reviewed Professional Journals (These publications should include at least three that are not part of the Ph.D. Thesis) may apply to the Council of PG Studies and research through proper channel, for recognition as a Ph.D. Guide\*.

Provided that in respect of the teacher/lecturer employed in this University the requirement of three years Post Ph.D. teaching experience may be relaxed by one year for every three completed years teaching experience in this University prior to obtaining the Ph.D. Degree.

Provided, however, that the teacher who is already recognized as Ph.D. guide in another University before joining this University and appointed in this University on a permanent position be recognized as a Ph.D. guide, irrespective of three years teaching experience in this University.

Provided, that he/she should have five research publications out of which minimum 3 publications should be after Ph.D. Degree.

A Teacher having a Ph.D. Degree of a recognized University and appointed on a permanent position directly as a **Reader** be recognized as Ph.D. guide irrespective of teaching experience provided he has a minimum of eight research papers out of which at least four papers should be other than the Ph.D. work, published in scholarly journals.

**(b) For the Teachers of Performing Arts and Fine Arts:**

- i. 5 Research Publications in referred Journals or Exhibits displayed in recognized Galleries or Performances and 3 years of experience after Ph.D. Degree as a Teacher on a permanent position at the M. S. University of Baroda.

**(c) For the purpose of clarification.**

- i. Research Publication means publication in referred Journals and / or Publications having ISSN Number.
- ii. Chapters in books or Presentations made at the National / International Seminar published in book form as a proceedings may also be considered as Research Publication.
- iii. This has to be certified clearly by Head of the Department/ Dean before forwarding for approval to the Council of Post-Graduate Studies and Research.

**(d) Guidelines for the Teachers of the Faculty of Medicine:**

1. Each Clinical Unit, under the different departments of the Medical College, Baroda is considered as a whole for purposes of registration of Post-graduate students and imparting instruction for the post-graduate courses. (While the Head of such a Unit should share the responsibility for post-graduate instruction with other recognized teachers of the Unit, he should have overall responsibility of certifying attendance statement, dissertations, etc.)
2. Professor in each full-time department be deemed recognized as a University teacher for imparting instruction for the Post-graduate courses.
3. Post-graduate Teacher in any subject should have 8 years of teaching experience out of which 5 years should be as Assistant Professor and above.
4. No teacher who is not holding a Medical Post-graduate degree can guide a Post-graduate student for medical degrees.
5. For Ph D Guides in Medicine Faculty minimum of 15 years teaching experience or 10 years experience as Post-Graduate Teacher is required.

Every recognized guide must be attached to Faculty/Institution of this University, and his recognition will continue so long as he answers the designation on the basis of which he was recognized. However, if a teacher has guided a student for Ph.D. studies and if he is willing to continue to guide the student concerned for the remaining period after leaving the Faculty/Institution under this University, he may be permitted to do so by the Vice-chancellor.

The Syndicate may, at any time, on the recommendation of the Council of Post-graduate Studies and Research withdraws the recognition.

**O. Ph. D. : 5-A**

The following shall be the guide lines to which the council of Post-graduate studies and Research will give due consideration while recognizing researchers as qualified for guiding candidates for Ph. D. Degree.

- (1) Directors / Chairman / President / Vice-president of Institutions / Laboratories be deemed recognized candidates for guiding Ph.D. Students without referring their cases to the Council of Post-Graduate Studies and Research and Syndicate, provided such persons are from Scientific/Technical cadre and having minimum Post-graduate degree in the respective subject. They should submit a formal application in the prescribed form to the University.
- (2) For Researchers other than Directors, Chairman mentioned in (1) the guide lines are as follows:
  - (i) A researcher should have a research Degree (PhD) of a recognized University.  
And
  - (ii) Research experience of at least 10 years and
  - (iii) Ten Patents/Original Research Publications in peer reviewed Journals after Ph.D. (These publications should not include those that are part of the Ph.D. Thesis)\*.

- II. Every-recognized guide must be permanent employee of the Institution / Laboratory and his recognition will continue so long as he answers the designation on the basis of which he was recognized and is in the employment of the same Institution. However, if a Researcher has guided Four Terms or more and if he is willing to continue after leaving the Institution laboratory recognized by this University, his application in this matter will be favourably considered by the University.
- III. The recognized guide should maintain active academic interaction with this University.
- IV. Viva-voce examination of the candidate be held in concerned University Department / Faculty.
- V. The Syndicate may at any time on the recommendation of the Council of Post-graduate studies and Research withdraw the recognition.
- VI. Not more than three guides be recognized from each organization apart from Chairman/Director/President/Vice-president.

### O. Ph. D.: 6

- (i) When any teacher is recognized to guide Ph.D. Students, initially he/she be permitted to register not more than four students at a time; and after the submission of two Ph.D. Theses under his guidance, he be permitted to register further Ph.D. students under his guidance up to a maximum of eight Ph.D. students. No teacher in the University shall be permitted to guide more than eight Ph.D. students at a given time. A teacher should not register Ph.D. students two years before retirement.
- (ii) A candidate desirous of changing his guide shall apply to the Registrar through both the old and the new guiding teachers, Head of the Department and the Dean. Provided that in the cases of death of a guide or long leave or prolonged sickness of a guide or the cases of similar nature, a candidate may apply to the Registrar for changing his guide and such application shall be forwarded by the Registrar to the Vice-Chancellor.

### O. Ph. D.: 7

- (i) Two months before submitting the thesis, the candidate shall forward to the Registrar through his guide, Head of the Department and the Dean, three copies of the Synopsis of the thesis along with the prescribed examination fee.

Ph.D. candidates shall publish one research paper in a referred journal before the submission of the thesis/monograph for adjudication, and produce evidence for the same in the form of acceptance letter or the reprint thereof\*.

- (i) The candidate shall have to submit his thesis within twelve months from the date of submission of the Synopsis. If he fails to do so, he shall have to pay examination fee again.
- (ii) The thesis can be submitted any time during the year.

### O. Ph. D.: 8

The thesis shall be submitted in a spiral binding so that changes/revisions, if any may be incorporated\*. The thesis shall contain an account of the research work carried out by the candidate leading to the discovery of new facts or techniques or new correlations of scientific facts already known, the work being of such quality that it makes a definite contribution to the advancement of knowledge.

The thesis shall be written in English only, or otherwise when its subject matter is related to or based on a Modern European or Indian Language, it may be written in the relevant language.

- (iii) The thesis shall be submitted through the guiding teacher, Head of the Department and the Dean of the Faculty. It shall contain a certificate to the effect that the thesis incorporates the results of independent investigations carried out by the candidate himself, and signed by the candidate and the guiding teacher and that he has fulfilled the requirements regarding attendance contained in O. Ph. D. 3(v).
- (iv) A candidate will not be permitted to submit thesis for which degree has already been conferred on him by this or any other University. But the candidate shall not be precluded for incorporating his work, which has already been submitted elsewhere for a degree, in his present thesis covering a wide field. In such a case, he shall so indicate in written statement, which shall accompany the thesis.
- (v) Each candidate shall be required to submit to the University Office three copies of the Summary of the thesis, consisting of not more than one thousand words at the time of the actual submission of the thesis. After the thesis is accepted for the award of the Ph. D. degree, this summary will be forwarded to Editor for being published in the University Journal.
- (vi) After the successful completion of the viva-voce examination, the supervisor shall certify that all suggested changes have been incorporated and candidates shall submit 3 hard bound copies of the thesis to the university for the award of the degree along with a CD of the thesis for hosting the thesis on the website of the University for a period of 30 days at least\*.

### O. Ph. D.: 9

- (i) The University Vice-Chancellor, from among at least six names (preferably Professors/ or equivalent in ranks) recommended by the Council of Post-graduate Studies and Research from the panel prepared by the relevant Board of Studies giving present or past designation and complete address of each of the persons on the panel, shall appoint Referees, consisting of three members. One of the three referees, ordinarily the guiding teacher under whom the candidate has worked shall be the internal Referee and the other two shall be the External Referee. Of the two Referees, at least one shall be a person residing in India. The two External Referees shall examine the thesis and submit individual reports, within the time specified for this purpose.

The External Referees shall submit the detailed report on the evaluation of the thesis and a clear recommendation in the following prescribed format\* :

Name of the Candidate :		
Title of the Thesis :		
(a)	Thesis is recommended for award in its present form	
(b)	The thesis be accepted for the award after minor revision You would like to examine the response before recommending for award	Yes / No
(c)	The thesis be accepted after major revision requiring rewriting a portion/ chapter of the thesis incorporating some additional work. You would like to examine the revised thesis before recommending for award (please note that the response of the candidate would be sent to you any way for approval).	Yes / No
(d)	Rewriting of the thesis after further research is recommended (Please note that the revised thesis would be sent to you before acceptance).	
(e)	The thesis to be rejected outright.	
Name & Address of the Examiner :		
Date :		Signature of the Examiner

- (ii) After receiving favourable reports from both the external referees, a Viva-Voce test by the Internal Referee with the help of one of the External Referees shall be arranged and the two Referees shall prepare a joint report on the Viva-Voce test.

An Open Seminar chaired by the external referee be held either before or after the Viva-voce test. The date and time of the seminar to be conducted be communicated to the University by the guide through proper channel. The open seminar however be not considered as part of Ph. D. Examination.

There shall be three examiners (one Supervisor and Two External examiners), and out of the Two External examiners one of them shall be from outside the State/Country\*.

However, the final report after the viva voce be submitted in consultation with the Supervisor\*.

- (iii) If the two External Referees consider the thesis unacceptable for the award of the degree, no viva-voce test of the candidate shall be held, and the reports of all the Referees will be placed before the Syndicate.
  - (iv) If the External Referees ask for certain clarifications before giving their recommendation, the Internal Referee may get in touch with the candidate to obtain the required informations, and communicate the same to the External Referees. In such cases, where the External Referees reserve their recommendations and suggest a viva-voce and if the candidate satisfies the referees present, on the points raised by the two External Referees, the internal referee may forward all the reports including that of the viva-voce, to the Registrar for the Syndicate's final decision.
  - (v) In case of difference of opinion between the two Experts Referees, the Vice-Chancellor shall appoint from the list recommended by the Council, a third External referee. If third External Referee finds the thesis unacceptable, no viva-voce will be held and the thesis be rejected. In case the third External Referee considers that there is a 'Prima facie' case for the award of the degree, the viva-voce test of candidate shall be held at which the External Referee who is in favour of the acceptance of thesis will be present.
- Provided further that when it is decided to appoint third referee the copies of the reports of both the referees, favourable as well as adverse, be sent to the third referee for his perusal, without disclosing the identity of the said both referees.
- (vi) Where no Internal Referee is appointed, Registrar or the Dean will arrange the viva-voce examination with the help of at least one of the two External Referees.
  - (vii) The Degree/Certificate awarded by the University, shall carry the title of the thesis and name of the department where the candidate was registered for Ph.D\*.
  - (viii) Upon successful completion of the evaluation process and announcements of the award of degree the University shall submit a soft copy of the thesis to the UGC within a period of thirty days, for hosting the same in INFLIBNET, accessible to all institutions/universities\*.
  - (ix) Along with the Degree, the university shall issue a provisional certificate certifying to the effect that the degree has been awarded in accordance with the provisions to the regulation of the UGC\*.
  - (x) An honorarium @ ₹. 2,000/- shall be paid for evaluation of the Thesis to each examiner. In addition, the Examiner conducting the Viva voce examination shall be paid Rs. 1,000/- as honorarium\*.

### O. Ph. D.: 10

A work that has been rejected may be resubmitted after the revision and subject to the payment of half of the examination fee. A thesis required to be revised, should be resubmitted within a period of not more than two years, failing which the candidate will be required to go in for re-registration. The revised thesis as far as possible be sent to the same Referees.

*Ordinances revised and approved vide S. R. No. 54(10) dated 27-02-1996.*

Amended O. Ph.D. I (i) and O. Ph.D. 5-I-2(A) - Vide S.R. No. 26(3) dated 19-1-98

Amendment O. Ph.D. in 1 (i), 1 (i), 3 (i), 3 (i), 4 (iii), 5.1 (b), 5 A (I) (1) are approved vide S.R. No. AC-2005/08/26 dated 1-9-2005.

Amendment O. Ph.D. 5-I (b) and t-I I(c) are approved vice S.R. No. Ac/2007/07/26 dated, 27-7-2007.

\* Amendment O. Ph.D. 1, 2, 3, 4, 5, 5-A, 7, 8, 9 are approved vide S.R. No. 29(9) dated 12-10-2009.



**THE MAHARAJA SAYAJIRAO UNIVERSITY OF BARODA**

Fatehgunj, Vadodara – 390 002, Gujarat, INDIA

ACADEMIC SECTION - Telephone : • (Dy.R. Exams/Academics) 2750267 • (Academics) 2789485

office-academics@msubaroda.ac.in

dr-academic@msubaroda.ac.in

ACA71 355

Date: 14-12-2020

To,  
The Dean, Faculty of Technology & Engineering,  
The Maharaja Sayajirao University of Baroda,  
Vadodara.

Subject : Issuance of Ph.D. Course Work completion Certificate.

Sir/Madam,

Please find an enclosed certificate towards completion of Ph.D. Course work of the below specified Research Scholar:

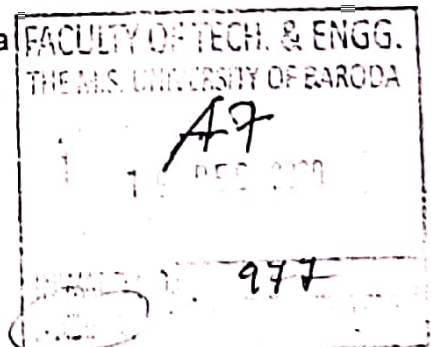
Name of the Research Scholar : **Vikas Kumar Rana**  
Registration Number : **950**  
Registration Date : **09/02/2018**  
Ph.D. course work certificate number : **FOTE/950**

Since the certificate being a pre-requisite for the submission of the synopsis, you are requested to arrange to send the certificate to the Research Scholar concerned through the concerned guide for further necessary actions.

  
Deputy Registrar (Academics)  
For Registrar (Offg.)  
The Maharaja Sayajirao University of Baroda.

Enclosure:  
Ph.D. Course Work completion Certificate of Vikas Kumar Rana

Copy to:  
• Section Examination



*19/12/2020*



# THE MAHARAJA SAYAJIRAO UNIVERSITY OF BARODA

## CERTIFICATE

[As per O.Ph.D. 2 under UGC (Minimum Standards and Procedure for Awards of M.Phil./Ph.D. Degree) Regulation, 2009 for 15 Credits to be earned by Ph.D. Scholars]

This is to certify that **Vikas Kumar Rana**, Research Scholar, registered under UGC (Minimum Standards and Procedure for Awards of M.Phil./Ph.D. Degree) Regulation, 2009, vide Registration Certificate Number **950** dated **09/02/2018**, for pursuing Ph.D. on has undertaken and completed the course work with the Grade **A**.

### STATEMENT OF CREDITS EARNED

Name of Research Scholar: **Vikas Kumar Rana**

Faculty/Institution: Faculty of Technology & Engineering

Department: Department of Civil Engineering

Paper Number	Course Title	Course Credits	Grade Earned
<b>Core Courses – 09 Credits [Offered at University Level]</b>			
I.	Introduction to Research & Research Writing	3	D
II.	Quantitative Research Techniques	3	A
III.	Introduction to Basic Computer Functions & Applications for Research	3	B
<b>Departmental Courses – 06 Credits [Offered at Departmental Level]</b>			
IV.	Computer Aided Design in Irrigation Water Management	3	A
V.	Watershed Management	3	A
<b>Overall Grade</b>			<b>A</b>

UC : 37 Batch III (9<sup>th</sup> September, 2018 to 28<sup>th</sup> February, 2019)

DC : 1206 (091220)

FOTE/950

Date of Issue: 15/12/2020

Place: Vadodara

  
17/12/2020  
Registrar (Offg.)

### Grade Conversion Table and Grade Calculation Formula

Grade	Grade Points	Range
O	10	Above 9.01
A	9	8.01 – 9.00
B	8	7.01 – 8.00
C	7	6.01 – 7.00
D	6	5.01 – 6.00
E	5	4.01 – 5.00
F	4	Below 4.00

$$\text{Overall Grade} = \frac{\sum (\text{Grade Points} \times \text{Credits})}{\sum \text{Credits}}$$



THE MAHARAJA SAYAJIRAO UNIVERSITY OF BARODA

CERTIFICATE

Date of Registration: 09/02/2018

Registration No.: FOTE/950

Certified that **Vikas Kumar Rana** has registered the name as a post-graduate student of this University for the Degree of Ph.D. under the guidance of **Dr. T.M.V. Suryanarayana** in Department of Civil Engineering in the Faculty of Tech. & Engg..

The title of the thesis is **Remote Sensing and Geographic Information System Approach for Hydrological, Morphometrical and Spatial Analysis of Vishwamitri Watershed.**

VADODARA  
DATE: 16/02/2018

  
DY. REGISTRAR  
(Academics)



THE MAHARAJA SAYAJIRAO UNIVERSITY OF BARODA

**Faculty of Technology & Engineering**

**Account Section Copy**

Academic Year 2020-21

Programme : Ph.D. in : CIVIL ENGINEERING

Name : VIKAS KUMAR RANA

Mobile No : 9033908837

Registration No. & Date : FOTE/950 03/02/18

Received the sum of : ₹. 8880/-

(Rupees in Words) : Eight Thousand Eight Hundred Eighty.

Being the payment towards Ph.D. fees for registered candidate at the University.

Year (s)	I	II	III	IV	V	VI	VII	VIII		
Term (s)	FIRST (I)					SECOND (II) ✓				

**Fees Receipt for Boys**

Code	Fees	
1	Tuition Fees:	1757
2	Common Fees:	2564
2(a)	Faculty Development & Maintenance Fund	513
2(b)	University Development & Maintenance Fund	512
2(c)	Library Registration Fees	146
2(d)	Internal Assessment Fees	74
2(e)	Facilities & Services Charges	1025
2(f)	Academic Activity Fees	74
2(g)	MSU Union Membership Fees	19
2(h)	Faculty Students' Association Fees	19
2(i)	Sports & Physical Education Activities Fees	36
2(j)	Eco. Disadvantaged Students' Support Fund	146
3	Other Fees:	4392
3(a)	Library resources fees	1464
3(b)	Laboratory fees / Field-work fees / Consumables fees etc.	1464
3(c)	Equipments & Maintenance fees	1464
4	Miscellaneous Fees	167
<b>Total:</b>		<b>8880</b>

Candidates Signature

Signature of Accounts Official  
For Chief Account Officer

Date: 08/01/2021



THE MAHARAJA SAYAJIRAO UNIVERSITY OF BARODA

**Faculty of Technology & Engineering**

**Academic Section Copy**

Academic Year 2020-21

Programme : Ph.D. in : CIVIL ENGINEERING

Name : VIKAS KUMAR RANA

Mobile No : 9033908837

Registration No. & Date : FOTE/950 03/02/18

Received the sum of : ₹. 8880/-

(Rupees in Words) : Eight Thousand Eight Hundred Eighty

Being the payment towards Ph.D. fees for registered candidate at the University.

Year (s)	I	II	III	IV	V	VI	VII	VIII		
Term (s)	FIRST (I)					SECOND (II) ✓				

**Fees Receipt for Boys**

Code	Fees	
1	Tuition Fees:	1757
2	Common Fees:	2564
2(a)	Faculty Development & Maintenance Fund	513
2(b)	University Development & Maintenance Fund	512
2(c)	Library Registration Fees	146
2(d)	Internal Assessment Fees	74
2(e)	Facilities & Services Charges	1025
2(f)	Academic Activity Fees	74
2(g)	MSU Union Membership Fees	19
2(h)	Faculty Students' Association Fees	19
2(i)	Sports & Physical Education Activities Fees	36
2(j)	Eco. Disadvantaged Students' Support Fund	146
3	Other Fees:	4392
3(a)	Library resources fees	1464
3(b)	Laboratory fees / Field-work fees / Consumables fees etc.	1464
3(c)	Equipments & Maintenance fees	1464
4	Miscellaneous Fees	167
<b>Total:</b>		<b>8880</b>

Candidates Signature

Signature of Accounts Official  
For Chief Account Officer

Date: 08/01/2021



THE MAHARAJA SAYAJIRAO UNIVERSITY OF BARODA

**Faculty of Technology Engineering**

**Student Copy**

Academic Year 2020-21

Programme : Ph.D. in : CIVIL ENGINEERING

Name : VIKAS KUMAR RANA

Mobile No : 9033908837

Registration No. & Date : FOTE/950 03/02/18

Received the sum of : ₹. 8880/-

(Rupees in Words) : Eight Thousand Eight Hundred Eighty

Being the payment towards Ph.D. fees for registered candidate at the University.

Year (s)	I	II	III	IV	V	VI	VII	VIII		
Term (s)	FIRST (I)					SECOND (II) ✓				

**Fees Receipt for Boys**

Code	Fees	
1	Tuition Fees:	1757
2	Common Fees:	2564
2(a)	Faculty Development & Maintenance Fund	513
2(b)	University Development & Maintenance Fund	512
2(c)	Library Registration Fees	146
2(d)	Internal Assessment Fees	74
2(e)	Facilities & Services Charges	1025
2(f)	Academic Activity Fees	74
2(g)	MSU Union Membership Fees	19
2(h)	Faculty Students' Association Fees	19
2(i)	Sports & Physical Education Activities Fees	36
2(j)	Eco. Disadvantaged Students' Support Fund	146
3	Other Fees:	4392
3(a)	Library resources fees	1464
3(b)	Laboratory fees / Field-work fees / Consumables fees etc.	1464
3(c)	Equipments & Maintenance fees	1464
4	Miscellaneous Fees	167
<b>Total:</b>		<b>8880</b>

Candidates Signature

Signature of Accounts Official  
For Chief Account Officer

Date: 08/01/2021

**IMPS Transaction Detail**

<b>Reference No.</b>	IMPS00147676447
<b>Debit Account Number</b>	00000033732750638
<b>Credit Account Number</b>	02010100009937
<b>Transaction Date</b>	08-Jan-2021
<b>Amount</b>	INR 8,880.00
<b>Status</b>	Success
<b>Reason</b>	Processed